

The impact of CO<sub>2</sub> on inorganic carbon  
supply and pH homeostasis in  
*Corynebacterium glutamicum*

**Inaugural-Dissertation**

**zur**

**Erlangung des Doktorgrades**

der Mathematisch-Naturwissenschaftlichen Fakultät

der Universität zu Köln

vorgelegt von

Katja Meike Kirsch

aus Saarbrücken

Köln, 2014

Berichterstatter:

Prof. Dr. Reinhard Krämer

Prof. Dr. Ulf-Ingo Flügge

Tag der Disputation: 14.03.2014

# Zusammenfassung

Bei dem Actinobacterium *C. glutamicum* handelt es sich um ein Bodenbakterium, das stark in der Biotechnologie genutzt wird, vor allem für die Produktion von L-Glutamat und L-Lysin. Ein wichtiger Aspekt bei der industriellen Fermentation mit hohen Zelldichten ist die Bildung großer Mengen  $\text{CO}_2$ . Da in *C. glutamicum*  $\text{CO}_2$  die Versorgung mit anorganischem Kohlenstoff ebenso beeinflusst wie den internen pH-Wert, wurden beide Aspekte in dieser Arbeit untersucht. Für die ausreichende Versorgung mit anorganischem Kohlenstoff ist die  $\beta$ -Carboanhydrase Bca vor allem bei niedrigem externen pH essentiell, denn die Umwandlung von  $\text{CO}_2$  zu Hydrogencarbonat ( $\text{HCO}_3^-$ ) ist entscheidend, damit es als Substrat für die Carboxylierung von PEP und Pyruvat zur Verfügung steht. Obwohl Bca-Aktivität auch zu einer beschleunigten Protonenbildung führt, scheint die pH-Homöostase durch das Enzym nicht beeinflusst zu sein. Auch erhöhte  $\text{CO}_2$ -Konzentrationen in der Zuluft haben keinen wachstumshemmenden Effekt und führten nur zu kurzen Effekten in Bezug auf pH-Homöostase. Ein Fehlen von Bca führt zu einem Wachstumsdefizit der Deletionsmutante *C. glutamicum*  $\Delta bca$ . Dieses kann durch die heterologe Expression von Genen ausgeglichen werden, die für ein cyanobakterielles Hydrogencarbonat-Aufnahmesystem kodieren, genannt SbtAB. Obwohl diese Komponente des Kohlenstoff-konzentrierenden Systems aus *Synechocystis* sp. PCC 6803 anorganischen Kohlenstoff in *C. glutamicum* bereitstellen kann, sind die positiven Auswirkungen auf den Wildtyp gering und beinhalten erhöhte Wachstumsraten auf Glukose und zum Teil auf Pyruvat. Die Aktivität von SbtAB konnte mit radiochemisch markiertem Hydrogencarbonat bestimmt werden. Zur Untersuchung der pH-Homöostase in *C. glutamicum* wurde ein Fluoreszenz-basiertes System zur *online*-Detektion entwickelt, das das ratiometrische GFP-Derivat pHluorin nutzt. Die Dynamik des Homöostaseprozesses konnte bestimmt werden, und die Ergebnisse zeigen die Fähigkeit von *C. glutamicum*, zwischen pH 6 und 8,5 effektiv pH-Homöostase zu betreiben. Verschiedene Komponenten, die an der pH-Homöostase beteiligt sind, wurden mit den entsprechenden Deletionsmutanten untersucht. Das Fehlen beider Endoxidasen der Atmungskette führt zum Kollaps der pH-Homöostase, während das Fehlen nur einer Komponente die Homöostasefähigkeit nicht beeinflusst. Das Fehlen der  $\text{F}_{(1)}\text{F}_{(0)}$ ATPase hat keine Auswirkung auf die pH-Homöostase in *C. glutamicum*.

## Abstract

The actinobacterium *C. glutamicum* is a soil bacterium which is extensively used in biotechnology, especially in the production of L-glutamate and L-lysine. An important aspect of industrial scale fermentation processes with high cell densities is the formation of large amounts of CO<sub>2</sub>. Since CO<sub>2</sub> is assumed to influence inorganic carbon provision as well as the internal pH of *C. glutamicum*, both aspects were investigated in this study. For a sufficient supply with inorganic carbon, the β-type carbonic anhydrase Bca is essential, especially at low external pH values, since conversion of CO<sub>2</sub> to bicarbonate (HCO<sub>3</sub><sup>-</sup>) is crucial before it can serve as a substrate for PEP and pyruvate carboxylation reactions. Although Bca activity also leads to an accelerated proton formation, the pH homeostasis seems not to be affected by this enzyme. Also, elevated CO<sub>2</sub> in the supply air did not lead to impaired growth and showed only short term effects on pH homeostasis. A lack of Bca leads to a growth deficit of the deletion mutant *C. glutamicum* Δ*bca*. This can be compensated by the heterologous expression of genes encoding a cyanobacterial system for bicarbonate import, called SbtAB. Although this component of the carbon concentrating mechanism of *Synechocystis* sp. PCC 6803 is able to provide inorganic carbon in *C. glutamicum*, there were only slight benefits observed in *C. glutamicum* wild type, including elevated growth rates on glucose and partly on pyruvate. The activity of SbtAB could be determined in uptake measurements using radio-labelled bicarbonate. The impact of SbtAB on pH homeostasis is negligible. To investigate the pH homeostasis of *C. glutamicum*, a fluorescence based assay for online detection of the intracellular pH was established using the ratiometric GFP variant pHluorin. The dynamic of the homeostasis process was determined and the results show the ability of *C. glutamicum* to perform effective pH homeostasis at external pH values from 6 to 8.5. Various possible components of the pH homeostasis machinery were observed by determination of the pH homeostasis capacity of the according deletion mutants. A complete lack of both branches of terminal oxidases of the respiratory chain leads to collapse of the pH homeostasis, while the absence of only one branch does not affect the ability to perform pH homeostasis. Also the absence of the F<sub>(1)</sub>F<sub>(0)</sub>ATPase has no effect on the of pH homeostasis in *C. glutamicum*.

# Abbreviations

ATP	Adenosine triphosphate
Bca	$\beta$ -type carbonic anhydrase
BCIP	5-Bromo-4-chloro-3-indolyl phosphate
BSA	Bovine serum albumine
CA	Carbonic anhydrase
CCCP	Carbonyl cyanide <i>m</i> -chlorophenyl hydrazone
CCM	Carbon concentrating mechanism
cdm	Cell dry mass
CO <sub>2</sub>	Carbon dioxide
cpm	Counts per minute
CTAB	Cetyltrimethylammonium bromide
DNA	Deoxyribonucleic acid
EDTA	Ethylenediaminetetraacetic acid
EYFP	Enhanced Yellow Fluorescent Protein
GFP	Green Fluorescent Protein
H <sub>2</sub> CO <sub>3</sub>	Carbonic acid
HCl	Hydrochloric acid
HCO <sub>3</sub> <sup>-</sup>	Bicarbonate
HEPPS	3-[4-(2-Hydroxyethyl)-1-piperazinyl]propane sulfonic acid
HPLC	High Pressure Liquid Chromatography
IPTG	Isopropyl $\beta$ -D-1-thiogalactopyranoside
K <sup>+</sup>	Potassium
K <sub>2</sub> HPO <sub>4</sub>	Dipotassium phosphate
kDa	Kilodalton
KH <sub>2</sub> PO <sub>4</sub>	Potassium dihydrogen phosphate
KP <sub>i</sub>	Potassiumphosphate buffer, inorganic
MES	2-(N-morpholino)ethanesulfonic acid
MOPS	3-(N-morpholino)propanesulfonic acid
Na <sup>+</sup>	Sodium
NaOH	Sodium hydroxide
NBT	Nitro blue tetrazolium
OD	Optical density
OPA	o-phthaldialdehyde/borate/2-mercapto-ethanol
PCR	Polymerase chain reaction
PEP	Phosphoenolpyruvate
pH <sub>i</sub>	Internal pH
PTS	Phosphotransferase system
PVDF	Polyvinylidene fluoride
SbtAB	Sodium-bicarbonate-transporter A and B
SDS	Sodium dodecyl sulfate

TAE	Tris-acetate-EDTA
TBS	Tris buffered saline
TC	Total counts
TCA	Tricarboinic acid

# Contents

1. Introduction .....	1
1.1 The model organism <i>Corynebacterium glutamicum</i> .....	1
1.2 CO <sub>2</sub> and the role of inorganic carbon in bacteria .....	2
1.2.1 The hydration of CO <sub>2</sub> and its impact on proton homeostasis .....	2
1.2.2 The role of CO <sub>2</sub> in inorganic carbon provision .....	3
1.3 Carbonic anhydrases .....	5
1.3.1 The catalytic reaction mechanism .....	5
1.3.2 Classification and functions of carbonic anhydrases .....	6
1.3.3 The Carbonic anhydrases of <i>C. glutamicum</i> .....	7
1.4 Cyanobacterial bicarbonate importers .....	8
1.5 Bacterial pH homeostasis .....	8
1.5.1 The importance of pH regulation .....	8
1.5.2 Mechanisms of pH homeostasis .....	9
1.6 Thesis objectives .....	11
2. Materials and Methods .....	12
2.1. Bacterial strains and culture conditions .....	12
2.1.1. Bacterial strains and plasmids .....	12
2.1.2. Culture conditions .....	15
2.1.3. Culture media and buffers .....	15
2.1.4 Growth experiments .....	16
2.2. Molecular biology techniques .....	17
2.2.1 Polymerase Chain Reaction (PCR) and product purification .....	17
2.2.2 Cloning of PCR fragments .....	19
2.2.3 Transformation of <i>E.coli</i> cells .....	20
2.2.4 Isolation of plasmid DNA and sequence analysis .....	20
2.2.5 Transformation of <i>C. glutamicum</i> cells .....	20
2.3. Uptake measurements .....	21
2.3.1 Cultivation prior to uptake measurements .....	21
2.3.2 Radiochemical detection of bicarbonate uptake .....	21

2.4. Determination of the intracellular pH .....	22
2.5. Protein biochemistry techniques.....	24
2.5.1. Gene expression for protein synthesis and cell disruption .....	24
2.5.2 SDS-Polyacrylamide gel electrophoresis (SDS-PAGE).....	24
2.5.3 Western blot analysis .....	25
2.6 Analytical methods.....	26
2.6.1 Lysine detection via HPLC analysis .....	26
2.6.2 Determination of osmolality.....	26
3. Results .....	27
3.1. The carbonic anhydrase Bca is essential in <i>C. glutamicum</i> .....	27
3.1.1 <i>C. glutamicum</i> $\Delta bca$ is not able to grow at atmospheric CO <sub>2</sub> .....	27
3.1.2 The <i>C. glutamicum</i> $\Delta bca$ phenotype is caused by the lack of Bca.....	28
3.1.3 The impact of <i>bca</i> overexpression in wild type cells is negligible.....	30
3.2 Heterologous expression of a cyanobacterial bicarbonate importer in <i>C. glutamicum</i> .....	34
3.2.1 SbtAB can restore growth of the <i>C. glutamicum</i> $\Delta bca$ strain .....	34
3.2.2 SbtAB has only slight impact on <i>C. glutamicum</i> wild type cells .....	39
3.2.3 The activity of SbtAB in <i>C. glutamicum</i> is difficult to display .....	44
3.2.4 SbtAB has no influence on the lysine yield in production strains .....	47
3.3 The pH homeostasis capacity of <i>C. glutamicum</i> .....	49
3.3.1 A method for online pH <sub>i</sub> measurement was established.....	49
3.3.2 The pH homeostasis in <i>C. glutamicum</i> is hardly affected by CO <sub>2</sub> .....	52
3.3.3 Bca and SbtAB do not interfere with pH homeostasis .....	53
3.3.4 Wild type cells perform pH homeostasis over a wide pH range .....	55
3.3.5 The process of pH homeostasis relies on the function of the respiratory chain .....	56
3.3.6 The F <sub>(1)</sub> F <sub>(0)</sub> ATPase is not involved in pH homeostasis.....	60
4. Discussion .....	62
4.1 Inorganic carbon supply in <i>C. glutamicum</i> .....	62
4.1.1 The impact of CO <sub>2</sub> on the physiology of <i>C. glutamicum</i> .....	62
4.1.2 Inorganic carbon supply in <i>C. glutamicum</i> $\Delta bca$ and the role of Bca in pH homeostasis .....	64

4.1.3 Inorganic carbon supply in <i>C. glutamicum</i> wild type.....	65
4.2 The impact of bicarbonate import via SbtAB .....	68
4.2.1 Consequences of additional bicarbonate in <i>C. glutamicum</i> .....	68
4.2.2 Possible alternatives to SbtAB.....	70
4.2.3 A model of inorganic carbon provision .....	71
4.3 The pH homeostasis machinery of <i>C. glutamicum</i> .....	73
4.3.1 The potential and possible limitations of the established $\text{pH}_i$ detection method .....	73
4.3.2 The role of the respiratory chain .....	74
4.3.3 A possible involvement of the $\text{F}_{(1)}\text{F}_{(0)}$ ATPase.....	75
4.3.4 Other putative components of the pH homeostasis machinery of <i>C. glutamicum</i> .....	76
5. Literature .....	78

# 1. Introduction

## 1.1 The model organism *Corynebacterium glutamicum*

The first description of the Gram-positive soil bacterium *Corynebacterium glutamicum* dates back to 1957 (Kinoshita, 1957). The GC-rich bacterium belongs to the family of *Mycobacteriaceae* which is part of the order of *Actinomycetales*. It is immobile, rod-shaped and its name refers to its typical club-like form (*coryne* [greek]: *club*). As *C. glutamicum* is non-pathogenic, it serves as a model organism for closely related pathogenic mycobacteria like *Mycobacterium leprae*, *Mycobacterium tuberculosis* and *Corynebacterium diphtheriae* (Minnikin, 1982; Stackenbrandt, 1997). It was discovered during the search for amino acid producing bacteria. Since then, *C. glutamicum* has been used extensively in industrial amino acid production.

Due to large efforts in metabolic engineering, *C. glutamicum* has become the most relevant organism for industrial L-lysine production with about 1.5 Mt/a. The L-glutamate production with *C. glutamicum* nowadays reaches a market size of almost 2.5 Mt/a (Becker & Wittmann, 2012). For example, a completely rationed lysine producer derived from a non-producing wild type strain was successfully designed in 2011 (Becker *et al.*, 2011). While L-lysine plays an important role in animal nutrition in industrial farming processes, L-glutamate is a popular flavour enhancer in convenience food. Further amino acids that are produced using *C. glutamicum* include L-methionine (Bolten *et al.*, 2010) and L-tryptophan (Ikeda, 2006). Production of the diamine cadaverine is also possible using *C. glutamicum* (Mimitsuka *et al.*, 2007). Above, biofuels (Blombach *et al.*, 2011; Inui *et al.*, 2004; Smith *et al.*, 2010), organic acids (Litsanov *et al.*, 2012) and vitamins (Vertes *et al.*, 2012) can be produced by *C. glutamicum*. Another biotechnological application of *C. glutamicum* which is of great economical importance is the production of various nucleotides, which serve for example as flavour enhancers and whose fermentative production has already been described in 1966 (Demain *et al.*, 1966).

Despite this huge impact of *C. glutamicum* in the field of biotechnology, many aspects of its physiology are still to be explored. Hence, not only strain improvement but also fundamental research in this field is still of interest. The study in hand contributes to

## 1. Introduction

this task by investigating physiological aspects of central importance. These are inorganic carbon supply and intracellular pH as well as basic mechanisms of proton homeostasis of *C. glutamicum* in general. All of them are basic physiological parameters that interfere with numerous cellular processes.

## 1.2 CO<sub>2</sub> and the role of inorganic carbon in bacteria

### 1.2.1 The hydration of CO<sub>2</sub> and its impact on proton homeostasis

Industrial scale fermentations in bioreactors using *C. glutamicum* are performed at extraordinary high cell densities (Knoll *et al.*, 2007). Under aerobic growth conditions, this leads to strongly elevated CO<sub>2</sub> concentrations of > 20 % due to the metabolic activity of the cells. This phenomenon shows up in particular at the bottom of large scale fermenters with volumes up to 750 m<sup>3</sup>, where elevated hydrostatic pressure leads to an increased solubility of CO<sub>2</sub> in the medium (Hermann, 2003). Also, local pH shifts of the medium occur during fermentation processes due to insufficient stirring (Kelle, 2005). Earlier experiments in *C. glutamicum* indicate a failure of pH homeostasis at an external pH of 6 and high CO<sub>2</sub> levels in the supply air (Follmann, 2008). Additionally, it has been reported that elevated CO<sub>2</sub> concentrations lead to an enhanced transcription of acid stress genes (Baez *et al.*, 2009). The underlying relation might be the proton formation during hydration of CO<sub>2</sub> in aqueous solution (Figure 1.1). It has to be noted that the first step which leads to the formation of carbonic acid (H<sub>2</sub>CO<sub>3</sub>) is not energetically favourable.



**Figure 1.1: Hydration of CO<sub>2</sub>.** If CO<sub>2</sub> is dissolved in aqueous solution, carbonic acid (H<sub>2</sub>CO<sub>3</sub>) is generated as a highly unstable intermediate. The weak acid dissociates to bicarbonate (HCO<sub>3</sub><sup>-</sup>) and a proton (H<sup>+</sup>) (Mostafa & Gu, 2003).

Gaseous CO<sub>2</sub> is able to enter the cell passively by diffusion via the cell membrane. As a consequence, the inner and outer concentrations are in equilibrium. The solubility of CO<sub>2</sub> changes dependent on temperature, hydrostatic pressure and above all the pH of the solution (Onken & Liefke, 1989). In an acidic surrounding, CO<sub>2</sub> is the major form

## 1. Introduction

while at an alkaline pH most of the emerging CO<sub>2</sub> is available as bicarbonate (HCO<sub>3</sub><sup>-</sup>). Two aspects of CO<sub>2</sub> are likely to cause negative effects on the pH homeostasis in *C. glutamicum*. On the one hand, the emerging protons from the hydration reaction intensify acidic stress at low external pH values. On the other hand, CO<sub>2</sub> is known to cause an elevated permeability of cell membranes, called the “anaesthetic effect”. This phenomenon might affect the proton gradient of the membrane and thereby interfere with pH homeostasis (Baez *et al.*, 2009; Sears & Eisenberg, 1961). Especially at low external pH values and high cell densities causing elevated CO<sub>2</sub> concentrations, these factors may lead to a collapse of pH homeostasis in *C. glutamicum*.

### 1.2.2 The role of CO<sub>2</sub> in inorganic carbon provision

Under neutral pH conditions, *C. glutamicum* is able to tolerate high CO<sub>2</sub> concentrations that occur during large scale fermentations (Bäumchen *et al.*, 2007). This is remarkable, since usually CO<sub>2</sub> has a noxious effect on microorganisms on various levels (Ballestra P., 1996; Garcia-Gonzalez *et al.*, 2007; Spilimbergo & Bertuccio, 2003) and has been used in food preservation long-since (Dixon & Kell, 1989). In contrast, *C. glutamicum* profits from elevated CO<sub>2</sub> levels especially at the beginning of fermentation processes. Inorganic carbon in its hydrated form of carbonate is added to the medium (personal note, Evonik Industries AG). The underlying reason for this observation may be the fact that inorganic carbon is required in carboxylation reactions like phosphoenol-pyruvate (PEP) and pyruvate carboxylation to perform gluconeogenesis, replenish TCA cycle intermediates and synthesise amino acids (Kronberg, 1966; Peters-Wendisch *et al.*, 1997; Peters-Wendisch *et al.*, 2001). The central significance of these reactions is represented by the PEP-pyruvate-oxaloacetate node pictured in Figure 1.2. Emanating from the oxaloacetate generated in the carboxylation reactions, the amino acid aspartate is formed which is the precursor molecule for the synthesis of asparagine, threonine, methionine, isoleucine and lysine. Although carboxylation and decarboxylation reactions seem to be in equilibrium during growth on glucose in wild type cells (Marx *et al.*, 1996; Petersen *et al.*, 2000), there are possible scenarios that enhance the need for external supply with inorganic carbon. Such conditions may be growth at low cell densities when the metabolic activity is still low, growth on gluconeogenic carbon sources such as pyruvate, lactate, acetate and glutamate (Gerstmeir *et al.*, 2003; Kramer *et al.*, 1990; Netzer *et al.*, 2004) or also in lysine producing strains.

## 1. Introduction

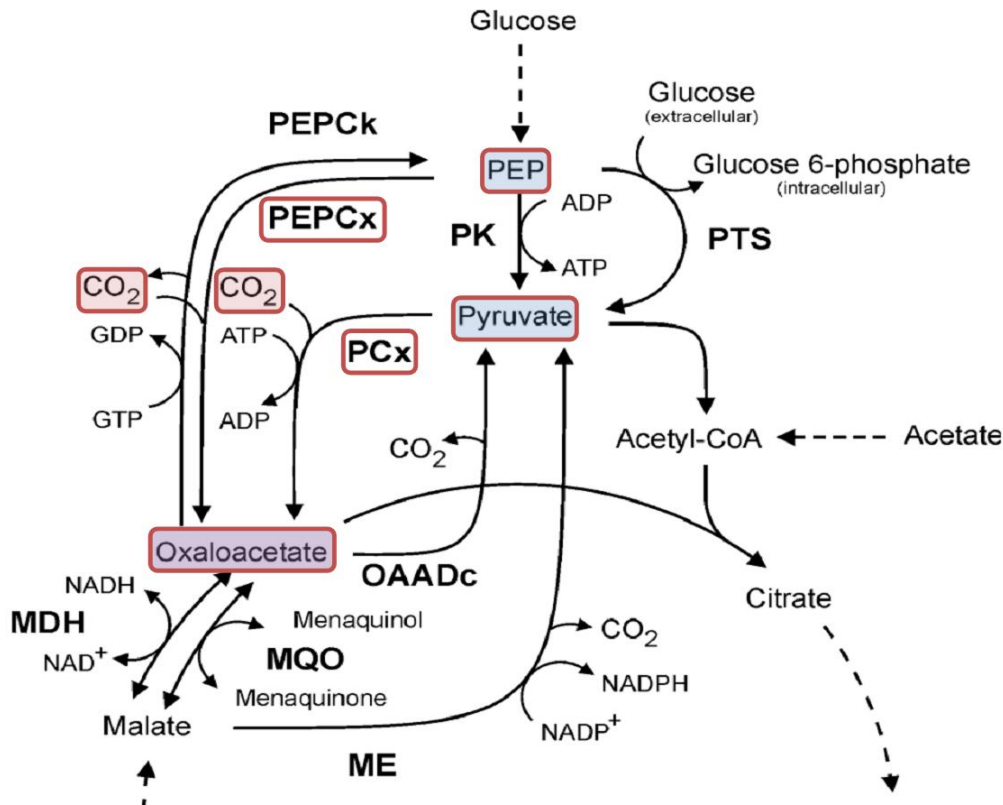


**Figure 1.2: Pyruvate, PEP, oxaloacetate and malate conversions in *C. glutamicum* (modified, (Netzer *et al.*, 2004)).** Solid arrows are marking reactions of the pyruvate kinase (PK), dashed arrows represent glycolysis, acetate activation and tricarboxylic acid cycle reactions. PTS, phosphotransferase system; PEPCk, PEP carboxy kinase; PEPCx, PEPcarboxylase; PCx, pyruvate carboxylase; OAADc, oxaloacetate decarboxylase; MDH, malate dehydrogenase; MQO, malate:quinone oxidoreductase; ME, malic enzyme. The coloured blocks highlight the carboxylation reactions of PEP and pyruvate catalysed by PEPCx and PCx, which lead to the formation of oxaloacetate.

In this context, it has to be noted that the actual substrate for the involved enzymes seems to be bicarbonate (Giordano *et al.*, 2003; Mitsuhashi *et al.*, 2004; Norici *et al.*, 2002; Okino *et al.*, 2008), which points out the importance of an efficient hydration of CO<sub>2</sub> as displayed in the equation in Figure 1.1. The reversible conversion from CO<sub>2</sub> to HCO<sub>3</sub><sup>-</sup> includes the formation of H<sub>2</sub>CO<sub>3</sub> as an unstable intermediate, a reaction that proceeds fairly slowly. In fact, this step is catalysed *in vivo* by a well described ubiquitous class of zinc metalloenzymes called carbonic anhydrases (CA, E.C.4.2.1.1), (Meldrum & Roughton, 1933; Stadie, 1933).

## 1.3 Carbonic anhydrases

### 1.3.1 The catalytic reaction mechanism

The central role of carbonic anhydrases (CAs) is represented by their appearance in all domains of life. They are divided into three major classes called  $\alpha$ -,  $\beta$ -, and  $\gamma$ -CAs. All classes evolved divergently and vary in sequence and structure (Hewett-Emmett & Tashian, 1996). Nevertheless, they all share a common active site containing a zinc ion involved in catalysis (Lindskog, 1997). The enzymatic conversion of  $\text{CO}_2$  is a two-step mechanism that is based on a nucleophilic attack on  $\text{CO}_2$  by a zinc-bound hydroxy-group ( $\text{OH}^-$ ) leading to bicarbonate formation, followed by regeneration of the active centre through ionisation of the now zinc-bound water (Lindskog, 1997). Figure 1.3 (a) displays the enzymatic conversion as well as the regeneration reaction. A crucial step is the replacement of bicarbonate by a water molecule, while the following proton transfer is the rate limiting step. Most CAs possess a  $k_{\text{cat}} > 10^4/\text{s}$ . Hence, this step requires a proton shuttle residue (PSR) to transfer protons to the final buffer in the solution. Usually, this is the His-64 residue of the active centre (Northrop & Simpson, 1998). This reaction step is shown in Figure 1.3 (b).

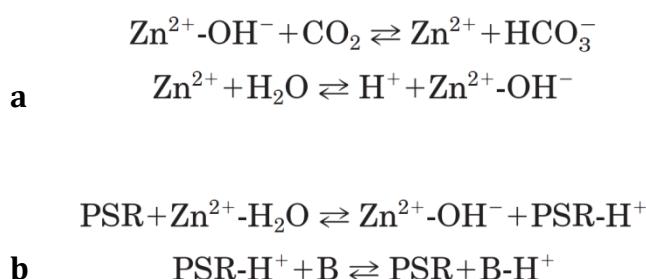


**Figure 1.3: Conversion of  $\text{CO}_2$  at the active site zinc ion of CAs.** The first step includes a nucleophilic attack by the zinc-bound hydroxide on  $\text{CO}_2$ . In a second step, the active site is regenerated by ionization of the zinc-bound water and the release of an  $\text{H}^+$  ion (a). To perform regeneration of the active centre via water ionisation, transfer of  $\text{H}^+$  to the proton shuttle residue (PSR) is necessary, before protons can be translocated to the actual buffer substance (B)(b)(Tripp *et al.*, 2001).

Although this reaction mechanism is common to all classes of carbonic anhydrases, the variations in their molecular structures are remarkable and many functions are described so far.

### 1.3.2 Classification and functions of carbonic anhydrases

While mammalian  $\alpha$ -CAs representing the best described group,  $\beta$ -,  $\gamma$ -CAs are mostly found in algae, bacteria and archaea. Especially the  $\beta$ -class has been detected in plants, algae and bacteria, showing various structures. A classification including a fourth  $\delta$ -class has been discussed years ago (Tripp *et al.*, 2001). Examples of the different structures are displayed in Figure 1.4.

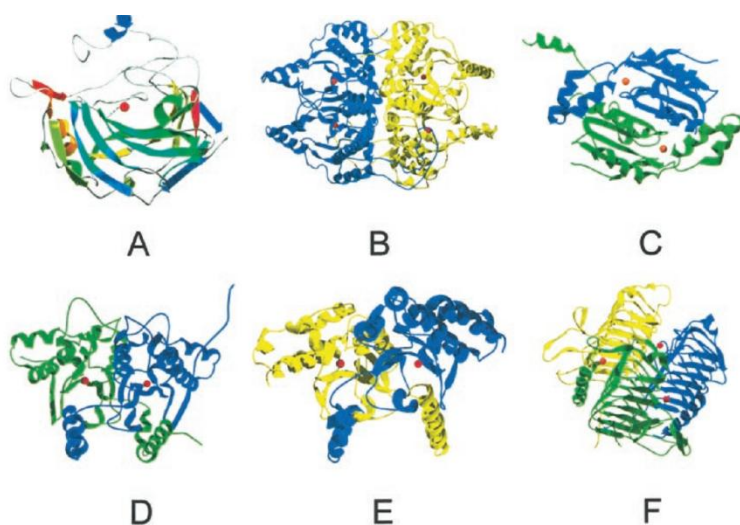


**Figure 1.4: Ribbon diagrams of the varying structures of the three different CA-classes (modified, (Tripp *et al.*, 2001)).** Each colour represents one monomer in the respective molecule. The active site zinc ions are displayed as red spheres. A,  $\alpha$ - class human isozyme II; B,  $\beta$ -class CA from the red algae *Porphyridium purpureum*; C,  $\beta$ -class CA from the pea plant *Pisum sativum*; D,  $\beta$ -class CA from the archeon *Methanobacterium thermoautotrophium*; E,  $\beta$ -class CA from the bacterium *Escherichia coli*; F,  $\gamma$ -class CA from the archeon *Methanosarcina thermophila*.

The physiological functions of CAs are diverse (Henry, 1996; Rowlett *et al.*, 2002; Smith & Ferry, 2000) and their activity is known to be pH dependent (Cronk *et al.*, 2001). For example, an involvement in lipid biosynthesis has been described as well as a role in photosynthesis related processes (Hoang & Chapman, 2002; Igamberdiev & Roussel, 2012; Lynch *et al.*, 1995). In one case, a function in oxidative stress response was postulated for a  $\beta$ -class CA in *Saccharomyces cerevisiae* (Götz *et al.*, 1999). The oxygen-sensitive phenotype of a  $\Delta nce103$  mutant was rescued by Mscal, a  $\beta$ -class CA from *Medicago sativa*. Unlike Mscal, the Bca-like NCE103 shows no CA activity in the CO<sub>2</sub>-based standard assay (Wilbur & Anderson, 1948). However, this observation was refuted later on (Clark *et al.*, 2004). CAs are of great medicinal interest as a suitable target for common groups of antibiotics (Lopez *et al.*, 2011; Nishimori *et al.*, 2010;

## 1. Introduction

Supuran, 2011). Above, they have been shown to enhance the activity of a bicarbonate importer in *Xenopus* oocytes (Schueler *et al.*, 2011) and serve anaplerotic functions in *Chlamydomonas reinhardtii* mitochondria (Giordano *et al.*, 2003). These examples underline the central importance of this group of enzymes in carbon metabolism.

### 1.3.3 The Carbonic anhydrases of *C. glutamicum*

Sequence analysis of the wild type strain *C. glutamicum* ATCC 13032 (Abe, 1967) revealed the existence of two carbonic anhydrase encoding genes called *bca* (*cg2954*) and *gca* (*cg0155*), belonging to the  $\beta$ - and  $\gamma$ -class, respectively (Mitsuhashi *et al.*, 2004). While transcription of the *gca* gene was not detectable and the deletion mutant did not behave different from the wild type, the *bca* gene is mainly expressed during exponential growth as well as during lysine production and a  $\Delta bca$  deletion mutant possesses a distinct phenotype. *C. glutamicum*  $\Delta bca$  shows a severe growth deficit at atmospheric CO<sub>2</sub> concentrations. Growth can be restored by cultivation at 5 % CO<sub>2</sub> in the supply air and by heterologous expression of the CA encoding *pca* gene from *Porphyridium purpureum* (Mitsuhashi *et al.*, 2004). These findings point towards the role of CAs in inorganic carbon supply. Dependency on the accelerated hydration of CO<sub>2</sub> catalysed by carbonic anhydrases to provide sufficient amounts of inorganic carbon appears likely. Since the influence of the *gca* gene seems negligible, the *bca* gene product Bca (Beta-typecarbonic anhydrase) is assumed to be the relevant carbonic anhydrase for *C. glutamicum*. Since its activity leads also to an accelerated proton formation, the deletion mutant *C. glutamicum*  $\Delta bca$  was expected to show better pH homeostasis at elevated CO<sub>2</sub> concentrations compared to the wild type. However, such an effect could not be observed (Follmann, 2008, unpublished). Nevertheless, elucidation of this connection needs further investigations. Also, the impact of the provided bicarbonate is of great interest in this context. Since this essential substrate cannot permeate the membrane like CO<sub>2</sub>, the necessity of Bca activity for its provision seems obvious. Creating an alternative way for its provision is a possible strategy to examine this aspect. The heterologous expression of a bicarbonate importer derived from an autotrophic organism is a possible strategy.

## 1.4 Cyanobacterial bicarbonate importers

The growth of many photosynthetic organisms depends on carbon concentrating mechanisms (CCMs) since the central enzyme for carbon fixation, the Ribulose-1,5-bisphosphatcarboxylase/oxygenase (RuBisCO), shows a very low substrate affinity for CO<sub>2</sub> (Kaplan & Reinhold, 1999). If the external pH is high, CO<sub>2</sub> mainly occurs in its hydrated form of HCO<sub>3</sub><sup>-</sup>, which can be converted back into CO<sub>2</sub> in the carboxysomes by carbonic anhydrases (Price *et al.*, 1992). Hence, bicarbonate importers are important for carbon supply in these organisms (Price *et al.*, 2008; Price, 2011). In the extensively studied cyanobacterial model organism *Synechocystis* sp. PCC 6803 (Grigorieva & Sestakov, 1982), two HCO<sub>3</sub><sup>-</sup> importers are encoded of which one has been identified as a Na<sup>+</sup>/HCO<sub>3</sub><sup>-</sup>-symporter. According to this function, it has been named SbtA (Sodium-bicarbonate-transport A)(Shibata *et al.*, 2002). SbtA is encoded by the *slr1512* gene. Transcriptional analyses revealed an elevated expression during alkaline stress (Summerfield & Sherman, 2008). This up-regulation of bicarbonate import makes sense at elevated pH values, since under these conditions bicarbonate is the most prominent form of inorganic carbon available. Also, the topology of SbtA has recently been described (Price *et al.*, 2011). Located next to *slr1512* is *slr1513*, the gene encoding SbtB, a periplasmic protein of unknown function. Both genes show similar expression patterns (Summerfield & Sherman, 2008). Hence, SbtB might be a crucial part of the functional transport system.

## 1.5 Bacterial pH homeostasis

### 1.5.1 The importance of pH regulation

In bacteria, an efficient pH homeostasis is essential to survive changing proton concentrations of their environment, since energy driven processes depend on a stable electrochemical proton gradient along the membrane for ATP generation. In aerobic organisms like *C. glutamicum*, this proton motive force is about 200 mV (Kashket, 1985; Mitchell, 1973). The fact that the external pH of the medium alters the bacterial metabolism has been known long-since (Gale & Epps, 1942), but the many ways of pH regulation in acidophilic, neutrophilic and alkalophilic bacteria are still not fully

understood. However, basic mechanisms have been described in detail earlier (Booth, 1985).

### 1.5.2 Mechanisms of pH homeostasis

A passive mechanism of pH regulation is the buffering capacity of the cytoplasm which has been determined for a number of bacteria (Booth, 1985). A regulation of the intracellular pH via proton consuming decarboxylation of amino acids is described as part of acidic stress response (Gale, 1946) and many examples for this function can be found (Castanie-Cornet *et al.*, 1999; Iyer *et al.*, 2003; Kashiwagi *et al.*, 1991; Senouci-Rezkallah *et al.*, 2011). Above, urease activity to produce alkalising ammonium, as well as membrane alterations and DNA repair mechanisms contribute to pH regulation (Cotter & Hill, 2003). However, no such mechanism has been described in *C. glutamicum* yet (Follmann, 2008).

Another aspect of pH regulation is the influence of cation/proton-antiporters. An involvement of sodium and potassium in alkaline and acidic stress response has long been discussed, since both play a role in maintenance of the proton motive force (Booth, 1985). In recent years, many examples for the involvement of both cations and  $\text{Na}^+(\text{K}^+)/\text{H}^+$ -antiporters in pH homeostasis have been described (Casey & Condon, 2002; Chapman *et al.*, 2006; Epstein, 2003; Kitko *et al.*, 2010; Krulwich *et al.*, 2009; Quinn *et al.*, 2012). In *C. glutamicum*, the potassium channel CgkK is known to be essential at acidic pH (Follmann *et al.*, 2009a). Also, two Mrp-type  $\text{K}^+(\text{Na}^+)/\text{H}^+$ -antiporters can be found in *C. glutamicum* and a role in alkaline pH homeostasis is discussed (Follmann, 2008).

The most likely players of pH regulation are proton pumps that can actively transfer  $\text{H}^+$  via the membrane. Of central importance in this context is the  $\text{F}_{(1)}\text{F}_{(0)}$ ATPase, which generates ATP using the electrochemical proton gradient. If the external pH is high, proton influx via ATPase activity is crucial to maintain a neutral intracellular pH (Barriuso-Iglesias *et al.*, 2006; Barriuso-Iglesias *et al.*, 2013; Bender *et al.*, 1986; Maurer *et al.*, 2005; Padan *et al.*, 2005; Sturr & Marquis, 1992). Also, a reverse function to export protons at acidic stress is possible and induction of the  $\text{F}_{(1)}\text{F}_{(0)}$  ATPase-operon by acidic pH has been reported in *Streptococcus*, *Lactococcus* and *Lactobacillus* (Koebsmann *et al.*, 2000; Kuhnert *et al.*, 2004; Kullen & Klaenhammer, 1999; Martin-Galiano *et al.*, 2001). In

## 1. Introduction

*C. glutamicum*, an involvement in alkaline stress response has been described (Barriuso-Iglesias *et al.*, 2006), while a reverse function in acidic stress response seems unlikely (Koch-Koerfges *et al.*, 2012). Proton export via the respiratory chain as part of pH homeostasis at acidic conditions is another possible scenario, which has not been taken into account yet. In *C. glutamicum*, two branches of proton exporting terminal oxidases exist (Bott & Niebisch, 2003). Especially the *bc1-aa3*-supercomplex with its ability to transfer  $6\text{ H}^+/2\text{ e}^-$  bears great potential to be involved in pH regulation. Figure 1.5 gives an overview of the postulated mechanisms for pH homeostasis in *C. glutamicum* with emphasis on the involvement of  $\text{CO}_2$ .

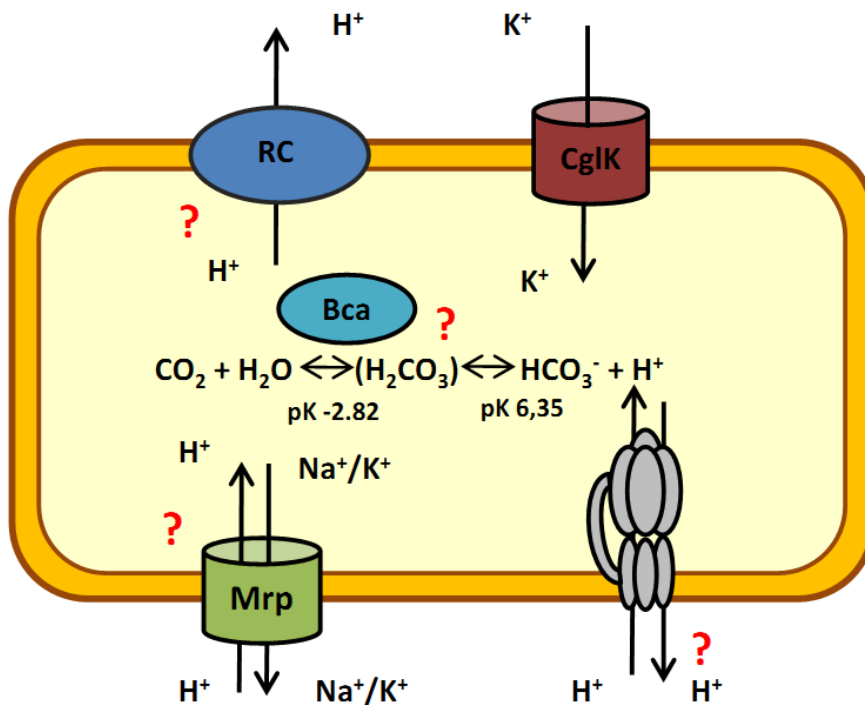


**Figure 1.5: Components involved in pH homeostasis in *C. glutamicum*.** Potassium import via CgIK was shown to be essential at acidic pH (Follmann *et al.*, 2009a). It is not clear to what extent Bca activity contributes to proton formation and pH homeostasis. While the respiratory chain (RC) might be used for proton export under acidic stress, the  $\text{F}_{(1)}\text{F}_{(0)}$ -ATPase (displayed in grey colour) is part of alkaline stress response and may be involved in proton export at acidic pH. Also, the role of the cation/proton-antiporters (Mrp) postulated in *C. glutamicum* is not clear yet. Abbreviations: CgIK, *C. glutamicum*  $\text{K}^+$  channel; RC, Respiratory chain.

The above figure illustrates the many aspects of pH regulation that are still unclear in *C. glutamicum*. Hence, investigation on the various candidates responsible for proton homeostasis is important. Understanding pH homeostasis is also basic to estimate the influence of  $\text{CO}_2$  in this context, since it is not clear to which extent its hydration interferes with proton homeostasis of the cell.

### 1.6 Thesis objectives

This work aims to give a better understanding of inorganic carbon metabolism and pH homeostasis in *C. glutamicum*. First of all, the examination of the carbonic anhydrase Bca and its influence on cellular processes is central to this. A second approach examines the possible benefits of bicarbonate import. An ideal scenario includes an optimised supply with inorganic carbon on the one hand and a better pH homeostasis at high CO<sub>2</sub> concentrations on the other hand. If import of bicarbonate shifts the balance of the CO<sub>2</sub> hydration reaction towards the educts, the negative influence of CO<sub>2</sub> on pH homeostasis is believed to be less severe since proton formation is attenuated at the same time. Hence, the potential of bicarbonate import for strain improvement by elevating the lysine yield is also of interest. A third topic is the profound investigation of pH homeostasis in *C. glutamicum*.

The experiments will include a deeper physiological characterisation of the *C. glutamicum*  $\Delta bca$  mutant, a strain which lacks the active  $\beta$ -type carbonic anhydrase Bca. Also, a test for possible benefits in carbon supply via overexpression of the *bca* gene in the wild type as well as a precise examination of the influence of Bca on pH homeostasis will be performed. To investigate benefits of elevated bicarbonate levels in *C. glutamicum*, heterologous expression of a bicarbonate importer is necessary. For this purpose, the SbtA transporter from *Synechocystis* sp. PCC 6803 will be tested in *C. glutamicum*. Since SbtA mediated bicarbonate uptake might also elevate the lysine yield in production strains, this will be measured as well. To investigate pH homeostasis, one aim is the establishment of a tool for online detection of the intracellular pH (pH<sub>i</sub>). Once such a system based on pH sensitive fluorescence proteins can be established, investigations towards the dynamics of pH homeostasis in general can be performed. Online pH<sub>i</sub> monitoring might be used to shed light on the influence of CO<sub>2</sub> on proton homeostasis and to characterise various components of pH homeostasis in *C. glutamicum*.

## 2. Materials and Methods

### 2.1. Bacterial strains and culture conditions

#### 2.1.1. Bacterial strains and plasmids

For cloning procedures, the *E. coli* strain DH5 $\alpha$  (Grant *et al.*, 1990) was used. All *C. glutamicum* strains in this work are based on the wild type strain ATCC 13032 (Abe, 1967), with the exception of the *C. glutamicum*  $\Delta bca$  strain which was provided by Kyowa Hakko Bio Co., LTD. and the production strain DM1933, which was provided by Evonik Industries AG. Table 2.1 gives an overview of all used bacterial strains.

**Table 2.1: List of bacterial strains, used in this study.** Explanations towards the features of the strains are given in the “Genotype” row.

Strain	Genotype	Origin
<i>E. coli</i>		
DH5 $\alpha$ mcr	<i>endA1 subE44 thi-1 <math>\lambda</math> recA1 gyrA96 relA1 deoR <math>\Delta(lacZYA-argF)</math> U196 <math>\phi 80DlacZ</math> <math>\Delta m15mcrA \Delta(mmr hsdRMS mcrBC)</math></i>	(Grant <i>et al.</i> , 1990)
<i>C. glutamicum</i>		
ATCC 13032	ATCC 13032 wild type	(Abe, 1967)
$\Delta F_1F_0$	ATCC 13032 with a deletion of the <i>atpBEFHAGDC</i> genes encoding F <sub>(1)</sub> F <sub>(0)</sub> -ATP synthase	(Koch-Koerfges <i>et al.</i> , 2012)
$\Delta qcr$	ATCC 13032 with a deletion of the <i>qcrCAB</i> genes encoding the cytochrome <i>bc1-aa3</i> branch of the respiratory chain	(Koch-Koerfges <i>et al.</i> , 2013)
$\Delta cydAB$	ATCC 13032 with a deletion of the <i>cydAB</i> genes encoding the cytochrome <i>bd</i> branch of the respiratory chain	(Koch-Koerfges <i>et al.</i> , 2013)
DOOR	ATCC 13032 with a deletion of the <i>cydAB</i> and <i>qcrCAB</i> genes ( <i>Devoid Of Oxygen Respiration</i> )	(Koch-Koerfges <i>et al.</i> , 2013)
DM 1933	DM 1730 ( <i>lysC</i> <sup>T3111</sup> - <i>pyc</i> <sup>P4585</sup> - <i>hom</i> <sup>V59A</sup> - $\Delta pck$ ),	Evonik Industries AG

## 2. Materials and Methods

	$2x(\text{lysC}^{\text{T3111}}\text{-asd-dapA-dapB-ddh-lysA-lysE})$	
$\Delta bca$	Kyowa Hakko strain with a deletion of the <i>bca</i> gene encoding the carbonic anhydrase Bca	Kyowa Hakko Bio Co., LTD.
$\Delta gca$	Kyowa Hakko strain with a deletion of the <i>gca</i> gene encoding the carbonic anhydrase Gca	Kyowa Hakko Bio Co., LTD.

All strains were stored as glycerol cultures at  $-80^{\circ}\text{C}$  using Roti®-Store tubes (Carl Roth GmbH & Co. KG, Karlsruhe). The *C. glutamicum* strains mentioned in this work were always equipped with the according pEKEx2-based plasmids. An overview of all constructs is given in Table 2.2.

## 2. Materials and Methods

**Table 2.2: List of plasmids, used in this study.** All plasmids were amplified in *E. coli* and used for expression in *C. glutamicum*.

Plasmid name	Properties	Origin
pEKEx2	Km <sup>R</sup> , lac promoter, oriV <sub>E.c.</sub> , oriV <sub>C.g.</sub> Expression vector	(Eikmanns <i>et al.</i> , 1991)
pGM1	Plasmid encoding the sequence for the fluorescence dye pHluorin (ratiometric)	(Miesenböck <i>et al.</i> , 1998)
pEKEx2_EYFP	pEKEx2 with the sequence encoding the fluorescence protein EYFP	(Faust, 2011)
pEKEx2_pHluorin	pEKEx2 with the sequence encoding the fluorescence protein pHluorin derived from the pGM1 plasmid	This work
pEKEx2_EYFP_Bca_Strep	pEKEx2_EYFP with the sequence encoding the carbonic anhydrase Bca from <i>C. glutamicum</i> and a Strep-tag	This work
pEKEx2_EYFP_SbtAB_Strep	pEKEx2_EYFP with the sequence encoding the SbtAB construct from <i>Synechocystis sp.</i> PCC 6803 and a Strep-tag	This work
pEKEx2_pHluorin_Bca_Strep	pEKEx2_pHluorin with the sequence encoding the carbonic anhydrase Bca from <i>C. glutamicum</i> and a Strep-tag	This work
pEKEx2_pHluorin_SbtAB_Strep	pEKEx2_pHluorin with the sequence encoding the SbtAB construct from <i>Synechocystis sp.</i> PCC 6803 and a Strep-tag	This work
pEKEx2_SbtA	pEKEx2_pHluorin with the sequence encoding the bicarbonate importer SbtA from <i>Synechocystis sp.</i> PCC 6803	Ines Ochrombel

### 2.1.2. Culture conditions

*E. coli* cells were cultivated on solid LB complex medium (Sambrook, 1989) plates containing 1.5 % agar. For liquid cultures, 5 ml LB-medium was used. The cultivation was performed at 37 °C. Liquid cultures were shaken on an agitator at 125 rpm.

*C. glutamicum* pre-cultures were grown on BHI complex medium (*Brain-Heart-Infusion*, Oxoid Thermo Scientific, Hampshire, UK) either on solid plates containing 1.5 % agar or in liquid cultures of 10 ml. Pre-cultures of the *C. glutamicum* DOOR mutant were cultivated on BHI complex medium containing 0.2 M MOPS and 22 mM glucose. Cells were cultivated at 30 °C. Liquid cultures were shaken at 125 rpm with the exception of cultures treated with elevated CO<sub>2</sub> concentrations in the supply air. In this case, no agitation was possible due to technical reasons.

### 2.1.3. Culture media and buffers

Main cultures that were used in the described experiments were grown in CgXII minimal medium with modifications depending on the experimental setup. The basic composition was as follows:

#### CgXII minimal medium

(NH <sub>4</sub> ) <sub>2</sub> SO <sub>4</sub>	20 g/l
Urea	5 g/l
K <sub>2</sub> HPO <sub>4</sub>	1,6 g/l
KH <sub>2</sub> PO <sub>4</sub>	1 g/l
MOPS	42 g/l
MgSO <sub>4</sub>	0.25 g/l
CaCl <sub>2</sub>	0.01 g/l
Protocatechuic acid	0.03 g/l
Biotin	0.2 mg/l
Trace elements solution	1 ml/l

#### Trace elements solution

FeSO <sub>4</sub> x7H <sub>2</sub> O	10 g/l
MnSO <sub>4</sub> xH <sub>2</sub> O	10 g/l
ZnSO <sub>4</sub>	1 g/l
CuSO <sub>4</sub> x5H <sub>2</sub> O	0.2 g/l
NiCl <sub>2</sub> x6H <sub>2</sub> O	20 mg/l

## 2. Materials and Methods

As organic carbon sources, either 5.5 mM (corresponding to 1 % w/v) glucose or 50 mM pyruvate were used.

If a pH below 7 or above 7.5 was required, 0.2 M MES or 0.2 M HEPPS instead of 0.2 M MOPS were used, respectively. During media preparation the pH was set using 10 M NaOH and 5 M HCl.

### 2.1.4 Growth experiments

All growth experiments were performed in 500 ml Erlenmeyer shaking flasks containing 50 ml liquid culture. For the selection of cells carrying the desired pEKEx2 plasmids, kanamycin was added to a final concentration of 50 mg/l. To induce gene expression via the *lac* promoter, 0.1 mM IPTG were used in the experiments. Cultures were incubated at 125 rpm and 30 °C. If cultures were treated with additional CO<sub>2</sub> in the supply air, they were grown in custom made glass tubes (Figure 2.1) in a culture volume of 25 ml at 30 °C.



**Figure 2.1: Glass vessels for CO<sub>2</sub> supplementation.** The sterile filtered air/CO<sub>2</sub>-mixture was lead into the culture via thin glass tubes. The culture volume for optimal mixing was 25 ml.

As a growth parameter, the cell density was determined photometrically at a wavelength of 600 nm. Derived from the monitored growth curves, the growth rate  $\mu$  [1/h] for exponential growth stages was determined using Microsoft Excel (Microsoft Corporation, Redmond, WA, USA).

## 2.2. Molecular biology techniques

### 2.2.1 Polymerase Chain Reaction (PCR) and product purification

To amplify the pHluorin encoding DNA sequence, the pGM1 plasmid (Miesenböck *et al.*, 1998) was used as DNA template. In case of the *bca* sequence encoding the carbonic anhydrase Bca, genomic DNA from *C. glutamicum* was used. The DNA template for amplification of the *slr1512-slr1513* region encoding the SbtAB construct was genomic DNA from *Synechocystis* sp. PCC 6803. The PCR reaction was performed using the Phusion® High-Fidelity-PCR system (Thermo Scientific, Fisher Scientific Germany GmbH, Schwerte, Germany) with HF-buffer as recommended by the supplier. A typical reaction mix consisted of the following components:

H2O	ad 50 µl
Template-DNA	0,5-3 µl
5x HF-buffer	10 µl
dNTP mix 10 mM	1 µl
Forward primer 10 µM	2.5 µl
Reverse primer 10 µM	2.5 µl
DMSO	1.5 µl
Phusion® Polymerase	0.5 µl

A typical program for amplification included the following steps:

98 °C, 2 min	Initial denaturation
98 °C, 15 s	Denaturation
50 °C, 15 s	Oligonucleotide binding
72 °C, 1-2.5 min	Elongation
72 °C, 5 min	Final elongation
Repetition of steps 2-4	30-35 x
8 °C, ∞	Short term storage

The oligonucleotides that were used as primer molecules in the PCRs were synthesised by Eurofins MWG Operon (Eurofins MWG Operon AG, Ebersberg, Germany) and are listed in Table 2.3.

## 2. Materials and Methods

**Table 2.3: List of oligonucleotides, used for PCR and control sequencing in this study.** All samples were stored as a 100  $\mu$ M aqueous solution at -20 °C.

Oligonucleotide name	Properties	Sequence
pHluoForBam (5'superecBam)	pHluorin encoding, forward	5'GGGATCCAGGAGGAATTAACCATGAGTAA AGGAGAAGAACTTTTC
pHluoRevBam (3'superecBam)	pHluorin encoding, reverse	5'GGGATCCTTATTTGTATAGTTCATCCATGC
bcaASfKpnIYFP	<i>bca</i> encoding, first of two possible transcription starts, forward	5'TATGGTACCCATGACCTAAATGATTGTACT GACTGGC
bcaSTREPrKpnIYF	<i>bca</i> encoding with Strep- tag sequence, reverse	5'TATGGTACCTTATTTTTTCGAACTGCGGGTG GCTCCAACCCAGGTTCTTGCTAATTACAGGT TCAGTACGACC
slrRBSforKpnIYFP	<i>sbtA</i> encoding with ribosome binding site, forward	5'TATGGTACCAGGAGACAATTTACATTATG GA
slrSTREPrSacIYFP	<i>sbtB</i> encoding with Strep-tag sequence, reverse	5'TATGAGCTCTTATTTTTTCGAACTGCGGGTG GCTCCAACAGCCCTCAGGGCCACA
pEKEEx2for	Sequencing primer pEKEEx2- <i>mcs</i> forward	5'ATCGGCTCGTATAATGTG
pEKEEx22for2	Sequencing primer pEKEEx2- <i>mcs</i> forward	5'GGCATACTCTGCGACATCG
pHluo.end.for	Sequencing primer, binds at the end of the pHluorin encoding sequence	5'TACCTGTCCTACCAATCTGCCCTTTTCG
pEKEEx2rev	Sequencing primer pEKEEx2- <i>mcs</i> reverse	5'CCGCTTCTGCGTTCTGATTT

The integrity of plasmid DNA in *E. coli* or *C. glutamicum* was confirmed via PCR using the EconoTaq®Plus Green 2x Master Mix (Lucigen Corporation, Middleton, WI, USA)

## 2. Materials and Methods

according to manufacturer's instructions. 1 µl per 10 µM oligonucleotide primer was added. With a sterile pipette tip, small amounts of colony material were transferred directly from the agar plate into the PCR mix. A typical example of the PCR program chosen for this so called "Colony-PCR" was as follows:

95 °C, 10-15 min	Cell lysis and Initial denaturation
95 °C, 30 s	Denaturation
50 °C, 30 s	Oligonucleotide binding
72 °C, 1-3 min	Elongation
72 °C, 7 min	Final elongation
Repetition of steps 2-4	30-35 x
8 °C, ∞	Short term storage

After completion of the PCR, the samples were analysed by agarose-gel electrophoresis using 1 % agarose in TAE buffer pH 8. For sizing of the DNA fragments, the GeneRuler™ 1 kb DNA ladder (Thermo Scientific, Fisher Scientific Germany GmbH, Schwerte, Germany) was used. DNA fragments that were to be used in cloning procedures were sliced out and purified using the "Nucleo Spin®Gel and PCR Clean-up" kit (Macherey-Nagel GmbH und Co. KG, Düren, Germany) or the "High Pure PCR Product Purification Kit" (Roche Diagnostics Deutschland GmbH, Mannheim, Germany) according to manufacturers' instructions.

### 2.2.2 Cloning of PCR fragments

To introduce purified PCR fragments into the pEKEx2 plasmid, both gene fragment and vector DNA were incubated with the according restriction enzymes. In case of the pHluorin encoding fragment, this was *Bam*HI, *Kpn*I was chosen for the *bca* fragment, while the SbtAB encoding fragment was flanked by *Kpn*I and *Sac*I restriction sites. All enzymes were purchased from Thermo Scientific (Fisher Scientific Germany GmbH, Schwerte, Germany) in the FastDigest® version. Samples containing the plasmid were additionally treated with the thermo-sensitive alkaline phosphatase FastAP (Fisher Scientific Germany GmbH, Schwerte, Germany) to prevent recirculation of the vector molecules. Reactions were performed at 37 °C for 30 min, followed by a purification step via agarose gel electrophoresis.

## 2. Materials and Methods

After purification, ligation was performed using T4 DNA ligase (Fisher Scientific Germany GmbH, Schwerte, Germany) in a total volume of 15 µl as recommended by the supplier. After inactivation for 10 min at 65 °C, the ligation mix was used for *E. coli* transformation.

### 2.2.3 Transformation of *E.coli* cells

Chemical-competent *E. coli* cells were prepared as described by Inoue *et al* (Inoue *et al.*, 1990). 100 µl cell suspension were transformed with approximately 5 µl ligation mix or 100 ng plasmid-DNA by incubation on ice for 30 min, followed by a heat shock at 42 °C for 45 s. Afterwards, cells were again incubated on ice for 2 min. 500 µl LB medium was added and the cell suspension was incubated for 30-60 min at 37 °C in 1.5 ml tubes at 500 rpm. Cells were then spread on LB-agar plates and incubated at 37 °C for about 16 h.

### 2.2.4 Isolation of plasmid DNA and sequence analysis

Plasmid-DNA was isolated from *E. coli* cells with the “Nucleo Spin® Plasmid” (Macherey-Nagel GmbH und Co. KG, Düren, Germany) or the “High Pure Plasmid Isolation Kit” (Roche Diagnostics Deutschland GmbH, Mannheim, Germany) according to manufacturers’ instructions.

Control sequencing of the isolated plasmids was performed by GATC Biotech AG (Konstanz, Germany).

### 2.2.5 Transformation of *C. glutamicum* cells

*C. glutamicum* cells were made electro-competent as described earlier (Liebl *et al.*, 1989). For transformation, approximately 300-500 ng plasmid-DNA were added to 50 µl cell suspension on ice. The transformation was performed with an electrical pulse of 2.5 kV, followed by immediate addition of 1 ml BHIS medium. After incubation for 1 h at 125 rpm and 30°C in a 15 ml tube, cells were spread on BHI-agar plates and further incubated at 30 °C. After about two days, the occurring colonies were isolated and the integrity of the inserted plasmids was checked via Colony-PCR.

## 2.3. Uptake measurements

### 2.3.1 Cultivation prior to uptake measurements

Wild type cells of *C. glutamicum* equipped with a pEKEx2 plasmid with and without SbtAB were cultivated overnight in BHI complex medium with 50 mg/l kanamycin and 0.1 mM IPTG. If the *C. glutamicum*  $\Delta bca$ +SbtAB strain was used, the overnight cultures were additionally supplied with 10 % CO<sub>2</sub>. Prior to conduction of a measurement cells were transferred into 25 ml CgXII minimal medium with 5.5 mM glucose, pH 8.5 at a starting OD of 1. Both *C. glutamicum* wild type and  $\Delta bca$ +SbtAB cultures were grown at atmospheric CO<sub>2</sub>. Uptake measurements were started when the cultures had reached an OD of about 5 in case of the wild type and 2 in case of the *C. glutamicum*  $\Delta bca$ +SbtAB strain.

### 2.3.2 Radiochemical detection of bicarbonate uptake

Uptake measurements with wild type cells were performed at 30 °C in a water bath using glass tubes and a magnetic stirrer, while *C. glutamicum*  $\Delta bca$ +SbtAB cells were incubated in 25 ml Erlenmeyer flasks on an agitator at 125 rpm and 30 °C. In the latter case, uptake was monitored during further growth. This growth of *C. glutamicum*  $\Delta bca$ +SbtAB at atmospheric CO<sub>2</sub> concentrations was used as an indicator for the functionality of SbtAB. Each 25 ml pre-culture was separated in two and one sample was treated with 50 µM CCCP to uncouple any membrane potential and thereby serve as a negative control for bicarbonate uptake. All cultures were spiked with 100 µM <sup>14</sup>C labelled bicarbonate (NaH<sup>14</sup>CO<sub>3</sub>). At defined time points, 500 µl of the culture were filtered via a glass fibre filter (Merck Millipore, Billerica, MA, USA) followed by an immediate washing step using 2 x 2.5 ml CgXII medium pH 8.5. The filter was placed in a tube containing 3.8 ml scintillation cocktail which had been alkalisied by addition of 50 µl/3.8 ml 10 M NaOH. The use of alkaline pH values throughout the experiment was essential to prevent bicarbonate loss by CO<sub>2</sub> formation. After incubation for at least three hours to avoid quenching effects by un-dissolved filter residues, the samples were analysed in the scintillation counter LS 6500 (Beckman Coulter Inc., Brea, CA, USA). The bicarbonate uptake at each defined time point was calculated using the following equation:

## 2. Materials and Methods

$$\text{uptake [nmol HCO}_3^-/\text{mgDW]} = (\text{cpm}(\text{cell}_{(t_x)}) * n \text{ HCO}_3^- \text{ [nmol]}) / (\text{cpm}(\text{TC}_{(t_0)}) * \text{OD} * V_{\text{sample}}[\text{ml}] * 0,36 \text{mg/ml})$$

DW: dry weight, Cpm: counts per minute, TC: total counts in the sample, OD: optical density, t: time

The uptake rate  $v$  was determined by extrapolation of the resulting graph.

### 2.4. Determination of the intracellular pH

In order to measure the intracellular pH of *C. glutamicum*, the pH sensitive GFP derivate pHluorin (Miesenböck *et al.*, 1998) was used. Prior to each measurement, 10 ml pre-culture were washed and transferred into 50 ml CgXII minimal medium supplemented with 5.5 mM glucose at pH 7.4 without MOPS buffer. Selection of plasmid carrying cells was ensured with 50 mg/l kanamycin. Expression of the pHluorin-containing pEKEx2 plasmids was performed using 0.1 mM IPTG. After cultivation for about three hours, the cells had reached an OD between 5 and 7. This value was chosen since it corresponds to sufficient amounts of pHluorin in the culture to ensure precise detection. In case of the DOOR mutant, 50 ml pre-cultures were washed and transferred into 50 ml CgXII minimal medium three hours prior to the experiment, since growth of the mutant on minimal medium was rather poor.

The intracellular pH of the whole culture was determined with the Aminco Bowmann® Series 2 Luminescence Spectrometer (SLM Instruments, Urbana, IL, USA) by monitoring excitation scans from 350 nm to 480 nm with a scan rate of 8 nm/s. This rate corresponds to a time of 17 s per spectrum. pHluorin possesses two excitation maxima at 396 nm and 468 nm and the ratio 396 nm/468 nm is pH dependent. The chosen emission wavelength was 505 nm and the intracellular pH was calculated based on a calibration curve. This curve was determined using cultures of pHluorin expressing *C. glutamicum* cells that were treated with 0.25 % CTAB to equalise the inner and outer pH by uncoupling of the membrane potential. The signal strength is represented in the measuring voltage applied for signal amplification. Since this parameter interferes with

## 2. Materials and Methods

the accuracy of the calculated pH values, an additional correction factor was implicated as well. Usually, a voltage below 800 V was ensured to gain reproducible raw data.

Prior to measurement, the 50 ml cultures were transferred into a 100 ml custom made small bioreactor. The vessel was equipped with inlets for acid and base as well as aeration, and a pH electrode. The temperature was kept at 30 °C with a water jacket. Cells were lead through a sample loop including a half-micro flow-through quartz glass cuvette (Starna GmbH, Pfungstadt, Germany), which was placed in the spectrometer for fluorescence detection. The remaining time in the loop was 21 s, corresponding to a flow rate of 18 ml/min.

To shift and regulate the external pH, 1 M  $\text{KH}_2\text{PO}_4$  and 1 M  $\text{K}_2\text{HPO}_4$  were used. Controlling and monitoring of the external pH was performed using a regulation program written by Arthur Reuter from the in-house electronics department. The aeration unit was equipped with a two-way mixing system for ambient air and  $\text{CO}_2$ , so various  $\text{CO}_2$  concentrations could be applied. Optimal mixing and aeration were ensured by a magnet stirrer and a glass frit at the end of the air pipe. Figure 2.2 shows a sketch of the experimental setup.

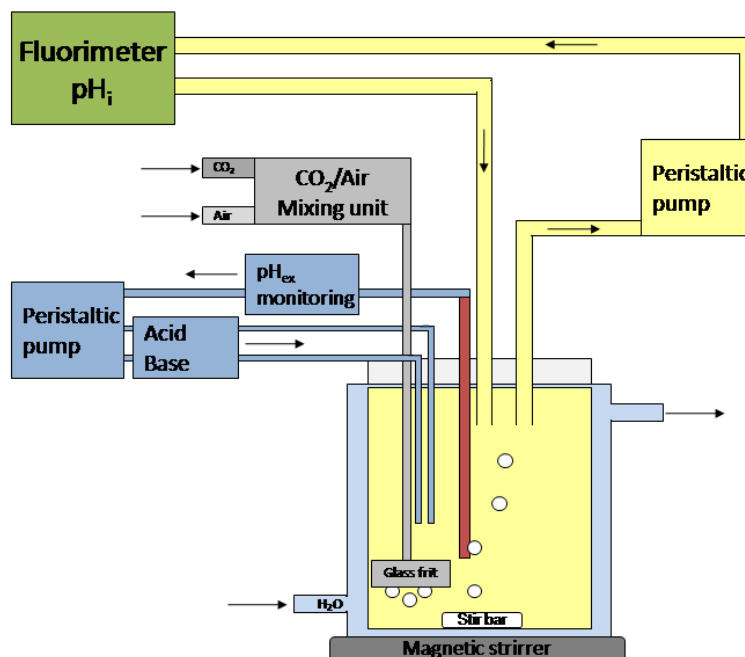


**Figure 2.2: Setup for  $\text{pH}_i$  measurements.** The culture is kept in a small bioreactor equipped with aeration, pH control, mixing unit and a water jacket. It enables a constant flow through the sample loop for pHluorin fluorescence detection.

The duration of a pH homeostasis measurement was usually 30-40 min. For the first 10 minutes, a stable pH of 7.4 was adjusted before a rapid shift towards an acidic or alkaline pH was performed. After the pH shift, the culture was further monitored for 15-20 min. The raw data gained from these measurements consist of a number of excitation spectra monitored over time. From each spectrum, the 396 nm and 468 nm intensity values were used to calculate the ratio which then was used to derive the according pH from the calibration curve. Hence, one pH value was monitored every 17 s.

### **2.5. Protein biochemistry techniques**

#### **2.5.1. Gene expression for protein synthesis and cell disruption**

To induce overproduction of proteins in *C. glutamicum*, cells were grown in 50 ml BHI complex medium spiked with 50 mg/l kanamycin and 0.1 mM IPTG for about 16 hours. After centrifugation, the cell pellet was resuspended in 2 ml buffer containing 50 mM Tris\*HCl pH 7.4 and 100 mM NaCl. Also, the protease inhibitor “Roche cOmplete Mini, EDTA-free” (Roche Diagnostics Deutschland GmbH, Mannheim, Germany) was added according to manufacturer’s instructions.

Cell disruption was performed with 600 µl of the sample in 1.5 ml screw cap vials with 400 µl glass beads using the homogeniser FastPrep™ (Thermo Scientific, Fisher Scientific Germany GmbH, Schwerte, Germany) at maximum speed for 3 x 45 s. In between the homogenisation steps, cells were chilled on ice for 5 min. To gain crude extracts of the cytoplasm, the samples were centrifuged at 14,000 rpm and 4 °C for 30 min. Further centrifugation of the crude extract in the Optima™ TLX Ultracentrifuge (Beckman Coulter Inc., Brea, CA, USA) at 4 °C and 80,000 rpm in the TLA 120.2 rotor for 20 min was performed to isolate the membrane fraction if desired.

#### **2.5.2 SDS-Polyacrylamide gel electrophoresis (SDS-PAGE)**

Prior to gel electrophoresis, the protein concentration of the samples was determined. For crude extracts, the Bradford method (Bradford, 1976) was applied using the “Roti NanoQuant®” reagent (Carl Roth GmbH & Co. KG, Karlsruhe). For samples containing the isolated membrane fraction, the amino-black-staining (Schaffner & Weissmann, 1973)

## 2. Materials and Methods

was used. In both cases, calibration curves were determined using dilutions of Bovine Serum Albumine (BSA).

The denaturing gel electrophoresis was performed based on the protocol described earlier (Laemmli, 1970) with a separation gel matrix containing 12 % acrylamide. The protein amount per sample was about 20-30 µg. Prior to the analysis, samples were mixed with 4x loading buffer (20 % glycerol, 8 % SDS, 400 mM Tris\*HCl pH 6.8, 10 mM EDTA, 100 µM β-mercapto-ethanol, bromo-phenol-blue) and incubated for 5 min at 95 °C. Each gel was prepared in two replicates. After electrophoresis at 175 V, one gel was stained with Coomassie brilliant blue dye for protein visualisation (Sambrook, 1989), while the second one was used for immuno-blotting (Towbin *et al.*, 1979) via Western Blot analysis.

### 2.5.3 Western blot analysis

Transfer of proteins from the gel matrix to a PVDF membrane (Immobilon P 0.45 µm, Merck Millipore, Billerica, MA, USA) was conducted using the semi-dry blot method (Kyhse-Andersen, 1984) at 12 V (~ 70 mA) for 45 minutes. Afterwards, for blocking of free binding sites, the membrane was incubated in 3 % milk powder diluted in TBS buffer (50 mM Tris\*HCl pH 7.4, 0.9 % NaCl). The same milk powder-buffer was used for incubation with the mouse-anti-streptag<sup>®</sup> antibody (StrepMAB-Classic, Iba GmbH, Göttingen, Germany; dilution of the antibody 1:10,000) for the detection of the Strep-tagged proteins. After three washing steps with TBS buffer, incubation with the secondary antibody (1:10,000 goat-anti-mouse with alkaline phosphatase conjugation, Sigma-Aldrich, St. Louis, MO, USA) was performed. Both antibodies were incubated for 1 h at room temperature. Visualisation of tagged proteins was based on the reaction of BCIP with NBT, catalysed by the alkaline phosphatase which results in staining of the according bands (McGadey, 1970).

## 2.6 Analytical methods

### 2.6.1 Lysine detection via HPLC analysis

The lysine concentration in the medium supernatant was analysed with the EliteLaChrom System from VWR/Hitachi in combination with the pump system L-2130, the column thermostat 2300 and the fluorescence detector L-2485.

Samples were derivatised using OPA reagent (o-phthaldialdehyde/borate/2-mercaptoethanol, Thermo Scientific, Fisher Scientific Germany GmbH, Schwerte, Germany) and the resulting fluorescence was detected using an excitation wavelength of 230 nm and an emission wavelength of 450 nm. As reversed-phase pre-column, the Multospher 4x40 mm (CS Chromatographie-Service GmbH, Langerwehe, Germany) was used. The reversed-phase main column was the NucleoDur® RP18 125x4 mm model (Macherey-Nagel GmbH & Co. KG, Düren, Germany). Elution was performed using a gradient of buffers A (40 mM sodium acetate, 0.06 % sodium azide, 5 % (v/v) methanol/acetonitrile 1:1) and B (50 % acetonitrile, 50 % methanol). Lysine concentrations used for calibration were 10 µM, 50 µM, 100 µM and 250 µM. The peak areas representing the amount of lysine were calculated with the applied HPLC-software.

### 2.6.2 Determination of osmolality

The osmolality of aqueous solutions was measured with the osmometer “Osmomat 030” (Gonotec GmbH, Berlin, Germany). Calibration solutions of 0.1-1.2 osmol/kg were used and samples were analysed as recommended by the manufacturer.

## 3. Results

### 3.1. The carbonic anhydrase Bca is essential in *C. glutamicum*

#### 3.1.1 *C. glutamicum* $\Delta bca$ is not able to grow at atmospheric CO<sub>2</sub>

Basic to the investigations towards the influence of the  $\beta$ -type carbonic anhydrase Bca was confirmation of the *C. glutamicum*  $\Delta bca$  growth phenotype (Mitsuhashi *et al.*, 2004) also in the *C. glutamicum*  $\Delta bca$  Kyowa Hakko strain. For this purpose, the deletion mutant was compared to the *C. glutamicum* ATCC 13032 wild type strain at various CO<sub>2</sub> concentrations on solid BHI medium. The results displayed in Figure 3.1 confirm the growth phenotype. At atmospheric 0.04 % CO<sub>2</sub>, the *C. glutamicum*  $\Delta bca$  strain is not able to grow. As displayed in Figure 3.1, this growth deficit can be overcome by elevated CO<sub>2</sub> levels in the supply air.

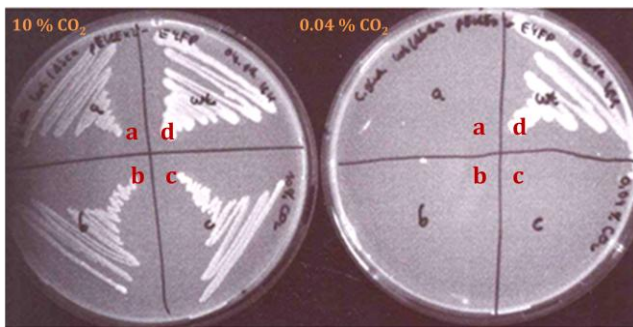


**Figure 3.1: Growth of *C. glutamicum* wild type and  $\Delta bca$  on solid BHI complex medium.** Since both strains were equipped with a pEKEx2\_EYFP plasmid, 50  $\mu$ g/ml kanamycin were added to the medium for selection. Displayed is the growth at 30 °C after 16 h incubation at 10 % CO<sub>2</sub> (left) and 0.04 % CO<sub>2</sub> (right). (a), (b), (c): three replicates of the *C. glutamicum*  $\Delta bca$  strain, (d): *C. glutamicum* wild type.

Based on these findings, a possible pH dependency of the growth deficit was investigated. This experiment was performed on solid medium, too. In this case, CgXII minimal medium of pH values from 5.5 up to 8 was used and cells were treated with CO<sub>2</sub> concentrations of 5, 10 and 20 % in the supply air. 2  $\mu$ l of cells of various densities in 0.9 % NaCl were applied. The chosen ODs were 10<sup>-1</sup>, 10<sup>-2</sup>, 10<sup>-3</sup> and 10<sup>-4</sup> for each strain and condition. Here, the *C. glutamicum*  $\Delta gca$  strain was examined as well to confirm the wild type-like growth behaviour that has been described earlier (Mitsuhashi *et al.*, 2004). The results are displayed in Figure 3.2. Indeed, *C. glutamicum* wild type and  $\Delta gca$  grew equally well at all conditions tested. However, the *C. glutamicum*  $\Delta bca$  strain

### 3. Results

showed pH dependent growth behaviour at 5 % CO<sub>2</sub>. At pH 5.5 and 6, no growth was observed and also growth at pH 7 was not as efficient as it was at pH 8. This observation was not made at 10 or 20 % CO<sub>2</sub> in the supply air. Here, the *C. glutamicum*  $\Delta bca$  strain grew at every pH value.

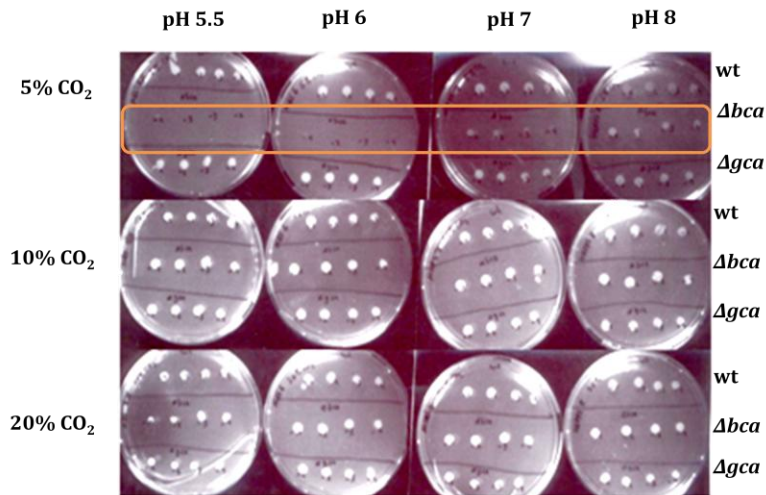


**Figure 3.2: Growth of *C. glutamicum* wild type,  $\Delta bca$  and  $\Delta gca$  at various CO<sub>2</sub> concentrations and pH values.** Each row of cell dots consists of 2  $\mu$ l cell suspensions with an OD of 10<sup>-1</sup> to 10<sup>-4</sup> from left to right. As solid medium, CgXII with 1 % glucose and 50  $\mu$ g/ml kanamycin was used, since all strains were harbouring the pEKEx2\_EYFP plasmid. Cells were incubated for 16 h at 30 °C. The relevant phenotype of *C. glutamicum*  $\Delta bca$  is highlighted with an orange frame.

This result not only confirms the *C. glutamicum*  $\Delta bca$  and  $\Delta gca$  phenotypes described earlier (Mitsuhashi *et al.*, 2004). It also shows a pH dependency for complementation of the *C. glutamicum*  $\Delta bca$  mutant with elevated CO<sub>2</sub> concentrations. This is a hint towards the close connection between inorganic carbon provision and the pH of the medium.

#### 3.1.2 The *C. glutamicum* $\Delta bca$ phenotype is caused by the lack of Bca

To ensure that the phenotypical characteristics of *C. glutamicum*  $\Delta bca$  are actually caused by deletion of the *bca* gene, a complementation mutant was constructed. *C. glutamicum*  $\Delta bca$  pEKEx2\_EYFP\_Bca was expected to show plasmid mediated *bca* expression. Western Blot analysis actually revealed the presence of Strep-tagged Bca protein (Figure 3.3). The construct of the Bca protein with a C-terminal Strep-tag is supposed to have a size of 26.55 kDa, which could be confirmed in the Western Blot analysis.

### 3. Results

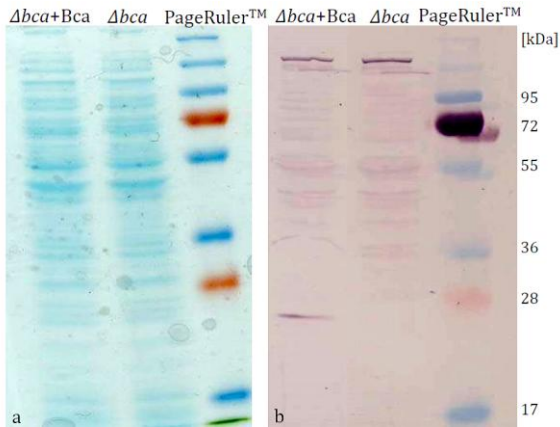


**Figure 3.3: Coomassie stained SDS-PAGE-gel (a) and Western Blot analysis (b) of Bca in *C. glutamicum*  $\Delta bca$ .**  $\Delta bca+Bca$ : *C. glutamicum*  $\Delta bca$  harbouring the pEKEx2\_EYFP\_Bca plasmid,  $\Delta bca$ : *C. glutamicum*  $\Delta bca$  harbouring the pEKEx2-EYFP plasmid as a negative control. About 12  $\mu$ g of protein were used in each analysis. Detection was performed using a mouse-anti-streptag<sup>®</sup> antibody.

Growth experiments on solid and liquid CgXII minimal medium were conducted to display a successful complementation on a physiological scale. The test on solid medium was performed at various pH values. Plasmid mediated expression of the *bca* gene can restore growth of the *C. glutamicum*  $\Delta bca$  strain at atmospheric CO<sub>2</sub> concentrations over a pH range from 5.5 to 8 (Figure 3.4). This is a clear hint that the *C. glutamicum*  $\Delta bca$  growth phenotype is due to the absence of Bca activity.

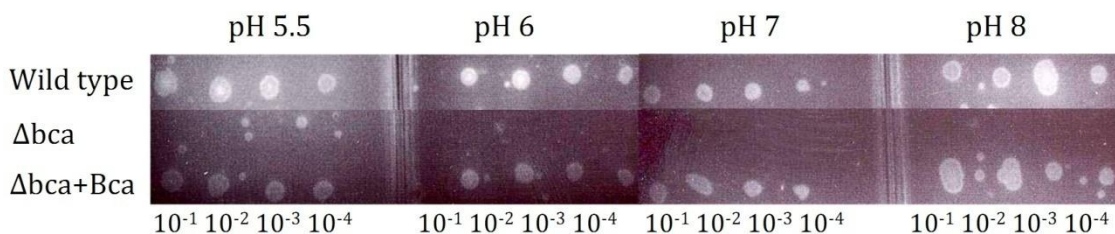


**Figure 3.4: Complementation of the *C. glutamicum*  $\Delta bca$  mutant via *bca* expression.** 2  $\mu$ l of cell suspension with dilutions from OD 10<sup>-1</sup> to OD 10<sup>-4</sup> were applied on solid CgXII medium with 1 % glucose, 50  $\mu$ g/ml kanamycin and 0.1 mM IPTG with pH values from 5.5 to 8. *C. glutamicum* wild type and  $\Delta bca$  were equipped with a pEKEx2\_EYFP plasmid. The complementation strain ( $\Delta bca+Bca$ ) was equipped with the pEKEx2\_EYFP\_Bca plasmid. Cells were incubated at atmospheric CO<sub>2</sub> concentrations and 30 °C for 16 hours.

The successful complementation of *C. glutamicum*  $\Delta bca$  could also be shown in liquid cultures. Figure 3.5 displays the kinetics of growth (Figure 3.5.a) and the resulting growth rates (Figure 3.5.b) at atmospheric CO<sub>2</sub> in CgXII liquid medium with 1 % glucose at a pH of 7.4. Clearly, *C. glutamicum* depends on inorganic carbon supply via Bca activity to be able to grow at atmospheric CO<sub>2</sub> levels.

### 3. Results

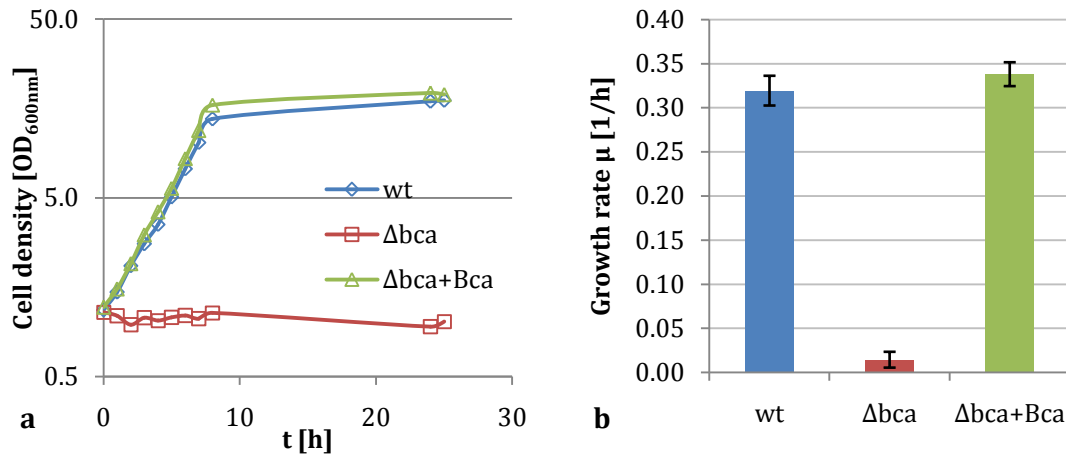


**Figure 3.5: Growth kinetics (a) and growth rates (b) of *C. glutamicum* wild type,  $\Delta bca$  and  $\Delta bca+Bca$  at atmospheric CO<sub>2</sub>.** Cells were cultivated in CgXII minimal medium with 1 % glucose, 50 μg/ml kanamycin and 0.1 mM IPTG at pH 7.4. wt: *C. glutamicum* wild type with the pEKEx2\_pHluorin plasmid,  $\Delta bca$ : *C. glutamicum*  $\Delta bca$  with the pEKEx2\_pHluorin plasmid,  $\Delta bca+Bca$ : *C. glutamicum*  $\Delta bca+Bca$  with the pEKEx2\_pHluorin\_Bca plasmid. The black error bars displayed in (b) represent the standard deviations of growth rates and are based on three independent replicates.

The results gained from the characterisation of the *C. glutamicum*  $\Delta bca$  strain underline the central role of the carbonic anhydrase in *C. glutamicum* and point out the importance of inorganic carbon provision even in this heterotrophic organism. Based on these findings, investigations towards possible growth benefits from overexpression of the *bca* gene came into focus.

#### 3.1.3 The impact of *bca* overexpression in wild type cells is negligible

To investigate possible benefits of *bca* overexpression in the *C. glutamicum* wild type strain, various stress conditions were chosen to examine the growth behaviour. First of all, various pH values of the medium were compared. The results are shown in Figure 3.6. It has to be noted that the differences observed between the two strains were not significant. Generally, growth kinetics at pH 7.4 strongly differed from those at pH 6 and 8.5, although the same final OD was reached (Figure 3.6.a). Also, the growth rates rather depend on the chosen pH value. While at a neutral pH the growth rate is about 0.3/h, it is only 0.2/h at pH 6 and hardly more than 0.1/h at pH 8.5 (Figure 3.6.b).

### 3. Results

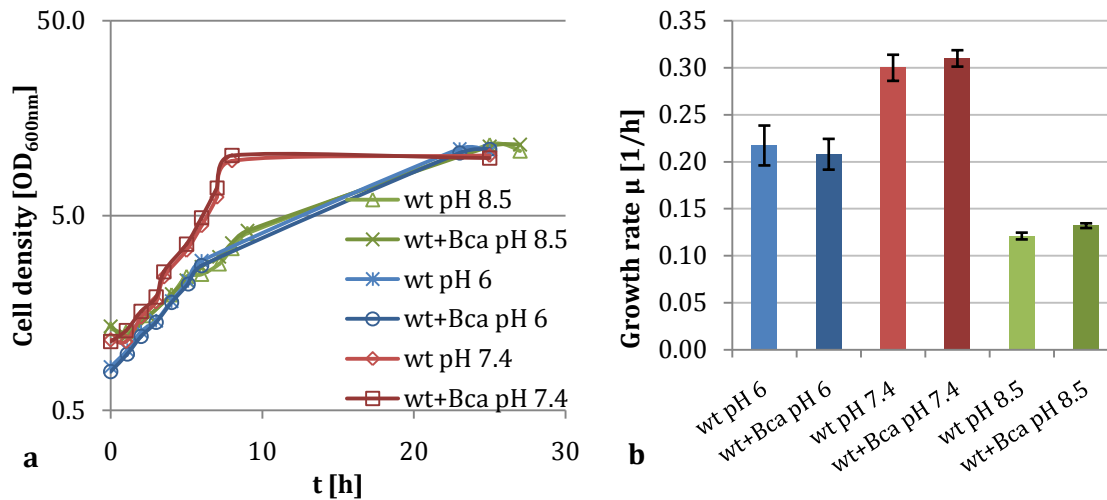


**Figure 3.6: Growth kinetics (a) and growth rates (b) of *C. glutamicum* wild type with and without *bca* overexpression at various pH values.** Cells were cultivated in CgXII minimal medium with 1 % glucose, 50  $\mu$ g/ml kanamycin and 0.1 mM IPTG at 30 °C. wt: *C. glutamicum* wild type with the pEKEx2\_pHluorin plasmid, wt+Bca: *C. glutamicum* wild type with the pEKEx2\_pHluorin\_Bca plasmid. The black error bars displayed in (b) represent the standard deviations of growth rates and are based on three independent replicates.

The results from the pH stress scenario led to the assumption that *bca* overexpression does not support a better pH homeostasis, since growth rates hardly differed at the same pH value. To further investigate the underlying physiological situation, crude extracts were compared towards their reaction upon acidification via CO<sub>2</sub> treatment. The results revealed a slight difference of the internal pH between the wild type and the overexpression mutant (Figure 3.7). If *bca* expression is elevated, the pH of the crude extract is about 6.9, while the wild type cytoplasm displays a pH of 7.1. When the crude extracts were treated with 100 % CO<sub>2</sub> at 30 °C, their pH values decreased to the same extent until a value of about 5.8 was reached. An acceleration of CO<sub>2</sub> derived acidification in the overexpression mutant caused by a more efficient CO<sub>2</sub> conversion was not observed.

### 3. Results

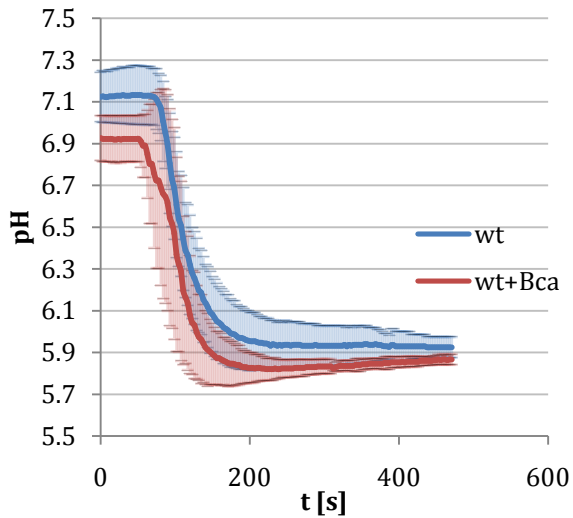


**Figure 3.7: pH of crude extracts from *C. glutamicum* with and without *bca* overexpression upon CO<sub>2</sub> mediated acidification.** Crude extracts were treated with 100 % CO<sub>2</sub> at 30 °C 60 s after start of the experiment, while the pH was monitored with a pH electrode. Wt: *C. glutamicum* wild type with a pEKEx2\_pHluorin plasmid; wt+Bca: *C. glutamicum* wild type with a pEKEx2\_pHluorin\_Bca plasmid for *bca* overexpression. The buffer for crude extract preparation consisted of 100 mM NaCl, 50 mM Tris pH 7.4.

This correlates with the insignificant differences between wild type and overexpression mutant illustrated in Figure 3.6. Apart from a possible influence on proton homeostasis, an elevated level of Bca in the cytoplasm caused by plasmid-mediated *bca* overexpression might also affect the availability of inorganic carbon. To test this hypothesis, two scenarios that possibly imply a strong need for inorganic carbon were investigated. First, growth at a relatively low cell density at the beginning of cultivation was determined. This setup was based on the assumption that in this case, CO<sub>2</sub> levels in the medium are rather low due to the fact that only few cells provide CO<sub>2</sub> by their metabolic activity. A higher level of Bca in the cell might compensate for this lack and thereby lead to a shorter lag-phase. As displayed in Figure 3.8, the *bca* overexpression mutant did not show different growth behaviour than the wild type of *C. glutamicum*. In both cases, a one hour lag-phase was observed. Growth at the beginning was generally slow, probably caused by low cell densities.

### 3. Results

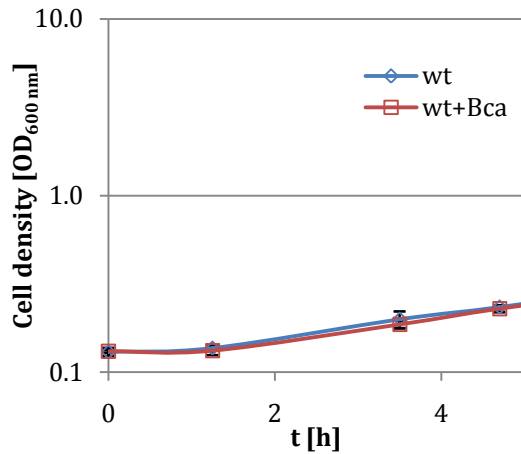


**Figure 3.8: Growth of *C. glutamicum* wild type with and without *bca* overexpression at a low starting OD.** Cells were cultivated in CgXII minimal medium with 1 % glucose, 50  $\mu\text{g/ml}$  kanamycin and 0.1 mM IPTG at pH 7.4. wt: *C. glutamicum* wild type harbouring the pEKEx2\_pHluorin plasmid; wt+Bca: *C. glutamicum* wild type harbouring the pEKEx2\_pHluorin\_Bca plasmid. The black error bars represent the standard deviations based on three independent replicates.

The second setup that was supposed to represent conditions of suboptimal inorganic carbon provision was growth on pyruvate as sole carbon source. Under such conditions, additional inorganic carbon is necessary for gluconeogenic processes. Hence, overexpression of *bca* was believed to ensure higher growth rates in the cultivation. As displayed in Figure 3.9, neither the final cell density (Figure 3.9.a) nor the growth rate (Figure 3.9.b) of the overexpression mutant differed from the *C. glutamicum* wild type.

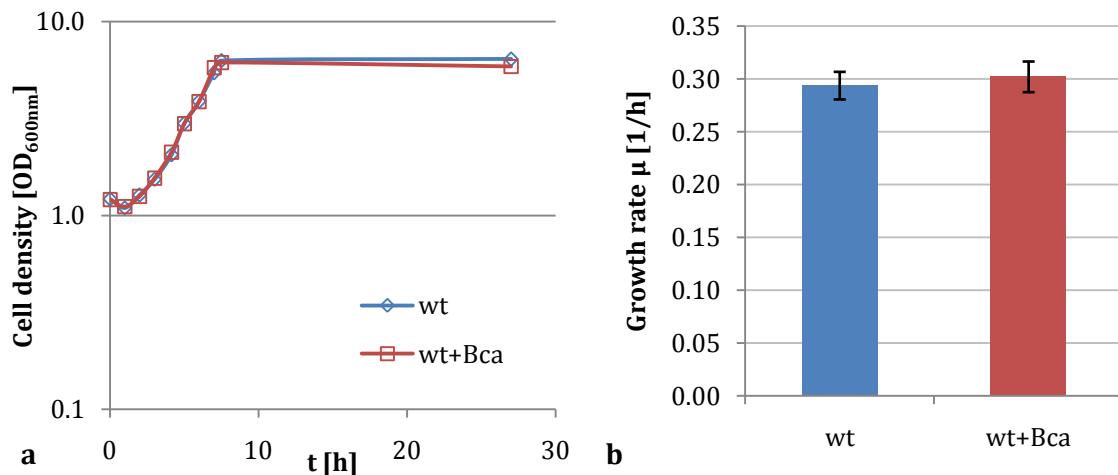


**Figure 3.9: Growth kinetics (a) and growth rates (b) of *C. glutamicum* wild type with and without *bca* overexpression on pyruvate as sole carbon source.** Cells were cultivated in CgXII minimal medium with 50 mM pyruvate, 50  $\mu\text{g/ml}$  kanamycin and 0.1 mM IPTG at pH 7.4. wt: *C. glutamicum* wild type harbouring the pEKEx2\_pHluorin plasmid; wt+Bca: *C. glutamicum* wild type harbouring the pEKEx2\_pHluorin\_Bca plasmid. The black error bars displayed in (b) represent the standard deviations of growth rates and are based on three independent replicates.

### 3. Results

It has to be noted that the initial decrease in cell density at the beginning of cultivation on pyruvate (Figure 3.9.a) has been observed repeatedly and seems to be a characteristic of the examined *C. glutamicum* strains on this substrate. Taken together, overexpression of the *bca* gene in *C. glutamicum* wild type cells does not seem to have influence on their growth behavior under various stress conditions like pH stress or a limitation of inorganic carbon supply.

## **3.2 Heterologous expression of a cyanobacterial bicarbonate importer in *C. glutamicum***

### **3.2.1 SbtAB can restore growth of the *C. glutamicum* $\Delta bca$ strain**

To ensure the functionality of the sodium/bicarbonate-symporter SbtA from *Synechocystis* sp. PCC 6803 in *C. glutamicum*, the predicted periplasmic protein SbtB was included in the cloning strategy for plasmid construction. This resulted in a construct consisting of the *slr1512-slr1513* gene region (encoding SbtA and SbtB, respectively) and a C-terminal Strep-tag encoding gene attached to *slr1513*. Hence, the transport system was named SbtAB. The resulting fusion protein of SbtB and the Strep-tag has a size of 13.2 kDa. Western Blot analysis based on detection of the Strep-tag revealed the presence of SbtB+Strep-tag in crude extracts of *C. glutamicum*  $\Delta bca$  harbouring the pEKEx2\_pHluorin\_SbtAB plasmid (Figure 3.10). However, it was difficult to actually show the presence of SbtB in the membrane fraction, so it is still not clear, whether SbtB is actually bound or attached to the membrane protein SbtA or not.

### 3. Results

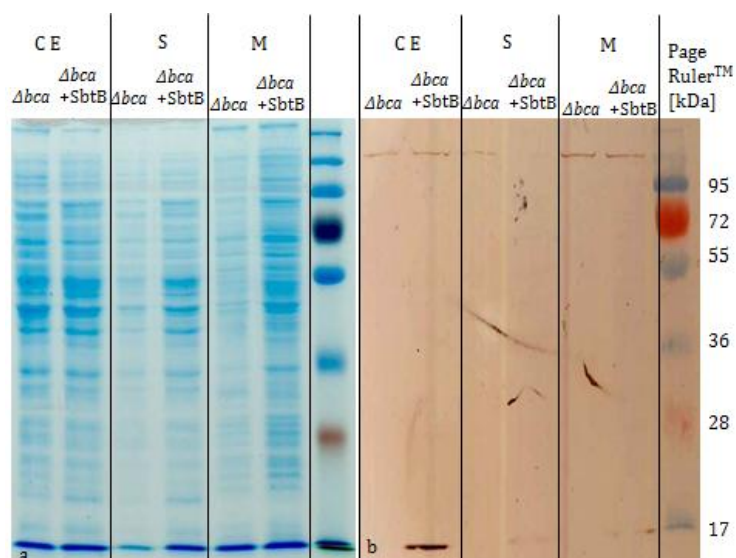


**Figure 3.10: Western Blot analysis to show synthesis of the cyanobacterial SbtB protein in *C. glutamicum*  $\Delta bca$ .** Part of the crude extract was separated into membrane fraction and supernatant. Displayed are (a) the Coomassie-stained PAGE-gel and (b) Western Blot analysis via Strep-tag antibody. CE: crude extract, S: supernatant from the membrane preparation procedure, M: membrane fraction; left lane  $\Delta bca$ : *C. glutamicum*  $\Delta bca$  equipped with the pEKEx2\_pHluorin plasmid; right lane  $\Delta bca$ +SbtB: *C. glutamicum*  $\Delta bca$  equipped with the pEKEx2\_pHluorin\_SbtAB plasmid, which allows immunochemical detection of the SbtB+Strep-tag fusion protein.

Another strong hint towards the successful heterologous expression of the cyanobacterial bicarbonate importer genes in *C. glutamicum* was given by the growth phenotype of *C. glutamicum*  $\Delta bca$  equipped with the pEKEx2\_pHluorin\_SbtAB plasmid. As displayed in Figure 3.11, expression of the SbtAB encoding genes restores growth of the mutant at atmospheric CO<sub>2</sub> in minimal medium. In CgXII medium with 1 % glucose and a pH of 7.4, *C. glutamicum*  $\Delta bca$  equipped with SbtAB grows to a final OD<sub>600nm</sub> of about 11 and shows a growth rate of 0.26/h similar to *C. glutamicum* wild type cells, which show a growth rate of 0.3/h under the same conditions (see Figure 3.6). This result is a strong hint towards the possibility that the cyanobacterial bicarbonate importer provides sufficient amounts of inorganic carbon, since even the lack of the essential Bca activity can be overcome by its presence in the *C. glutamicum*  $\Delta bca$  strain.

### 3. Results

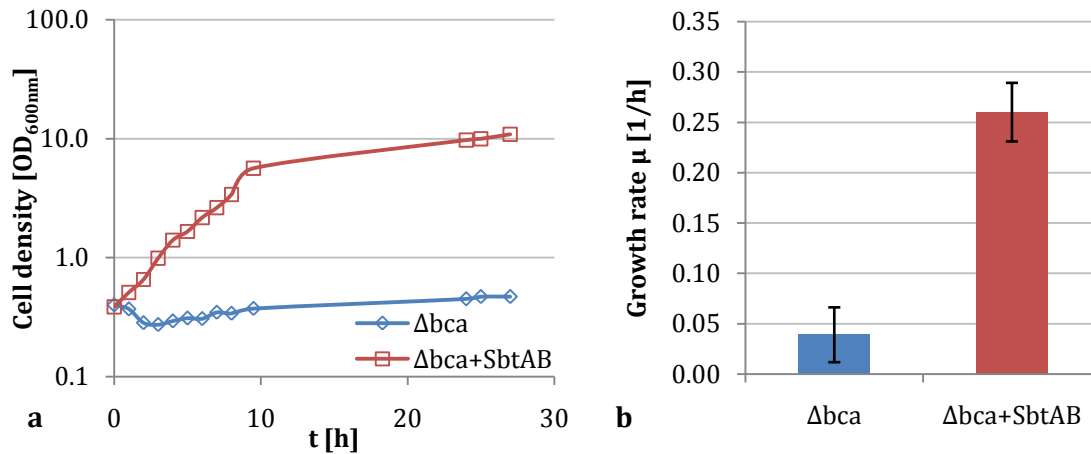


**Figure 3.11: Growth kinetics (a) and growth rates (b) of *C. glutamicum*  $\Delta bca$  with and without SbtAB at atmospheric CO<sub>2</sub>.** Cells were cultivated in CgXII minimal medium with 1 % glucose, 50  $\mu$ g/ml kanamycin and 0.1 mM IPTG at pH 7.4 and 0.04 % CO<sub>2</sub>.  $\Delta bca$ : *C. glutamicum*  $\Delta bca$  with the pEKEx2\_pHluorin plasmid,  $\Delta bca$ +SbtAB: *C. glutamicum*  $\Delta bca$  with the pEKEx2\_pHluorin\_SbtAB plasmid. The black error bars displayed in (b) represent the standard deviations of growth rates and are based on three independent replicates.

Based on these findings, pyruvate was tested as sole carbon source since it is believed to create a stronger need for inorganic carbon in anaplerotic reactions. *C. glutamicum* wild type,  $\Delta bca$  and  $\Delta bca$ +SbtAB were compared on solid minimal medium with either pyruvate or glucose as sole organic carbon sources at atmospheric (0.04 %) and elevated (10 %) CO<sub>2</sub>. To provide an additional inorganic carbon source, 0.5 mM bicarbonate (HCO<sub>3</sub><sup>-</sup>) was added. As illustrated in Figure 3.12, 10 % CO<sub>2</sub> in the supply air are not sufficient to ensure growth of *C. glutamicum*  $\Delta bca$  on pyruvate. This points towards an actual lack of inorganic carbon on this substrate, since growth at 10 % CO<sub>2</sub> was observed on glucose. While elevated CO<sub>2</sub> did not ensure growth of *C. glutamicum*  $\Delta bca$  on pyruvate, the SbtAB transport system actually did. In fact, growth of *C. glutamicum*  $\Delta bca$ +SbtAB was similar to the wild type. *C. glutamicum* wild type as well as *C. glutamicum*  $\Delta bca$ +SbtAB grew better on pyruvate if additional CO<sub>2</sub> was provided. Generally, better growth on glucose was observed. Here again, cells grew slightly better at elevated CO<sub>2</sub>. As expected, growth of *C. glutamicum*  $\Delta bca$  was not possible at atmospheric CO<sub>2</sub>, but could be restored on glucose by 10 % CO<sub>2</sub>. Taken together, *C. glutamicum*  $\Delta bca$ +SbtAB was able to grow on both substrates and at both CO<sub>2</sub> concentrations. On pyruvate, SbtAB activity was the only way to restore growth of the *C. glutamicum*  $\Delta bca$  mutant. These results underline the potential of SbtAB for inorganic carbon provision in *C. glutamicum*.

### 3. Results

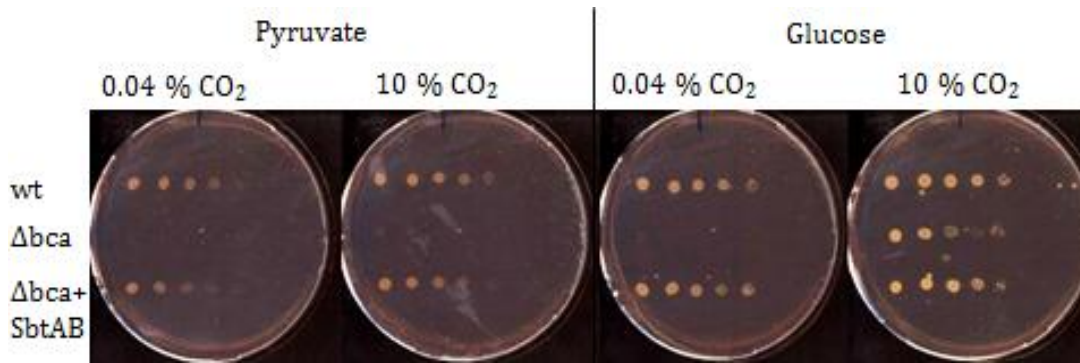


**Figure 3.12: Growth of *C. glutamicum* wild type,  $\Delta bca$  and  $\Delta bca+SbtAB$  on glucose and pyruvate at various  $CO_2$  concentrations.** 2  $\mu$ l of cell suspensions of  $OD_{600\text{ nm}}$  1,  $10^{-1}$ ,  $10^{-2}$ ,  $10^{-3}$ ,  $10^{-4}$  and  $10^{-5}$  from left to right were applied on solid CgXII minimal medium with 0.5 mM  $HCO_3^-$  and either 50 mM pyruvate or 5.5 mM glucose at pH 8.5. 50  $\mu$ g/ml kanamycin and 0.2 mM IPTG were added. Growth was observed at 30 °C for 40 hours. Wt: *C. glutamicum* wild type with pEKEx2\_EYFP;  $\Delta bca$ : *C. glutamicum*  $\Delta bca$  with pEKEx2\_EYFP;  $\Delta bca+SbtAB$ : *C. glutamicum*  $\Delta bca$  with pEKEx2\_EYFP\_SbtAB.

The next step to investigate the potential of SbtAB for carbon provision in *C. glutamicum* was to confirm the results displayed in Figure 3.12 in liquid culture. Figure 3.13 shows growth of *C. glutamicum*  $\Delta bca+SbtAB$  on pyruvate as sole carbon source at various  $CO_2$  concentrations and a pH of 7.4. Similar to growth on solid medium, cells grew almost equal to a final  $OD_{600\text{ nm}}$  3 and 4.2 at 0.04 %  $CO_2$  and 10 %  $CO_2$ , respectively (Figure 3.13.a). Also, the growth rate was about 0.09/h in both cases (Figure 3.13.b). Although this growth rate is lower than observed for the wild type on pyruvate (see Figure 3.9), it has to be noted that pyruvate as sole carbon source is sufficient to ensure SbtAB mediated growth of *C. glutamicum*  $\Delta bca+SbtAB$  in liquid culture.

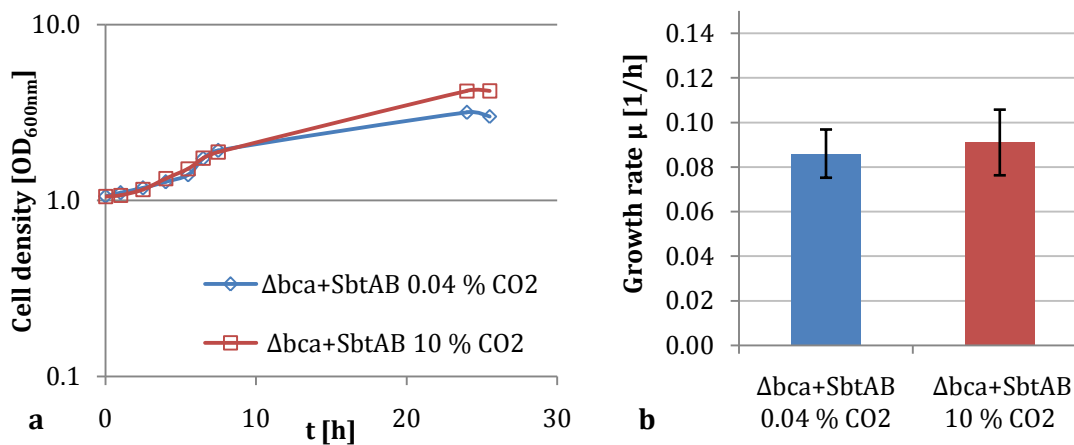


**Figure 3.13: Growth kinetics (a) and growth rates (b) of *C. glutamicum*  $\Delta bca+SbtAB$  on pyruvate at various  $CO_2$  concentrations.** Cells were cultivated in CgXII minimal medium with 1 % glucose, 50  $\mu$ g/ml kanamycin and 0.1 mM IPTG at pH 7.4.  $\Delta bca+SbtAB$ : *C. glutamicum*  $\Delta bca$  with pEKEx2\_pHluorin\_SbtAB. The black error bars displayed in (b) represent the standard deviations of growth rates and are based on three independent replicates.

### 3. Results

A completely different picture emerged when the same conditions were tested on the *C. glutamicum Δbca* strain without SbtAB. Figure 3.14 illustrates the results of growth experiments with the mutant on glucose and pyruvate both at atmospheric and elevated CO<sub>2</sub> concentrations. Surprisingly, growth on pyruvate was observed after 24 hours whether additional CO<sub>2</sub> was provided or not (Figure 3.14.a). Also, restoration of growth on glucose and 10 % CO<sub>2</sub> was rather poor and cells reached only an average growth rate of 0.025/h compared to 0.003/h at atmospheric CO<sub>2</sub>. The growth rate on pyruvate was 0.006/h at atmospheric CO<sub>2</sub> and 0.149/h at 10 % CO<sub>2</sub> (Figure 3.14.b).

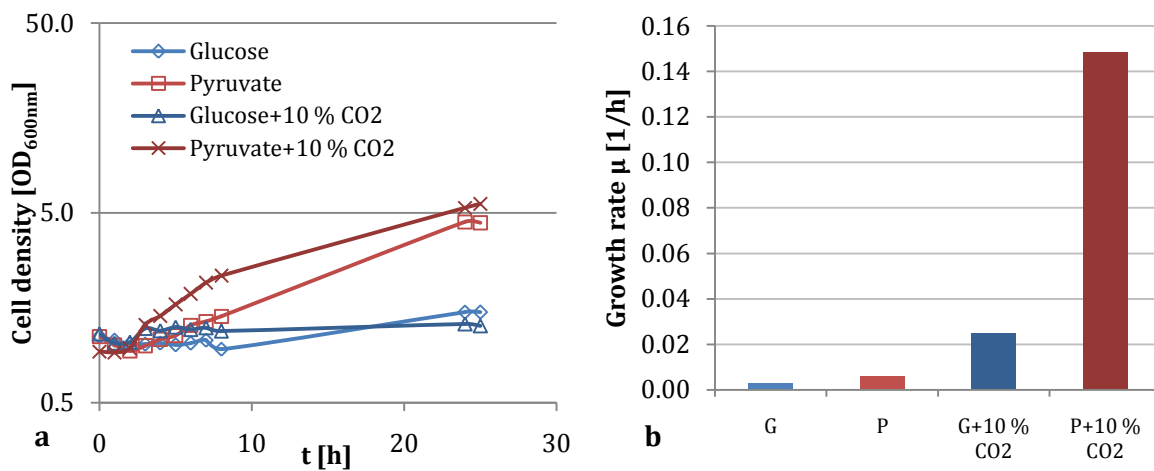


**Figure 3.14: Growth kinetics (a) and growth rates (b) of *C. glutamicum Δbca* on pyruvate and glucose at various CO<sub>2</sub> concentrations.** Cells were cultivated in CgXII minimal medium with 50 μg/ml kanamycin, 0.1 mM IPTG and either 5.5 mM (1 %) glucose or 50 mM pyruvate at pH 7.4. The values displayed represent the mean values of two independent measurements. Δbca: *C. glutamicum Δbca* with pEKEx2\_pHluorin; G: glucose, P: pyruvate.

These findings for *C. glutamicum Δbca* are in strong contradiction to the assumption that pyruvate as sole carbon source creates a stronger need for inorganic carbon in the cells. However, this growth pattern emerged repeatedly and it cannot be ruled out that there is an alteration in glucose uptake in the *C. glutamicum Δbca* strain, although this observation was not confirmed on solid medium (see Figure 3.12). To check whether the growth deficit of *C. glutamicum Δbca* at elevated CO<sub>2</sub> in minimal medium is specific to the substrate glucose, maltose was tested as an alternative substrate. As displayed in Figure 3.15, cells grew neither on glucose nor on maltose, while the *C. glutamicum* wild type control grew on both substrates. Hence, pyruvate is actually the only carbon source that ensures growth of *C. glutamicum Δbca* in liquid culture with 10 % CO<sub>2</sub>.

### 3. Results

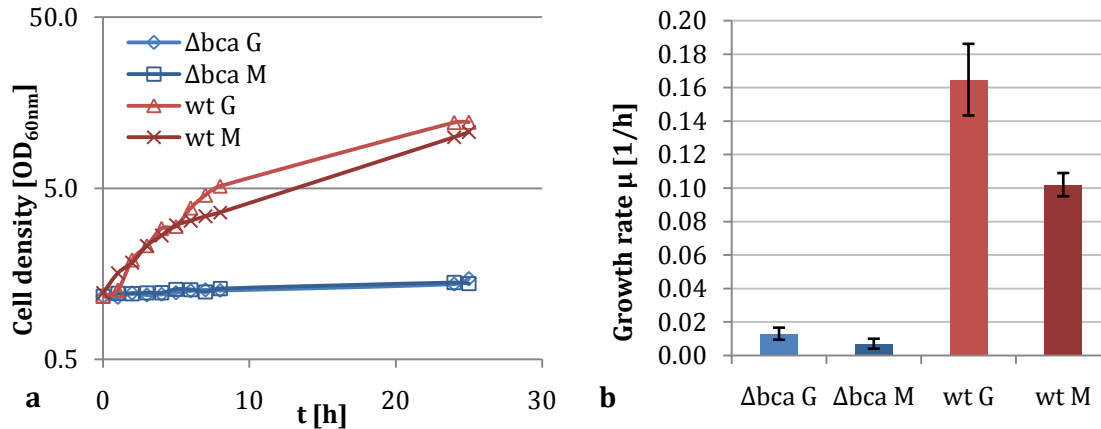


**Figure 3.15: Growth kinetics (a) and growth rates (b) of *C. glutamicum*  $\Delta bca$  and wild type on glucose and maltose at 10 % CO<sub>2</sub>.** Cells were cultivated in CgXII minimal medium with 50  $\mu$ g/ml kanamycin, 0.1 mM IPTG and either 1 % glucose or 1 % maltose at pH 7.4. The black error bars displayed in (b) represent the standard deviations of growth rates and are based on three independent replicates.  $\Delta bca$ : *C. glutamicum*  $\Delta bca$  with pEKEx2\_pHluorin; wt: *C. glutamicum* wild type with pEKEx2\_pHluorin G: glucose, M: maltose.

Despite the inconclusive results displayed in Figures 3.14 and 3.15, investigations towards the influence of SbtAB on *C. glutamicum*  $\Delta bca$  showed the positive impact of the cyanobacterial bicarbonate importer on inorganic carbon provision. Based on these promising observations, possible benefits by SbtAB were explored for the *C. glutamicum* wild type strain.

#### 3.2.2 SbtAB has only slight impact on *C. glutamicum* wild type cells

The close connection between the extracellular pH and the supply with inorganic carbon became obvious during the experiments towards Bca activity in *C. glutamicum* (see Figures 3.2 and 3.6). Hence, the import of bicarbonate could also be influenced by the external pH value. Also, additionally imported bicarbonate might have an impact not only on carbon provision but also on the intracellular pH value. Therefore, impact of the bicarbonate import system SbtAB on growth of *C. glutamicum* wild type cells was examined at various pH values (Figure 3.16). Even in wild type cells, the influence of SbtAB led to enhanced growth rates (Figure 3.16.b). This effect was observed independent from the external pH value. However, final OD values were not influenced by SbtAB activity. Also, growth behaviour at pH 8 was slightly different from those at pH 6 and 7 (Figure 3.16.a).

### 3. Results

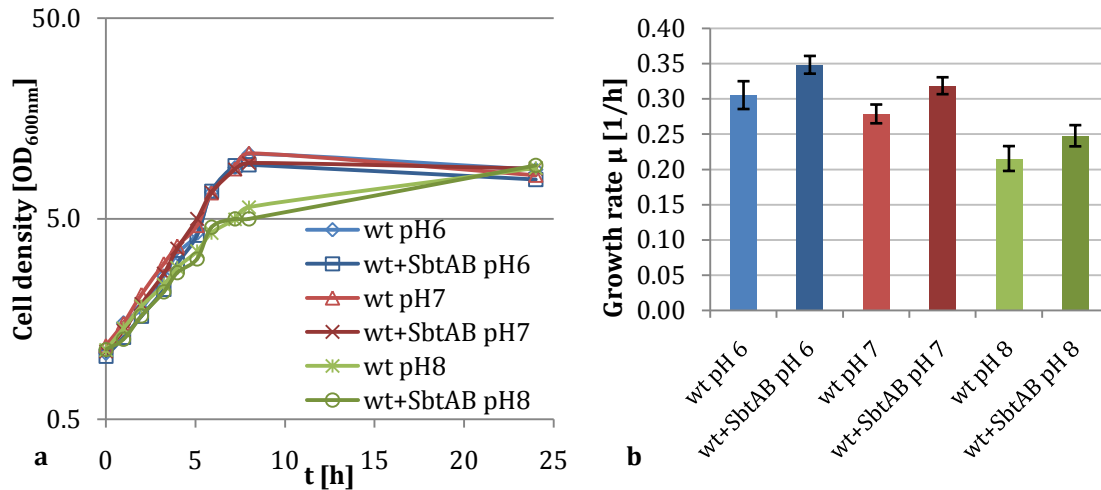


**Figure 3.16: Growth kinetics (a) and growth rates (b) of *C. glutamicum* wild type with and without SbtAB at various pH values.** Cells were cultivated in CgXII minimal medium with 1 % glucose, 50  $\mu\text{g/ml}$  kanamycin and 0.2mM IPTG at various pH values. Wt: *C. glutamicum* wild type harbouring the pEKEx2\_EYFP plasmid, wt+SbtAB: *C. glutamicum* wild type harbouring the pEKEx2\_EYFP\_SbtAB plasmid. The black error bars displayed in (b) represent the standard deviations based on three independent replicates.

To check whether the expression level might be a limiting factor to display the influence of SbtAB, two different concentrations of the inducer IPTG were compared. As illustrated in Figure 3.17, an elevated IPTG concentration of 1mM has no relevant effects on growth of *C. glutamicum* wild type+SbtAB.

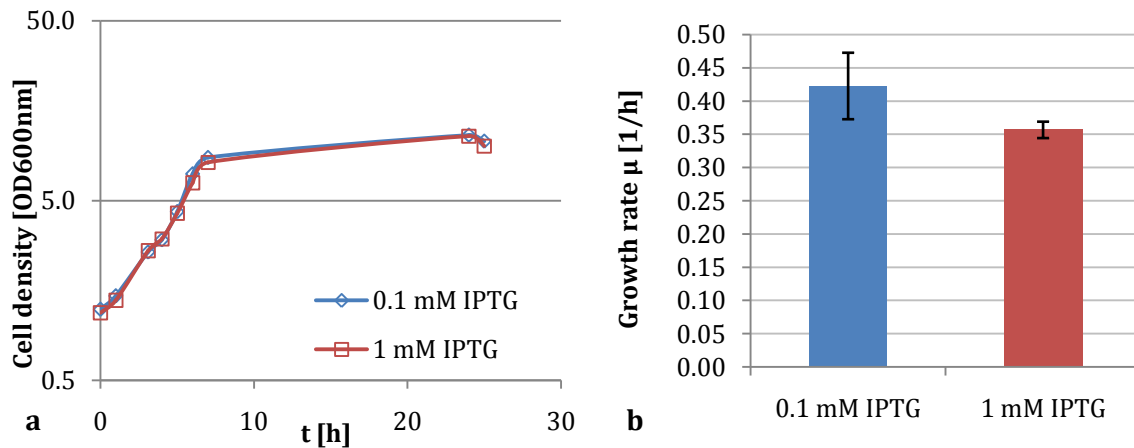


**Figure 3.17: Growth kinetics (a) and growth rates (b) of *C. glutamicum* wild type with SbtAB at various IPTG concentrations.** Cells were cultivated in CgXII minimal medium with 1 % glucose, 50  $\mu\text{g/ml}$  kanamycin and either 0.1 mM or 1 mM IPTG at pH 7.4. The *C. glutamicum* wild type cells were equipped with the pEKEx2\_pFluorin\_SbtAB plasmid. The black error bars displayed in (b) represent the standard deviations based on three independent replicates.

Based on the results illustrated in Figure 3.12, the influence of SbtAB on growth with pyruvate as organic carbon source was also tested for *C. glutamicum* wild type cells. As

### 3. Results

displayed in Figure 3.18, a remarkable growth advantage by SbtAB was observed on solid CgXII minimal medium at atmospheric CO<sub>2</sub>.

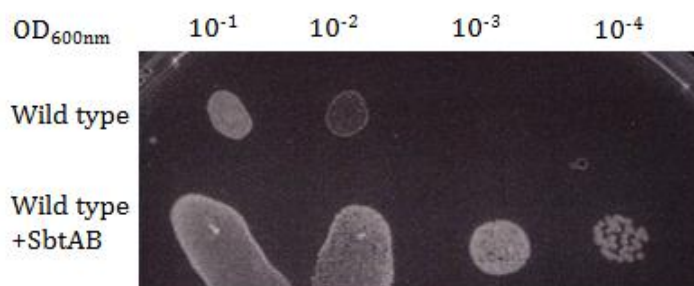


**Figure 3.18: Growth of *C. glutamicum* wild type with and without SbtAB on pyruvate.** 2  $\mu$ l of cell suspensions with ODs from  $10^{-1}$  to  $10^{-4}$  were applied on solid CgXII minimal medium with 50 mM pyruvate, 0.5 mM bicarbonate, 50  $\mu$ g/ml kanamycin and 0.2 mM IPTG at pH 8.5. The plates were incubated at 30 °C and atmospheric CO<sub>2</sub> for 54 hours. Wild type: *C. glutamicum* wild type with the pEKEx2\_ pHluorin plasmid; Wild type+SbtAB: *C. glutamicum* wild type with the pEKEx2\_ pHluorin\_SbtAB plasmid.

Although Figure 3.18 displays growth after 54 hours, it has to be noted that the positive effect of SbtAB on growth was observed right from the beginning of the experiment. This observation was made repeatedly, so confirmation in liquid culture was the next step. In a first experiment, growth on pyruvate as sole carbon source was performed at pH 7.4. Also no bicarbonate was added, since the inorganic carbon provided by the naturally occurring 0.04 % CO<sub>2</sub> in the supply air seems to serve as a sufficient substrate for SbtAB in liquid culture during growth of *C. glutamicum*  $\Delta bca$  on glucose (see Figure 3.11). However, this was not the case for *C. glutamicum* wild type+SbtAB. In contrast, cells equipped with the bicarbonate importer grew even worse under the chosen conditions (Figure 3.19). While the wild type reached a mean final OD<sub>600nm</sub> of 4.3, the wild type with SbtAB reached merely 3.8 (Figure 3.19.a). The mean growth rates differed even more with 0.44/h for *C. glutamicum* wild type and 0.26/h for *C. glutamicum* wild type with SbtAB.

### 3. Results

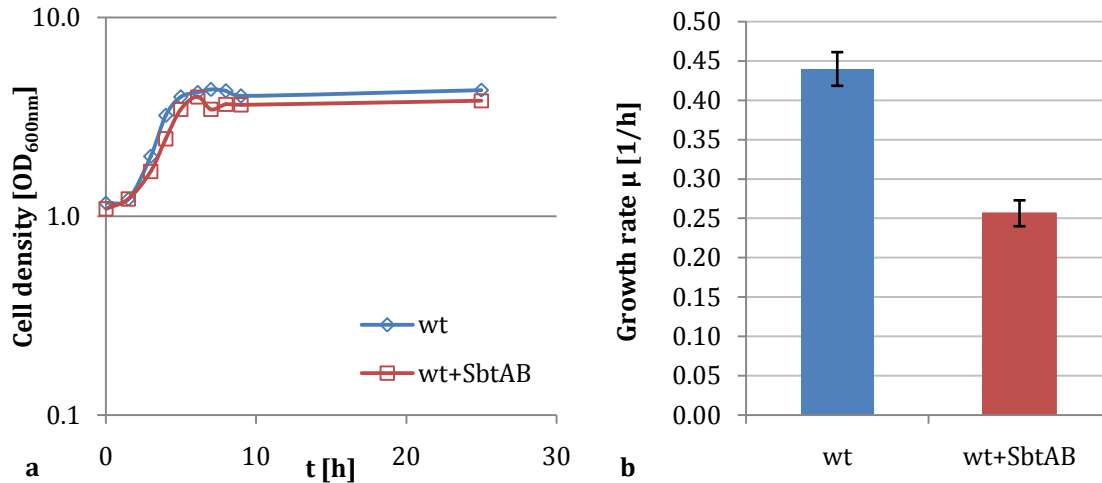


**Figure 3.19: Growth kinetics (a) and growth rates (b) of *C. glutamicum* wild type with and without SbtAB on pyruvate.** Cells were cultivated in CgXII minimal medium with 50 mM pyruvate, 50  $\mu$ g/ml kanamycin and 0.2 mM IPTG at pH 7.4 and atmospheric CO<sub>2</sub>. wt: *C. glutamicum* wild type with the pEKEx2\_EYFP plasmid, wt+SbtAB: *C. glutamicum* wild type with the pEKEx2\_EYFP\_SbtAB plasmid. The black error bars displayed in (b) represent the standard deviations of growth rates and are based on three independent replicates.

To have a more direct comparison to the conditions chosen for the cultivation on solid medium (Figure 3.18), cultivation in liquid culture was also performed with various bicarbonate concentrations to provide an additional substrate for SbtAB. Unlike cultivation on solid medium, a neutral pH of 7.4 was again chosen, since growth behaviour of *C. glutamicum* wild type at alkaline pH differs from that at acid or neutral pH (see Figure 3.16). The results for growth on pyruvate with additional 0.5 mM and 5 mM bicarbonate are shown in Figure 3.20. At least in the second case, growth was slightly decreased if SbtAB was present. There are hardly any differences in the final ODs with 1.63 for *C. glutamicum* wild type+SbtAB and 1.71 for *C. glutamicum* wild type at 0.5 mM bicarbonate (Figure 3.20.a). At 5 mM bicarbonate, the final ODs were higher with 2.08 and 2.22 with and without SbtAB, respectively (Figure 3.20.c). Although the final ODs are generally low, the growth rates reached normal levels of 0.21/h and 0.27/h with and without SbtAB at 0.5 mM bicarbonate, respectively (Figure 3.20.b). Growth rates at 5 mM bicarbonate were also higher with 0.28/h and 0.37/h with and without SbtAB, respectively (Figure 3.20.d).

### 3. Results

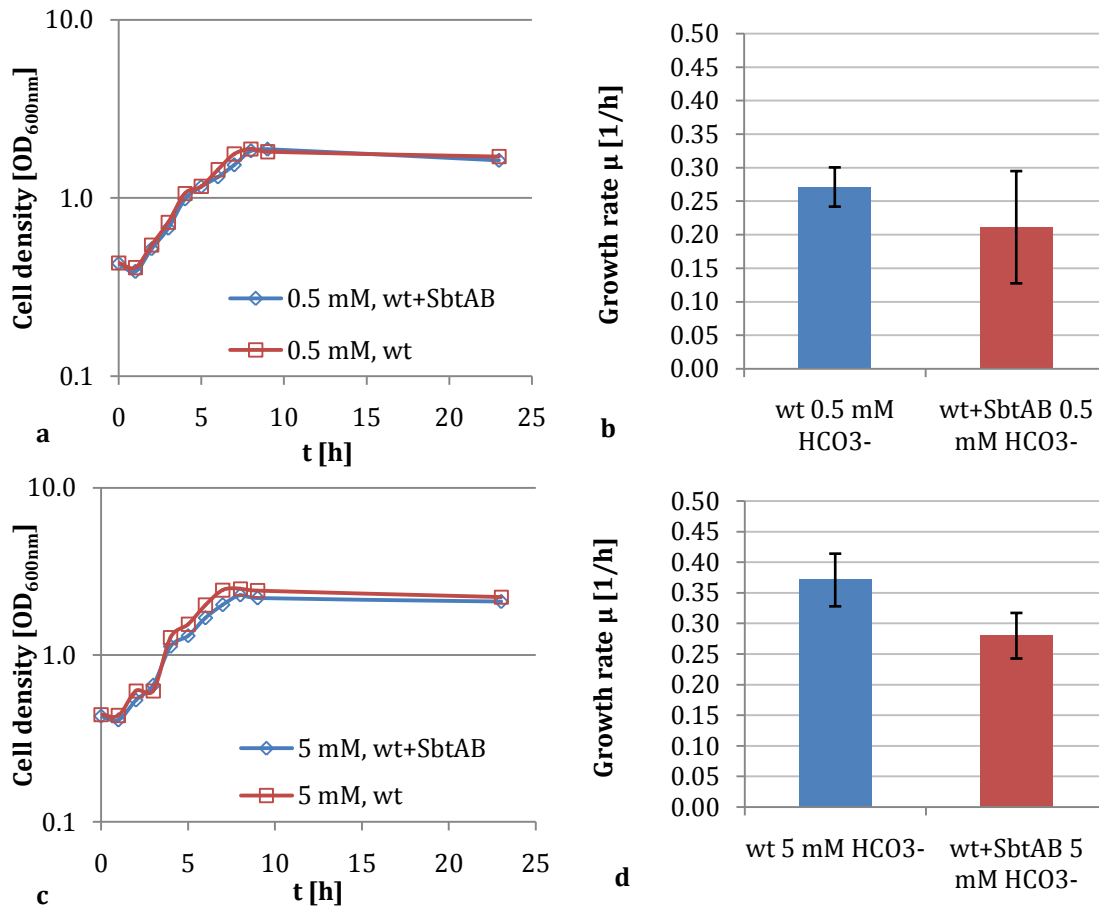


**Figure 3.20: Growth kinetics (a, c) and growth rates (b, d) of *C. glutamicum* wild type with and without SbtAB on pyruvate and various HCO<sub>3</sub><sup>-</sup> concentrations.** Cells were cultivated in CgXII minimal medium with 50 mM pyruvate, 50 μg/ml kanamycin, 0.1 mM IPTG and either 0.5 mM or 5 mM bicarbonate at pH 7.4. wt: *C. glutamicum* wild type harbouring the pEKEx2\_pHluorin plasmid, wt+SbtAB: *C. glutamicum* wild type harbouring the pEKEx2\_pHluorin\_SbtAB plasmid. The black error bars displayed in (b) and (d) represent the standard deviations of growth rates and are based on three independent replicates.

The same experimental setup was tested with 10 % CO<sub>2</sub> in the supply air as additional inorganic carbon source. Also, control measurements with 1 % (5.5 mM) glucose were performed in parallel. As illustrated in Figure 3.21, SbtAB led to better growth on glucose which is in agreement with the observations at atmospheric CO<sub>2</sub> (see Figure 3.16). For growth on pyruvate, no difference was observed. Generally, it has to be noted that the low growth rates and the high standard deviations are based on the experimental setup. Growth in the special vessels for CO<sub>2</sub> application is constricted by the suboptimal aeration. During growth on glucose, both *C. glutamicum* wild type with and without SbtAB reached a mean final OD of 10.6, whereas on pyruvate, mean final ODs of 2 and 4.1 were measured for the wild type with and without SbtAB, respectively (Figure 3.21.a). The growth rates for growth on glucose were 0.18/h and 0.16/h for *C. glutamicum* wild type with and without SbtAB, respectively. For growth on pyruvate,

### 3. Results

the mean growth rates were also very similar with 0.143/h and 0.14/h with and without SbtAB, respectively (Figure 3.21.b).

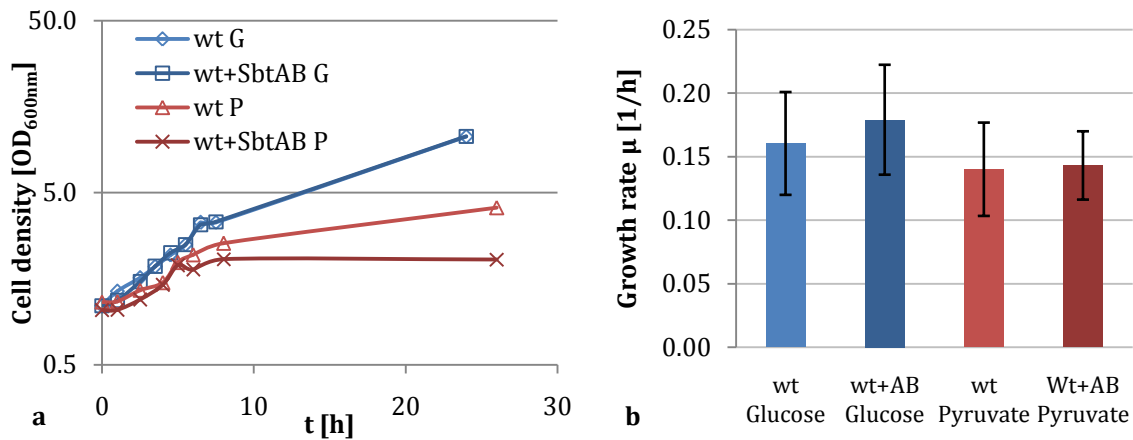


**Figure 3.21: Growth of *C. glutamicum* wild type with and without SbtAB on glucose and pyruvate with 10 % CO<sub>2</sub> in the supply air.** Cells were cultivated in CgXII minimal medium with either 5.5 mM (1 %) glucose or 50 mM pyruvate, 50 μg/ml kanamycin and 0.1 mM IPTG at pH 7.4. wt: *C. glutamicum* wild type harbouring the pEKEx2\_pHluorin plasmid, wt+SbtAB: *C. glutamicum* wild type harbouring the pEKEx2\_pHluorin\_SbtAB plasmid. The black error bars displayed in (b) represent the standard deviations based on three independent replicates.

Although the results describing the influence of the bicarbonate importer SbtAB gained from *C. glutamicum*  $\Delta bca$  clearly point towards the successful heterologous expression leading to functional proteins, the observations in *C. glutamicum* wild type remain inconclusive apart from the growth benefit displayed in Figure 3.16. Therefore, examinations towards the activity of SbtAB in *C. glutamicum* on a biochemical level are indispensable. In this study, radiochemical uptake measurements with <sup>14</sup>C labelled bicarbonate were performed to address this question.

#### 3.2.3 The activity of SbtAB in *C. glutamicum* is difficult to display

To measure the activity of the bicarbonate importer SbtAB in *C. glutamicum*, the amount of radio-labelled sodium bicarbonate (NaH<sup>14</sup>CO<sub>3</sub>) taken up by the cells was determined. During establishment of a suitable experimental setup, bicarbonate uptake by *C. glutamicum* wild type cells without SbtAB was observed repeatedly and it cannot be ruled out that unspecific uptake via anion importers takes place in *C. glutamicum*. A more promising test system was based on *C. glutamicum*  $\Delta bca$ +SbtAB growing at atmospheric CO<sub>2</sub>. The advantage lies in the fact that growth at atmospheric CO<sub>2</sub> is a direct hint towards an active SbtAB transport system, so uptake during growth should

### 3. Results

be detectable. Indeed, a higher uptake of bicarbonate was observed compared to *C. glutamicum* wild type without SbtAB (Figure 3.22). As an additional negative control using the same strain, *C. glutamicum*  $\Delta bca$ +SbtAB cells were treated with CCCP to abolish any membrane potential so no transport processes were possible any longer. Similar to the wild type without SbtAB, those cells did hardly show any bicarbonate uptake as well.

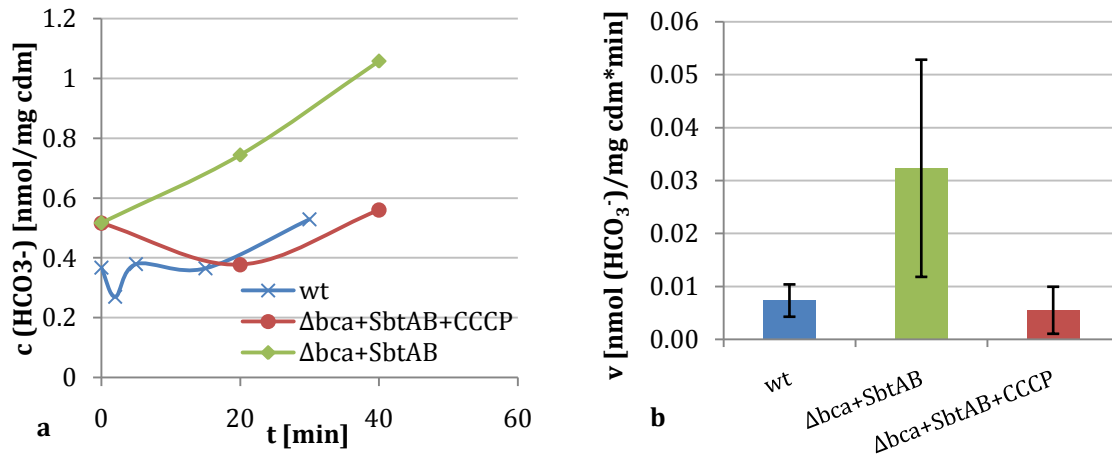


**Figure 3.22: Radioactively labelled intracellular bicarbonate (a) and the derived uptake rates of SbtAB (b).** Uptake was monitored during growth on CgXII minimal medium with 1 % glucose, 50  $\mu\text{g/ml}$  kanamycin and 0.1 mM IPTG at pH 8.5.  $^{14}\text{C}$  labelled bicarbonate was added to a concentration of 100  $\mu\text{M}$ . To abolish the membrane potential in the negative control, 50  $\mu\text{M}$  CCCP were added. wt: *C. glutamicum* wild type with the pEKEx2\_pHluorin plasmid,  $\Delta bca$ +SbtAB: *C. glutamicum*  $\Delta bca$  harbouring the pEKEx2\_pHluorin\_SbtAB plasmid. The black error bars displayed in (b) represent the standard deviations based on three independent replicates.

It is obvious that the uptake rates displayed in Figure 3.22 show high standard deviations. The reason for this lies in the experimental setup. An alkaline pH value was ensured during the whole process to avoid a loss of labelled bicarbonate by  $\text{CO}_2$  formation. However, another problem emerged that possibly made the results difficult to reproduce. The urea in the CgXII medium is converted to  $\text{CO}_2$  in the cells via urease activity. This  $\text{CO}_2$  serves as an additional source of inorganic carbon, which interferes with precise measurements towards the inorganic carbon supply in *C. glutamicum*, which is why the use of urea-free CgXII is mandatory in such experiments. Hence, growth of *C. glutamicum* wild type and  $\Delta bca$  with and without SbtAB in urea-free medium was examined first. The results for *C. glutamicum* wild type are illustrated in Figure 3.23. No difference between cells with and without SbtAB was observed. Compared to growth with urea (see Figure 3.16), growth at pH 6 was constricted in urea-free medium, probably because of the buffer function of urea. While the growth

### 3. Results

rates at pH 6 with urea were 0.35/h and 0.3/h, they were only 0.2/h and 0.19/h on minimal medium without urea for *C. glutamicum* wild type with and without SbtAB, respectively (Figures 3.16b and 3.23.b).

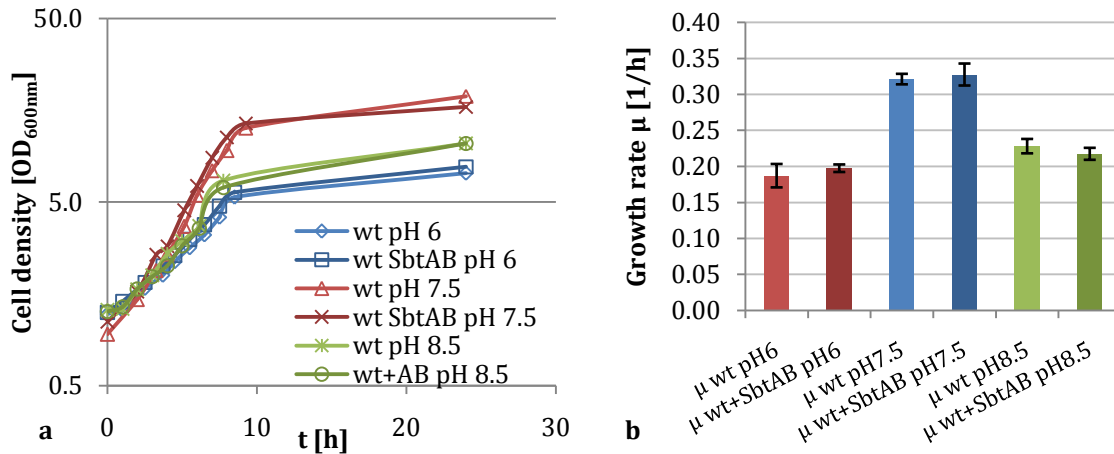


**Figure 3.23: Growth kinetics (a) and growth rates (b) of *C. glutamicum* wild type with and without SbtAB on urea-free medium.** Cells were cultivated in urea-free CgXII medium with 1 % glucose, 50  $\mu$ g/ml kanamycin and 0.1 mM IPTG at various pH values. wt: *C. glutamicum* wild type harbouring the pEKEx2\_pHluorin plasmid, wt+SbtAB: *C. glutamicum* wild type harbouring the pEKEx2\_pHluorin\_SbtAB plasmid. The black error bars displayed in (b) represent the standard deviations of growth rates and are based on three independent replicates.

In a next step, growth behaviour in urea-free medium was tested for *C. glutamicum*  $\Delta bca$ +SbtAB. The results show that growth of *C. glutamicum*  $\Delta bca$ +SbtAB at atmospheric CO<sub>2</sub> is no longer possible in the absence of urea, even if 5 mM bicarbonate are provided as a substrate for SbtAB (Figure 3.24.a and b). Growth can only be restored by *bca* expression in the complementation mutant *C. glutamicum*  $\Delta bca$ +Bca. The growth rates were 0.04/h for *C. glutamicum*  $\Delta bca$ , 0.07/h for *C. glutamicum*  $\Delta bca$ +SbtAB and 0.29/h for *C. glutamicum*  $\Delta bca$ +Bca with final ODs of 0.99, 0.67 and 3.58, respectively. This effect is less severe, if 10 % CO<sub>2</sub> in the supply air are provided (Figure 3.24.c and d). Here, the growth rates for *C. glutamicum*  $\Delta bca$ , *C. glutamicum*  $\Delta bca$ +SbtAB and *C. glutamicum*  $\Delta bca$ +Bca were 0.034/h, 0.089/h and 0.143/h, respectively. The according final ODs were 3.74, 8.34 and 15.32. Hence, only Bca and elevated CO<sub>2</sub> are able to compensate for the lack of inorganic carbon that emerges during cultivation in urea-free medium.

### 3. Results

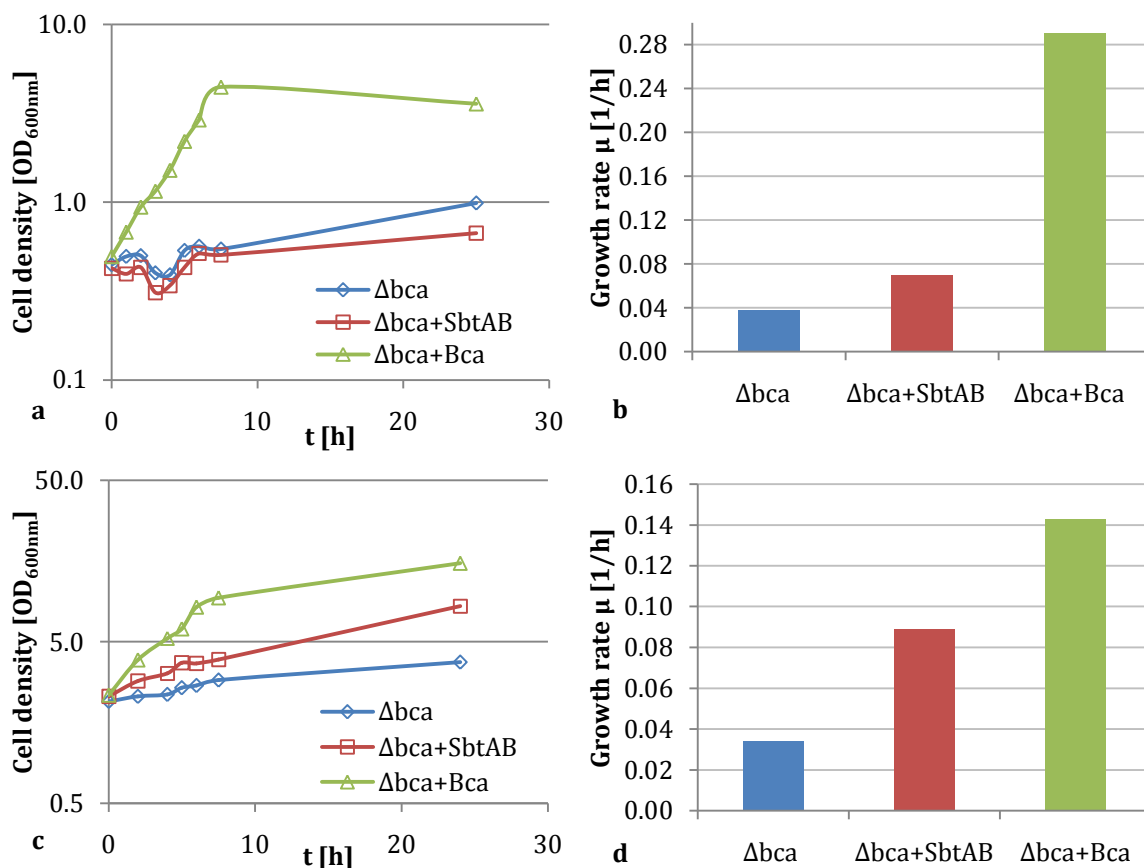


**Figure 3.24: Growth kinetics (a, c) and growth rates (b, d) of various *C. glutamicum*  $\Delta bca$  mutants in urea-free medium.** Cells were cultivated in urea-free CgXII minimal medium with 1 % glucose, 50  $\mu\text{g/ml}$  kanamycin, 0.1 mM IPTG and either 5 mM bicarbonate (a, b) or 10 % CO<sub>2</sub> (c, d) at pH 8.5.  $\Delta bca$ : *C. glutamicum*  $\Delta bca$  with the pEKEx2\_pHluorin plasmid,  $\Delta bca+SbtAB$ : *C. glutamicum*  $\Delta bca$  with the pEKEx2\_pHluorin\_SbtAB plasmid,  $\Delta bca+Bca$ : *C. glutamicum*  $\Delta bca$  with the pEKEx2\_pHluorin\_Bca plasmid. The experiments were performed in duplicates of which the mean values are displayed.

The results illustrated in Figure 3.24 show the impossibility to perform uptake measurements with *C. glutamicum*  $\Delta bca+SbtAB$  in urea-free medium, especially since the use of *C. glutamicum*  $\Delta bca$  as a correct negative control is also indispensable. The wild type also represents no suitable test system because of the background activity in SbtAB free cells. Hence, the results shown in Figure 3.22 can only serve as a hint to estimate the activity of SbtAB in *C. glutamicum*. A more precise setup could not be established, mostly because of the need for urea in *C. glutamicum*  $\Delta bca$ .

#### 3.2.4 SbtAB has no influence on the lysine yield in production strains

Independent from the results gained in the growth experiments described in chapter 3.2.2, which show only a slight influence of SbtAB on *C. glutamicum* wild type cells, an impact on lysine production was still a possible scenario. Hence, lysine yields in the

### 3. Results

production strain *C. glutamicum* DM1933 with and without SbtAB were determined. Cultivation was performed in 500 ml Erlenmeyer flasks and the lysine concentration of the medium was determined after 32 hours via HPLC analysis. As displayed in Figure 3.25, no difference between cells with and without SbtAB activity was observed.

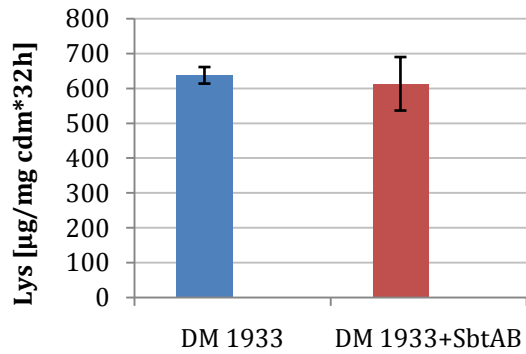


**Figure 3.25: Lysine concentration in the cultivation supernatant after 32 hours.** Cells were cultivated in CgXII minimal medium with 1 % glucose, 50 µg/ml kanamycin and 0.1 mM IPTG in 500 ml Erlenmeyer flasks. Samples were analysed via HPLC. DM 1933: *C. glutamicum* DM 1933 with the pEKEx2\_pHluorin plasmid, DM 1933+SbtAB: *C. glutamicum* DM 1933 with the pEKEx2\_pHluorin\_SbtAB plasmid. The black error bars represent the standard deviations based on three independent replicates.

Taken together, there is a clear impact of the cyanobacterial bicarbonate importer SbtAB on the inorganic carbon provision in *C. glutamicum*. The results for *C. glutamicum*  $\Delta bca$  shown in chapter 3.2.1 clearly point this out, since SbtAB can replace the carbonic anhydrase Bca in terms of inorganic carbon provision at atmospheric CO<sub>2</sub>. Nevertheless, benefits for the *C. glutamicum* wild type strain are hardly detectable (chapter 3.2.2). Also, the activity of SbtAB is difficult to measure in *C. glutamicum* and no influence on the lysine yield in DM 1933 was observed. The supply with inorganic carbon is closely connected to the availability of CO<sub>2</sub> and bicarbonate and thereby also to the internal pH of the cells. The latter factor has so far only been addressed in growth experiments but not in direct measurements of the internal pH. To close this gap, a tool for online pH-measurement was developed to gain insights into the dynamics of pH homeostasis and inorganic carbon supply in *C. glutamicum*.

### 3.3 The pH homeostasis capacity of *C. glutamicum*

#### 3.3.1 A method for online $\text{pH}_i$ measurement was established

First experiments regarding the use of pH sensitive fluorescence dyes for online detection of the intracellular pH ( $\text{pH}_i$ ) in *C. glutamicum* had been performed by Simone Faust (Faust, 2011). The established system was based on the Enhanced Yellow Fluorescence Protein (EYFP), which shows a decrease in intensity upon acidification of the cytoplasm. Although its functionality was shown in *C. glutamicum*, two great disadvantages emerged. First, the intensity maximum occurs at pH 8, which bears the necessity to set this pH in each culture at the beginning of the experiment to determine the reference value which corresponds to 100 % fluorescence intensity. Since this step already interferes with the physiology of the cell, it is not the procedure of choice for online measurements. Second, basic experiments in this study revealed aberrations in the intensity at the same pH value, probably caused by varying expression strengths. Since fluorescence intensity is the pH sensitive parameter of EYFP, this method based on absolute fluorescence amounts is not suitable for *C. glutamicum*. As an alternative, the pH sensitive fluorescence dye pHluorin (Miesenböck *et al.*, 1998) was tested in *C. glutamicum*. pHluorin is a derivative of the Green Fluorescence Protein (GFP) (Tsien, 1998), that possesses two pH dependent excitation maxima. The dye could be functionally expressed in *C. glutamicum* and its physical properties were determined by Simon Mayr (Mayr, 2011). Figure 3.26.a shows the excitation spectra at various pH values. Each pH leads to a different ratio of the two excitation maxima, from which a calibration curve was determined (Figure 3.26.b). Based on the function of this curve, the pH can be directly calculated from the ratio values derived from the 396 nm and 468 nm fluorescence values.

### 3. Results

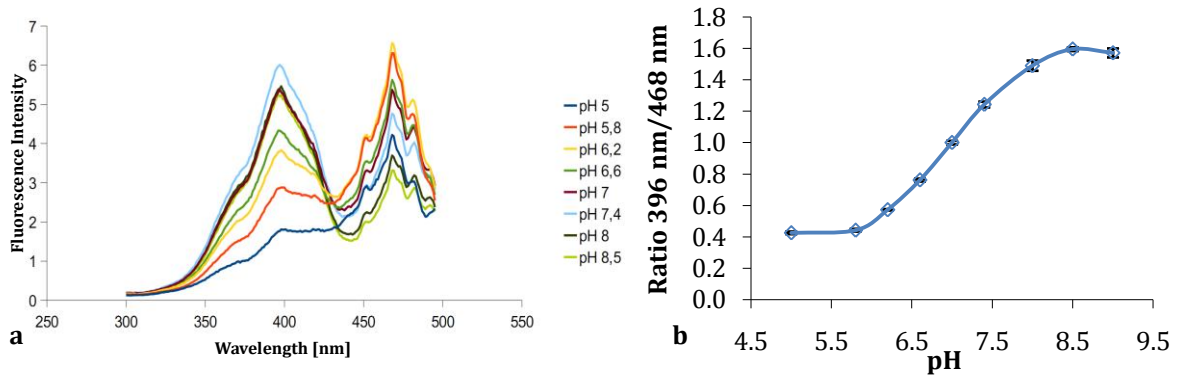


**Figure 3.26: Physical properties of pFluorin.** (a): Excitation spectra at various pH values in crude extracts of *C. glutamicum* (Mayr, 2011); (b): pKs curve of pFluorin. The pH values were set with KP<sub>i</sub> buffer and the ratios were determined *in vivo* after treatment with 0.25 % CTAB. The values were confirmed in crude extracts as well.

Once the functionality of pFluorin had been shown in *C. glutamicum*, a setup for online determination was developed. The aim was determination of the intracellular pH via fluorescence detection during cultivation. This approach was believed to minimise the influence on the cells' physiology. Also, cultivation conditions should be optimal even on a small scale level. These requirements could be fulfilled by the setup based on a small bioreactor (see Figure 2.2). As a suitable buffer system to regulate the external pH, 1 M K<sub>2</sub>HPO<sub>4</sub> and 1 M KH<sub>2</sub>PO<sub>4</sub> were chosen. An important factor here is the osmolality of the medium, since this parameter might interfere with the pH homeostasis capacity. Table 3.1 gives an overview of the osmolalities of the buffers that are used to regulate the external pH and the osmolalities of the cultivation medium before and after acidification. If the pH was shifted from pH 7.4 to pH 6, the osmolality only changed from 0.556 osmol/kg to 0.725 osmol/kg, making a possible negative influence on *C. glutamicum* unlikely.

**Table 3.1: Osmolalities of media and buffers used for online pH measurements.** CgXII medium without MOPS represents the cultivation medium at the beginning of the experiment. 0.2 M KH<sub>2</sub>PO<sub>4</sub> equals the average situation after acidification to pH 6.

Medium/buffer	Osmolality [osmol/kg]
CgXII, 1% glucose, without MOPS	0.556
1 M KH <sub>2</sub> PO <sub>4</sub>	1.427
1 M K <sub>2</sub> HPO <sub>4</sub>	2.016
CgXII, 1% glucose, 0.2 M KH <sub>2</sub> PO <sub>4</sub>	0.725

### 3. Results

Control measurements without a shift of the external pH but with the addition of  $KP_i$  buffer of the according pH 7.4 also ensured that occurring shifts in extracellular osmolality did not affect the internal pH value.

First online measurements revealed a fast shift of the internal pH upon extracellular pH shifts. These fast changes of the proton concentration are quickly overcome by pH homeostasis mechanisms, so a physiological pH is restored after about five minutes (Figure 3.27).

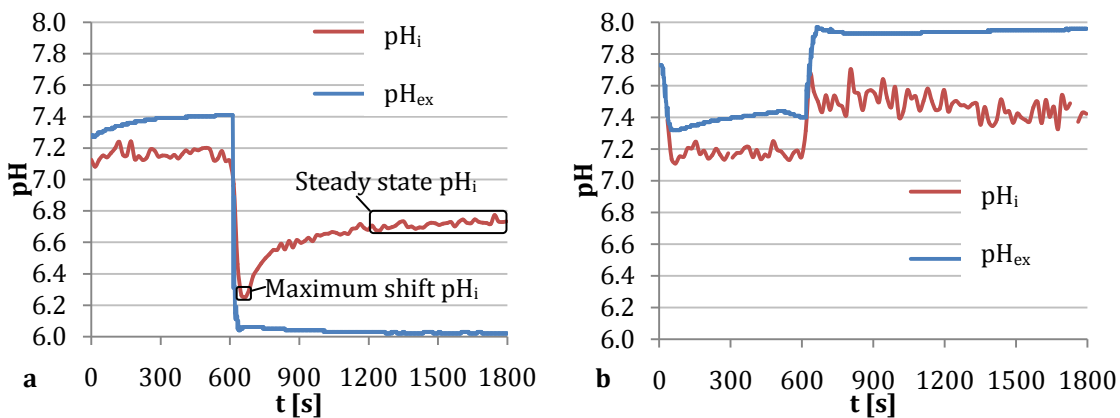


**Figure 3.27: pH homeostasis pattern of *C. glutamicum* wild type after acidification (a) and alkalisiation (b) of the outer medium.** *C. glutamicum* wild type cells harbouring the pEKEx2\_pHluorin plasmid were incubated in CgXII medium without MOPS, pH 7.4 and 1 % glucose for 10 minutes before the external pH was shifted towards pH 6 (a) and 8 (b) using 1 M  $KP_i$  buffers; pH<sub>i</sub>: intracellular pH, pH<sub>ex</sub>: extracellular pH.

Taken together, pHluorin is functionally expressed in *C. glutamicum* and possesses two excitation maxima at 396 nm and 468 nm that can be measured with an emission wavelength of 505 nm. The ratio 396 nm/468 nm is pH dependent and allows calculation of pH values from pH 5.8 to 8.5 independent from absolute fluorescence intensities (see Figure 3.26). The intracellular pH of *C. glutamicum* in 50 ml-cultures can be monitored online so the process of pH homeostasis can be followed over time. Usually *C. glutamicum* shows an internal pH of 7.0 to 7.2 at an external pH of 7.4. Two parameters to describe the homeostasis capacity were chosen. The first one is the strongest shift the intracellular pH undergoes after a rapid change of the external pH and it is called “maximum shift pH<sub>i</sub>”. The second parameter is the mean pH value of the last ten minutes of a measurement and represents the final pH that can be achieved by pH homeostasis. It is called “steady state pH<sub>i</sub>” (see Figure 3.27.a). Based on the

### 3. Results

developed tool for online  $\text{pH}_i$  monitoring, the actual influence of  $\text{CO}_2$  on  $\text{pH}$  homeostasis in *C. glutamicum* was investigated.

#### 3.3.2 The $\text{pH}$ homeostasis in *C. glutamicum* is hardly affected by $\text{CO}_2$

A negative influence of high  $\text{CO}_2$  concentrations on intracellular  $\text{pH}$  at acidic external  $\text{pH}$  values has been observed in *C. glutamicum* earlier (Follmann, 2008). However, the dynamics of this influence are not clear since the results were based on samples taken at discrete time points which did not allow the monitoring of  $\text{pH}_i$  over time. The advantage of pHluorin based online measurements without sample preparation was hence applied to close this gap. For this purpose, *C. glutamicum* wild type cells were exposed to a shift of the external  $\text{pH}$  towards  $\text{pH}$  6 at atmospheric  $\text{CO}_2$  and to  $\text{pH}$  6.2 at 10 %  $\text{CO}_2$ . The latter shift was less severe to ensure values within the detection range of pHluorin. The results illustrated in Figure 3.28 show a deeper drop of the internal  $\text{pH}$  in cells treated with  $\text{CO}_2$  although the external shift was even less severe. To this point, earlier results (Follmann, 2008) could be confirmed. However, during the further course of the measurements, a different picture emerged. Although the  $\text{pH}_i$  was lower at 10 %  $\text{CO}_2$ , the steady state  $\text{pH}_i$  was similar to the steady state  $\text{pH}_i$  at atmospheric  $\text{CO}_2$ .

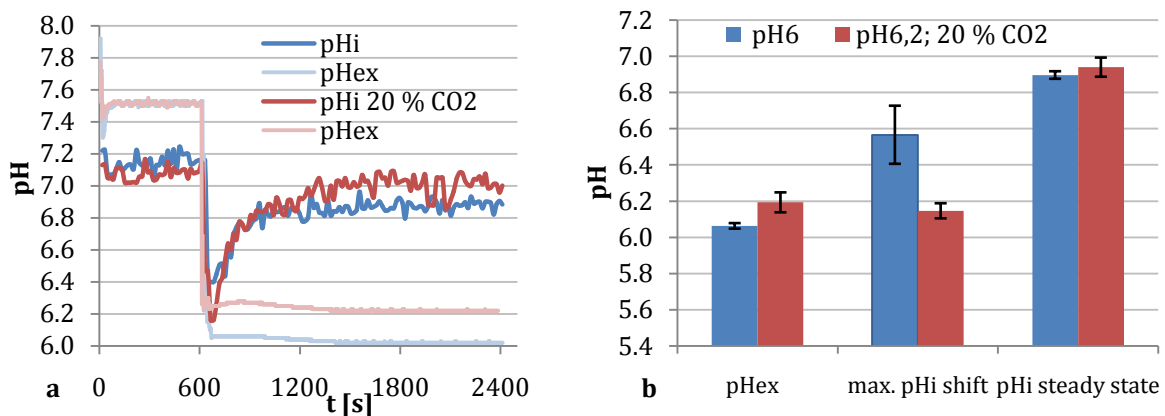


**Figure 3.28: The influence of  $\text{CO}_2$  on  $\text{pH}$  homeostasis after acidification.** *C. glutamicum* wild type cells harbouring the pEKEx2\_pHluorin plasmid were incubated in CgXII medium with 1 % glucose at atmospheric and elevated  $\text{CO}_2$  for 10 minutes before the external  $\text{pH}$  was shifted towards  $\text{pH}$  6 and 6.2, respectively. Displayed is an example of an online pattern (a) and the average values for the maximum shift  $\text{pH}_i$  and the steady state  $\text{pH}_i$  (b). The black error bars displayed in (b) represent the standard deviations based on three independent replicates. Cells were grown in 50 ml CgXII minimal medium  $\text{pH}$  7.5 without MOPS. Acidification was performed using 1M  $\text{KH}_2\text{PO}_4$ .  $\text{pH}_{\text{ex}}$ : external  $\text{pH}$ , max.  $\text{pH}_i$  shift: lowest  $\text{pH}_i$  after acidification,  $\text{pH}_i$  steady state: highest  $\text{pH}_i$  achieved by homeostasis, mean value from the last 10 minutes of measuring.

### 3. Results

These results show that *C. glutamicum* is indeed hardly affected by elevated CO<sub>2</sub> levels at an acidic pH, giving a strong hint towards a remarkable resistance of *C. glutamicum* against CO<sub>2</sub> derived pH stress. There actually is an influence of CO<sub>2</sub> on the intracellular proton concentration, represented in the deeper shift of the internal pH at the beginning, but the steady state pH<sub>i</sub> values show the ability of the cells to compensate this additional stress. To gain a better understanding of the underlying processes during pH homeostasis, the influence of the carbonic anhydrase Bca and the cyanobacterial bicarbonate importer SbtAB were investigated.

#### 3.3.3 Bca and SbtAB do not interfere with pH homeostasis

Based on the fact that Bca activity accelerates proton formation in *C. glutamicum*, an involvement in proton homeostasis seems likely. First investigations using the *C. glutamicum*  $\Delta bca$  mutant showed a lower buffer capacity of the cytoplasm and a less efficient pH homeostasis upon acidification to pH 6.2, regardless whether CO<sub>2</sub> is elevated or not (Figure 3.29). While the maximum shift is pH 6.2 in *C. glutamicum* wild type at elevated CO<sub>2</sub> and pH 6.57 at atmospheric CO<sub>2</sub> (see Figure 3.28.b), shift below the cut-off value of pH 5.8 occurred in *C. glutamicum*  $\Delta bca$ . The steady state values with and without additional CO<sub>2</sub> were 6.43 and 6.47 in *C. glutamicum*  $\Delta bca$ , while the according values in the wild type were 6.94 and 6.9.

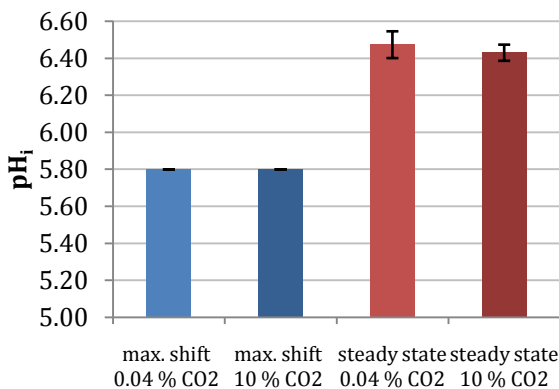


**Figure 3.29: pH homeostasis parameter of *C. glutamicum*  $\Delta bca$  upon acidification at various CO<sub>2</sub> concentrations.** Cells were equipped with the pEKEx2\_pHluorin plasmid. The maximum shift values were below the cut-off of 5.8, which is the limit of pHluorin. The black error bars represent the standard deviations based on three independent replicates. Cells were incubated in CgXII with 1 % glucose at atmospheric (0.04 %) and elevated (10 %) CO<sub>2</sub> for 10 minutes before acidification to pH 6.2 of the outer medium was performed using 1 M KH<sub>2</sub>PO<sub>4</sub>.

### 3. Results

This stands in contradiction to the fact that Bca activity increases the amount of protons in the cell. However, control measurements using the *C. glutamicum*  $\Delta bca$ +Bca strain lead to inconclusive results, since the stability of pHluorin could not be ensured in this strain. Thus, it cannot be excluded that the results shown in Figure 3.29 are caused by a strain-specific property of *C. glutamicum*  $\Delta bca$ . Hence, the impact of *bca* overexpression was tested in *C. glutamicum* wild type. Since a higher amount of Bca might be beneficial at elevated pH values, the maximum shift and steady state values upon alkalisation were determined as well. The results are shown in Figure 3.30, where the maximum shift (Figure 3.30.a) and the steady state values (Figure 3.30.b) are each compared at external pH values of 6 and 8. Apart from a slight and insignificant drop of the internal pH in the overexpression strain upon acidification, no differences between the wild type with and without *bca* overexpression were observed.

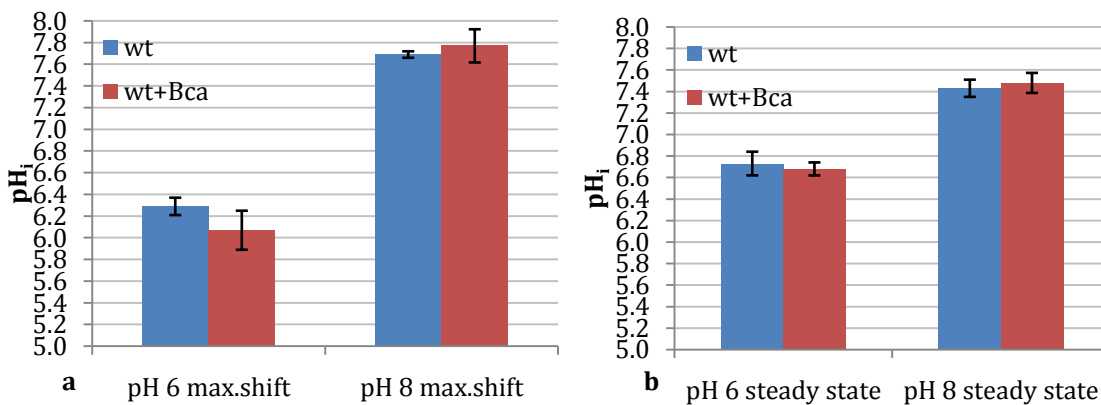


**Figure 3.30: Maximum shift (a) and steady state values (b) of *C. glutamicum* wild type with and without *bca* overexpression upon acidification and alkalisation.** Cells were cultivated in CgXII medium without MOPS, pH 7.4, 1% glucose at atmospheric CO<sub>2</sub>. Acidification and alkalisation were performed via addition of 1 M KH<sub>2</sub>PO<sub>4</sub> and 1 M K<sub>2</sub>HPO<sub>4</sub>, respectively. Wt: *C. glutamicum* wild type with the pEKEx2\_pHluorin plasmid, wt+Bca: *C. glutamicum* wild type with the pEKEx2\_pHluorin\_Bca plasmid. The black error bars represent the standard deviations based on three independent replicates.

In a next step, the influence of the bicarbonate import system SbtAB was tested at acidic pH stress. The imported bicarbonate was assumed to serve as a buffer and thereby enhance the pH homeostasis capacity of *C. glutamicum* at an acidic external pH value. To test this hypothesis, *C. glutamicum* wild type with and without SbtAB was exposed to an external shift to pH 6 at atmospheric CO<sub>2</sub> and the two homeostasis parameters “maximum shift pHi” and “steady state pHi” were determined. The results are illustrated in Figure 3.31. Indeed, cells equipped with SbtAB seem to possess a higher buffer capacity of the cytoplasm since the maximum shift is less severe (pH 6.5 instead of pH

### 3. Results

6.3). However, pH homeostasis after acidification is similar to cells without SbtAB, since achieved steady state  $pH_i$  values are almost equal and lie around pH 6.7.

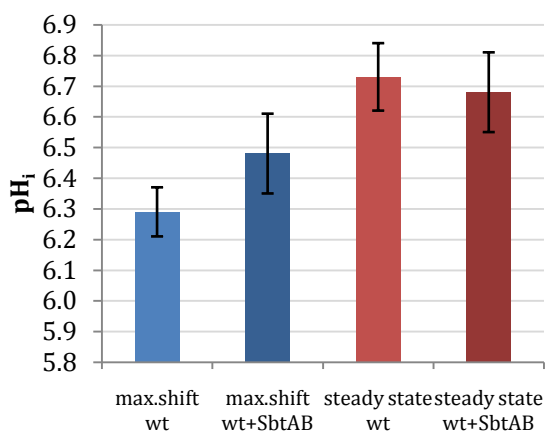


**Figure 3.31: pH homeostasis parameter of *C. glutamicum* wild type with and without SbtAB upon acidification of the medium.** Cultures were cultivated in CgXII medium with 1 % glucose at atmospheric  $CO_2$ . Shift of the external pH from 7.4 to 6 was performed with 1 M  $KH_2PO_4$ . Wt: *C. glutamicum* wild type with the pEKEx2\_pHluorin plasmid, wt+SbtAB: *C. glutamicum* wild type with the pEKEx2\_pHluorin\_SbtAB plasmid. The black error bars represent the standard deviations based on three independent replicates.

Similar to  $CO_2$ , Bca and SbtAB have only a slight effect on the maximum shift of the internal pH of *C. glutamicum* but not on the pH homeostasis capacity of the organism. These observations point towards a very efficient and robust pH resistance of *C. glutamicum*. Hence, a more detailed description of the homeostasis capacity in *C. glutamicum* wild type cells was the next step.

#### 3.3.4 Wild type cells perform pH homeostasis over a wide pH range

To get a detailed picture of the ability of *C. glutamicum* to perform pH homeostasis, *C. glutamicum* wild type cells were exposed to various rapid shifts of the external pH value. Cells were cultivated in CgXII medium at pH 7.4. Since this extracellular pH increased sometimes during the three hours of pre-cultivation, it was corrected to pH 7.4 again at the beginning of the measurement and maintained constant for 10 minutes before the shift was applied. The cultures were shifted towards pH 6, 6.5, 7 and 8. As a control,  $KP_i$  buffer of pH 7.4 was added in one case to exclude possible changes of the internal pH derived from adding the buffer. For each shift, the maximum shift  $pH_i$  and the steady state  $pH_i$  were determined. Figure 3.32 shows the emerging homeostasis pattern for *C. glutamicum* wild type. At external pH values from 6 to 8, the maximum

### 3. Results

shifts range from pH 6.2 to 7.6, while the steady state pH is kept constant at values between 6.7 and 7.35.

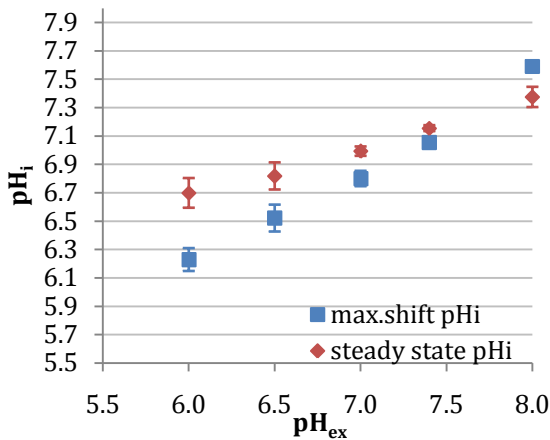


**Figure 3.32: pH homeostasis pattern of *C. glutamicum* wild type cells.** Cultivation and measurements were performed in CgXII minimal medium without MOPS, pH 7.4 and 1 % glucose. External pH shifts were generated using 1 M  $\text{KP}_i$  buffer. Wt: *C. glutamicum* wild type cells harbouring the pEKEx2\_pHluorin plasmid,  $\text{pH}_i$ : intracellular pH,  $\text{pH}_{\text{ex}}$ : external pH. The error bars represent the standard deviations based on at least three independent replicates.

The results show that shortly after a rapid shift of the outer pH, the intracellular pH shifts to a certain degree as well. However, the steady state values were always within a physiological range. The fact that pH homeostasis takes only about five minutes after an external shift to pH 6 to reach these values (see Figure 3.27) underlines the remarkable efficiency of proton homeostasis in *C. glutamicum*. Hence, the underlying mechanisms were studied in greater detail. In a first attempt, proton transporting components of the respiratory chain were investigated towards their role in pH homeostasis.

#### 3.3.5 The process of pH homeostasis relies on the function of the respiratory chain

As mentioned in chapter 1.5, the two branches of terminal oxidases of *C. glutamicum* might be involved in pH homeostasis, since the cytochrome *bd1* oxidase branch exports two protons per electron pair, while the cytochrome *bc1-aa3*-supercomplex branch exports even six protons per electron pair. To investigate their role in pH homeostasis, three deletion mutants were provided by the group of Prof. Michael Bott at the FZ Jülich (Koch-Koerfges *et al.*, 2013). The *C. glutamicum*  $\Delta\text{cydAB}$  mutant shows a deletion of the *bd1* oxidase genes, while *C. glutamicum*  $\Delta\text{qcr}$  lacks the *bc1-aa3*-supercomplex encoding genes. The *C. glutamicum* DOOR mutant is a double deletion mutant that lacks both

### 3. Results

branches of terminal oxidases. The strain cannot use oxygen as electron acceptor, hence its name based on the acronym DOOR for “Devoid Of Oxygen Respiration”. It was assumed that, based on the number of protons transported by the various oxidases, *C. glutamicum*  $\Delta$ *cydAB* would possibly behave like the wild type, while *C. glutamicum*  $\Delta$ *qcr* and DOOR should be significantly constrained in their proton homeostasis capacity. The same pH homeostasis patterns like the one illustrated for *C. glutamicum* wild type in Figure 3.32 were determined for each strain. Figure 3.33 displays one example of a homeostasis run of each strain after acidification of the outer medium to pH 6. For *C. glutamicum*  $\Delta$ *cydAB* and  $\Delta$ *qcr*, a wild type-like pattern was observed (Figure 3.33.a, b). The maximum shift and the steady state  $pH_i$  hardly differed from those of the wild type displayed in Figure 3.33.d. Neither did the speed of the homeostasis process. A different picture emerged for *C. glutamicum* DOOR. As shown in Figure 3.33.c, the internal pH is unusually low at the beginning and even drops below the external pH upon acidification. After the shift, no homeostasis process could be observed.

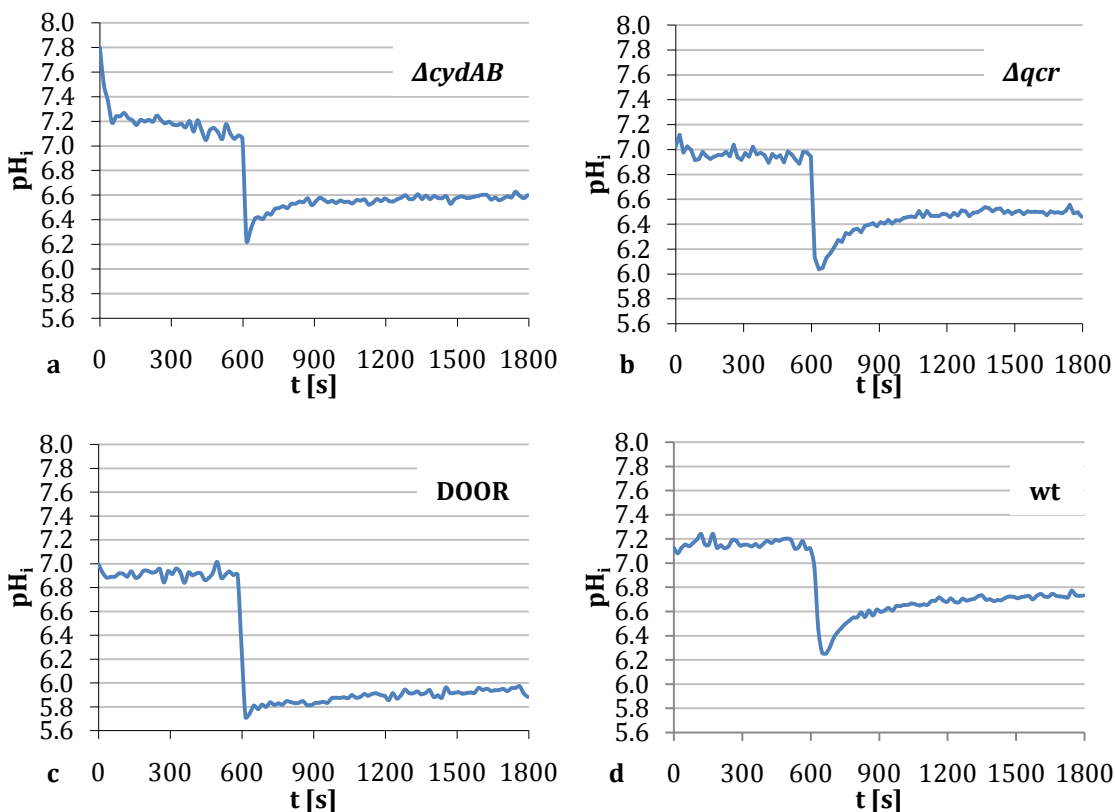


**Figure 3.33: Intracellular pH of the three respiratory chain mutants of *C. glutamicum* compared to the wild type after acidification to pH 6.** Cultivation and measurements were performed in CgXII minimal medium without MOPS pH 7.4, 1 % glucose. After 10 minutes, the external pH was shifted towards pH 6 using 1 M  $KH_2PO_4$ . (a): internal pH ( $pH_i$ ) of *C. glutamicum*  $\Delta$ *cydAB*, (b): internal pH ( $pH_i$ ) of *C. glutamicum*  $\Delta$ *qcr*, (c): internal pH ( $pH_i$ ) of *C. glutamicum* DOOR, (d): internal pH ( $pH_i$ ) of *C. glutamicum* wild type (wt), each strain harbouring the pEKEx2\_pHluorin plasmid.

### 3. Results

The observation that *C. glutamicum*  $\Delta cydAB$  and  $\Delta qcr$  possess a pH homeostasis capacity similar to that of *C. glutamicum* wild type was made at each pH value of the homeostasis patterns (Figures 3.34.a and b). Also, the fact that *C. glutamicum* DOOR is hardly able to perform any pH homeostasis was confirmed over a wide range of external pH values from 6 to 8 (Figure 3.34.c).

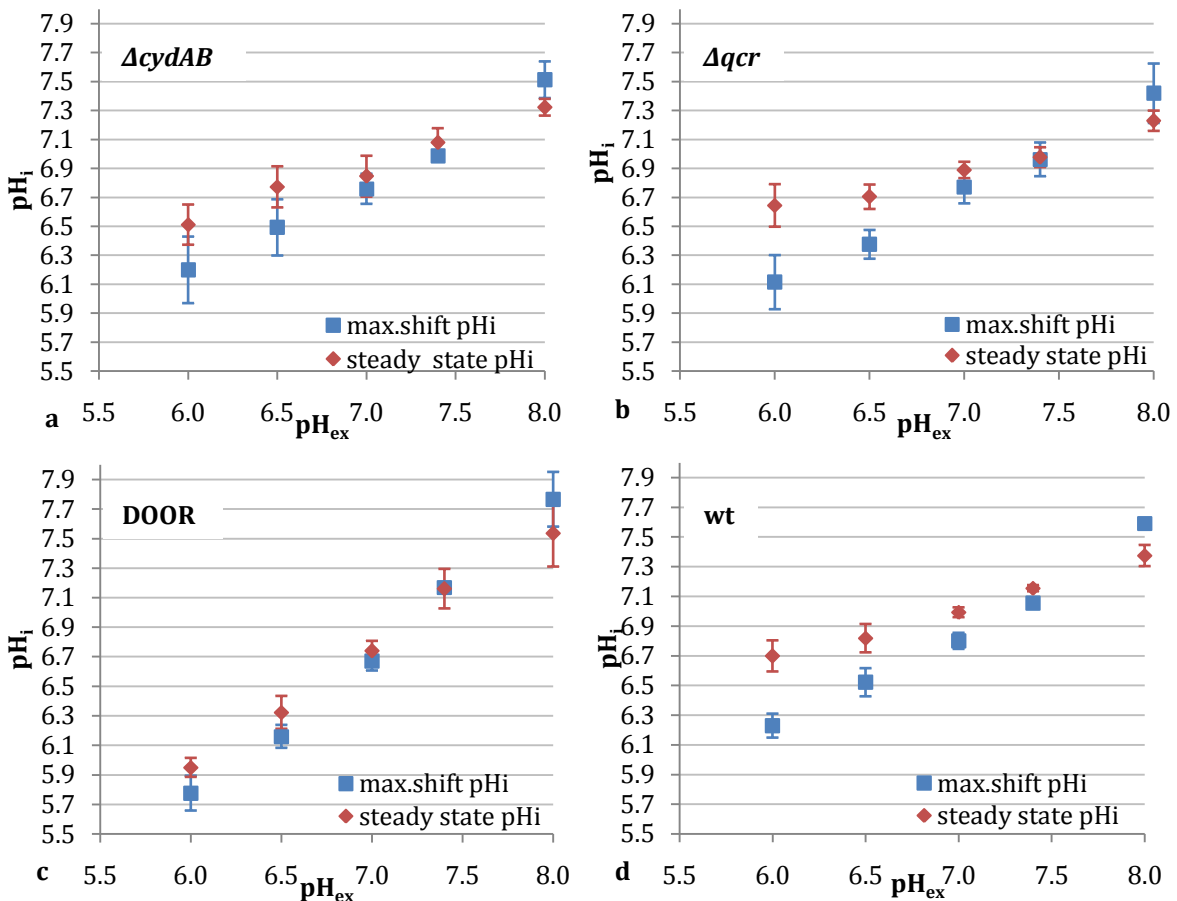


**Figure 3.34: pH homeostasis patterns of *C. glutamicum*  $\Delta cydAB$ ,  $\Delta qcr$  and DOOR compared to *C. glutamicum* wild type.** Cultivation and measurements were performed in CgXII minimal medium without MOPS pH 7.4, 1 % glucose. After 10 minutes, the external pH was shifted using KP<sub>i</sub> buffers. (a): homeostasis pattern of *C. glutamicum*  $\Delta cydAB$ , (b): homeostasis pattern of *C. glutamicum*  $\Delta qcr$ , (c): homeostasis pattern of *C. glutamicum* DOOR, (d): homeostasis pattern of *C. glutamicum* wild type (wt); pH<sub>i</sub>: intracellular pH, pH<sub>ex</sub>: external pH, wt: wild type. The error bars represent the standard deviations based on at least three independent replicates. All strains were equipped with the pEKE<sub>x2</sub>\_pHluorin plasmid.

The pH homeostasis patterns in Figure 3.34 clearly show the differences between *C. glutamicum*  $\Delta cydAB$  and  $\Delta qcr$  on the one hand and *C. glutamicum* DOOR on the other hand. As long as at least one branch of the respiratory chain is still present, pH homeostasis is hardly affected. However, if the cells lack both terminal oxidases as it is the case in the *C. glutamicum* DOOR mutant, the intracellular pH is somewhat lower than the external pH and the cells are unable to perform efficient pH homeostasis, since the

### 3. Results

determined steady state pH values hardly differ from the maximum shift pH values. Figure 3.35 displays a direct comparison of the three respiratory chain mutants and the wild type of *C. glutamicum*.

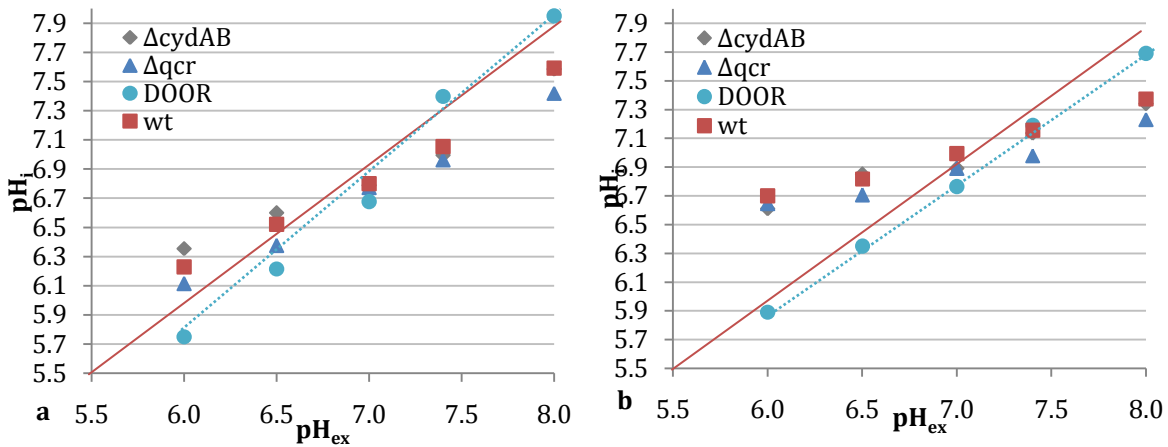


**Figure 3.35: Maximum shift (a) and steady state (b) pH values of the respiratory chain mutants and the wild type of *C. glutamicum* at various external pH values.** The red line represents the situation of equal values of internal and external pH, a situation of no cytoplasmic buffer capacity and no active pH homeostasis.  $pH_i$ : intracellular pH,  $pH_{ex}$ : extracellular pH, wt: *C. glutamicum* wild type,  $\Delta cydAB$ : *C. glutamicum*  $\Delta cydAB$ ,  $\Delta qcr$ : *C. glutamicum*  $\Delta qcr$ , DOOR: *C. glutamicum* DOOR; all strains were equipped with the pEKEx2\_pHluorin plasmid.

Although pH homeostasis is hardly affected by the absence of one of the two branches of terminal oxidases, the results from the *C. glutamicum* DOOR strain strongly suggest an involvement of the respiratory chain in the pH homeostasis of *C. glutamicum*. In this mutant, proton homeostasis seems severely disturbed, since the internal pH drops below the external pH upon acidification. Hence, the cytoplasm seems to possess no significant passive buffer capacity. Also, not only the maximum shift values (Figure 3.35.a) but also the steady state values (Figure 3.35.b) of *C. glutamicum* DOOR form a straight line (see dashed blue lines in Figures 3.35. a, b) which is almost in parallel to the red line representing the  $pH_i = pH_{ex}$  scenario. This is a strong hint that no pH homeostasis is possible without the terminal oxidases of *C. glutamicum*. Another possible component of the pH homeostasis machinery is the  $F_{(1)}F_{(0)}$ ATPase, which generates ATP via proton import, but is also assumed to possess a reverse function to conduct proton export from the cytoplasm during acidic stress response. The deletion mutant *C. glutamicum*  $\Delta F_{(1)}F_{(0)}$ , which lacks this enzyme complex was available from the group of Prof. Bott (Koch-Koerfges *et al.*, 2012). Hence, the involvement of the  $F_{(1)}F_{(0)}$ ATPase in pH homeostasis

### 3. Results

was investigated as well via determination of a homeostasis pattern of the *C. glutamicum*  $\Delta F_1F_0$  mutant.

#### 3.3.6 The $F_{(1)}F_{(0)}$ ATPase is not involved in pH homeostasis

To gain insight into the impact of the  $F_{(1)}F_{(0)}$ ATPase on the pH homeostasis of *C. glutamicum*, the same homeostasis pattern as illustrated before (Figures 3.32 and 3.34) was determined for the deletion mutant *C. glutamicum*  $\Delta F_1F_0$ . Figure 3.36.a shows an example of a pH homeostasis curve after acidification to pH 6 after 10 minutes. Although the maximum shift and the steady state values are slightly lower compared to a typical wild type pattern (see Figure 3.33.d), homeostasis proceeds just as fast as in *C. glutamicum* wild type. Also, it has to be noted that it is difficult to directly compare single measurements, since there were always aberrations due to slight variations in fitness of the cells. As displayed in Figure 3.36.b, at each pH value regarded in the homeostasis pattern, the situation is similar to *C. glutamicum* wild type. While the maximum shift pH values ranged from 6.2 to 7.6 in the wild type, they ranged from 6.14 to 7.34 in the *C. glutamicum*  $\Delta F_1F_0$  strain. The steady state pH values achieved by pH homeostasis ranged from pH 6.7 to 7.35 in *C. glutamicum* wild type and from pH 6.52 to 7.25 in the *C. glutamicum*  $\Delta F_1F_0$  mutant.

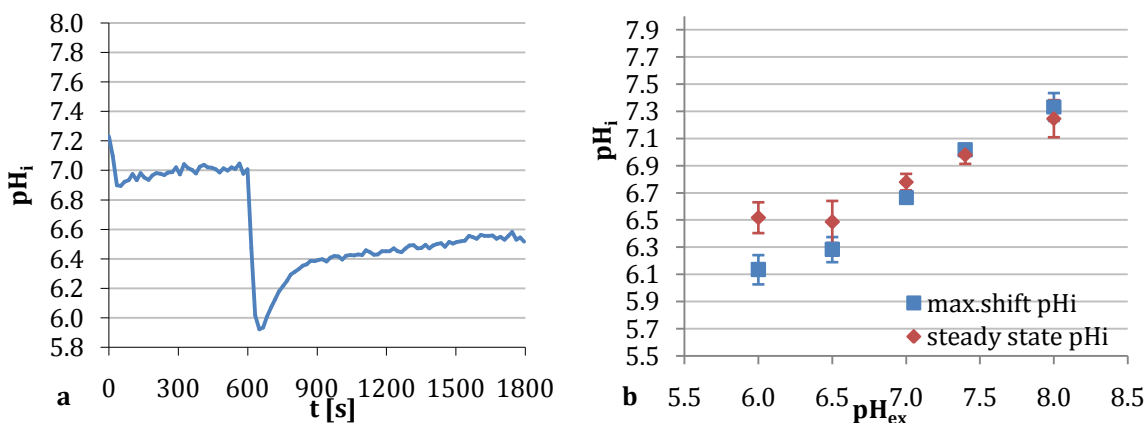


**Figure 3.36: Intracellular pH upon acidification of the medium to pH 6 (a) and pH homeostasis pattern (b) of *C. glutamicum*  $\Delta F_1F_0$ .** Cultivation and measurements were performed in CgXII minimal medium without MOPS pH 7.4, 1 % glucose. External pH shifts were generated using 1 M  $KP_i$  buffer.  $\Delta F_1F_0$ : *C. glutamicum*  $\Delta F_1F_0$  cells harbouring the pEKEx2\_pHluorin plasmid, pH<sub>ex</sub>: external pH. The error bars represent the standard deviations based on at least three independent replicates.

The wild type-like pH homeostasis pattern of *C. glutamicum*  $\Delta F_1F_0$  points towards a negligible impact of the  $F_{(1)}F_{(0)}$ ATPase on the pH homeostasis capacity of *C. glutamicum*.

### 3. Results

Neither is the pH homeostasis constrained at alkaline pH values, nor are there any hints towards a reverse function of the proton pump at acidic pH values.

Taken together, only *C. glutamicum* DOOR, which has no functional respiratory chain, shows a phenotype with significantly altered pH homeostasis. It was not possible to display statistically relevant differences between *C. glutamicum* wild type,  $\Delta cydAB$ ,  $\Delta qcr$  or  $\Delta F_1F_0$ . Table 3.2 sums up the homeostasis parameters determined for *C. glutamicum* wild type and the respiratory chain mutants as well as for *C. glutamicum*  $\Delta F_1F_0$  as displayed in Figures 3.34 and 3.36.b, respectively.

**Table 3.2: Overview of the pH homeostasis capacity of all *C. glutamicum* strains tested.** Displayed is the maximum shift the cells showed upon rapid external pH shifts (“max. shift acidic/alkaline”) and the steady state values that were achieved upon active homeostasis after external shifts from pH 6 to pH 8 (“steady state range”). All *C. glutamicum* strains were equipped with the pEKEx2\_pHluorin plasmid.

<i>C. glutamicum</i> strain	max. shift acidic/alkaline	steady state range
Wild type	6.2/7.6	6.7-7.35
$\Delta F_1F_0$	6.14/7.33	6.52-7.25
$\Delta cydAB$	6.2/7.5	6.5-7.3
$\Delta qcr$	6.1/7.45	6.65-7.25
DOOR	5.8/7.85	5.9-7.6

The results in chapter 3 display the remarkable ability of *C. glutamicum* for efficient pH homeostasis. This enables the cells to cope for example with unusually high CO<sub>2</sub> concentrations. However, no further detailed information towards possible components involved in pH homeostasis at elevated and atmospheric CO<sub>2</sub> concentrations was gathered. An exception is represented in the *C. glutamicum* DOOR strain which illustrated the importance of the respiratory chain for pH homeostasis in *C. glutamicum*.

## 4. Discussion

### 4.1 Inorganic carbon supply in *C. glutamicum*

#### 4.1.1 The impact of CO<sub>2</sub> on the physiology of *C. glutamicum*

The negative influence of CO<sub>2</sub> on microorganisms is based on two effects that cannot be regarded completely separate from each other. First, pH homeostasis is less effective at high CO<sub>2</sub> concentrations, since the amount of protons becomes elevated by the hydration of CO<sub>2</sub> in aqueous solution (Garcia-Gonzalez *et al.*, 2007). Second, CO<sub>2</sub> causes alterations in lipid structure of the cell membrane, which is probably based on dehydration and reduced water miscibility of the membrane known as the anaesthetic effect (Ballestra P., 1996; Sears & Eisenberg, 1961). These changes of the membrane topology might influence the stability of the proton gradient, since permeability of the membrane becomes increased in the presence of CO<sub>2</sub>. This effect is expected to have consequences on the pH homeostasis capacity at acidic pH values. It has to be noted that those negative effects of high CO<sub>2</sub> concentrations are severe enough to cause cell death, which is why application of high CO<sub>2</sub> pressures is used as a non-thermal food preservation method (Dixon & Kell, 1989; Garcia-Gonzalez *et al.*, 2007).

In this context, the results for *C. glutamicum* shown in this work are surprising since growth of *C. glutamicum* is not negatively affected by 10 % CO<sub>2</sub>. In contrast, such high CO<sub>2</sub> levels seemed to be even slightly beneficial in some cases (see Figure 3.12, growth on glucose). Although a similar observation was made for succinate production in *E. coli* fermentations (Lu *et al.*, 2009) and for growth of *C. glutamicum* on lactate (Bäumchen *et al.*, 2007), the result stands in contradiction to studies that revealed inhibited growth of *C. glutamicum* on glucose at elevated CO<sub>2</sub> (Bäumchen *et al.*, 2007). A noxious effect of elevated CO<sub>2</sub> levels in the supply air on the intracellular pH was observed in *C. glutamicum* before (Follmann, 2008). Additionally, increased expression levels of genes involved in acidic stress response were observed in *E. coli* at elevated CO<sub>2</sub> concentrations even if the pH was kept neutral (Baez *et al.*, 2009). Above, various examples of the inhibitory effect on biomass and product formation in industrial fermentations have already been reviewed in 1989 (Dixon & Kell, 1989). Physiological

#### 4. Discussion

investigations in yeast point towards a higher sensitivity towards elevated CO<sub>2</sub> at aerobic growth compared to fermentative metabolism (Aguilera *et al.*, 2005).

The online measurements of the intracellular pH in *C. glutamicum* established in this study only partly confirmed these observations. Cells treated with 10 % CO<sub>2</sub> for ten minutes shifted their internal pH to a deeper value after acidification of the outer medium than cells incubated at atmospheric CO<sub>2</sub> (see Figure 3.28). However, the cells were able to restore the same internal pH in the presence of high CO<sub>2</sub> as they did at atmospheric CO<sub>2</sub>. This is a further indication of a high resistance of *C. glutamicum* against elevated CO<sub>2</sub> concentrations. Prior to this study, it was assumed that especially the combination of elevated CO<sub>2</sub> and an acidic pH had a noxious effect on *C. glutamicum*. This assumption was supported by earlier results (Follmann, 2008). In the experiments of Martin Follmann, cells were cultivated at an acidic pH and elevated CO<sub>2</sub> was applied. In the present study, the cultivation conditions were different since the experiments were performed on a small scale level instead of using a 1.5 l bioreactor and the cells were pre-incubated at a neutral pH instead of an acidic pH value. Hence, it cannot be excluded that the cells in the experiment of Martin Follmann were in a different physiological state. On the one hand, fermentation ensures optimal growth conditions. On the other hand, cells were exposed to an acidic pH for a longer period of time before CO<sub>2</sub> stress was applied. These alterations in the experimental setup make the results less comparable, since the two stress parameters were applied in reverse order. However, a selection towards acid resistant cells might have been taken place in the fermenter based setup and those cells should be even more resistant against high CO<sub>2</sub> concentrations. This is the reason why a neutral pH during cultivation was chosen in the pHluorin based measurements. Observations towards a different pH homeostasis behaviour of pre-adapted cells were for example made in *E. coli* and *Salmonella typhimurium* (Foster, 1999). A pre-cultivation in acidic medium prior to online pH<sub>i</sub> measurements might help answering this open question.

Nevertheless, the results presented in this study strongly argue for a remarkable resistance of *C. glutamicum* against elevated CO<sub>2</sub> concentrations even at an acidic external pH value. The effective pH homeostasis after a rapid acidification was not constrained in the presence of 10 % CO<sub>2</sub> (see Figure 3.28). The ambivalent effect of CO<sub>2</sub> on bacterial cells characterised by beneficial effects at low concentrations and a growth

inhibiting effect at high concentrations (Onken & Liefke, 1989) was only partly confirmed in *C. glutamicum*, since no growth inhibition by elevated CO<sub>2</sub> concentrations was observed in this study. The low growth rates at elevated CO<sub>2</sub> concentrations measured in growth experiments (see Figures 3.13, 3.14, 3.15 and 3.21) are most likely caused by the suboptimal mixing conditions in the glass vessels used for CO<sub>2</sub>-aeration. More detailed investigations in fermenters applying at least 30 % CO<sub>2</sub> might reveal possible negative effects of CO<sub>2</sub> on *C. glutamicum*.

### **4.1.2 Inorganic carbon supply in *C. glutamicum* $\Delta bca$ and the role of Bca in pH homeostasis**

The growth deficit of *C. glutamicum*  $\Delta bca$  shows the need for inorganic carbon and the essential role the carbonic anhydrase Bca plays in providing it (Mitsuhashi *et al.*, 2004). The fact that elevated CO<sub>2</sub> in the supply air is able to rescue the *C. glutamicum*  $\Delta bca$  mutant points out that the growth deficit is actually based on a lack of inorganic carbon. The results shown in this work also point towards a stronger need for Bca activity at lower pH values of the outer medium (see Figure 3.2). At an acidic external pH, 5 % CO<sub>2</sub> were no longer sufficient to restore growth. It has to be noted that at pH values lower than 7.4, the balance of the hydration reaction of CO<sub>2</sub> shifts on the educt side, so bicarbonate is scarcely present if the pH is below 6 (Onken & Liefke, 1989) and its formation proceeds slowly even under neutral conditions. Hence, it seems obvious that bicarbonate is the actual substrate in carboxylation reactions as stated before (Mitsuhashi *et al.*, 2004; Norici *et al.*, 2002). This also explains the essentiality of Bca, since the enzyme strongly accelerates the hydration of CO<sub>2</sub>. As lipid membranes are 1000-fold more permeable for CO<sub>2</sub> compared to the negatively charged HCO<sub>3</sub><sup>-</sup> (Price, 2011), CO<sub>2</sub> is the basic external source of inorganic carbon and its fast conversion to bicarbonate is essential to prevent a depletion of inorganic carbon via passive CO<sub>2</sub> efflux. Hence, at atmospheric CO<sub>2</sub> concentrations, Bca activity is vital to ensure sufficient amounts of bicarbonate, although elevation of CO<sub>2</sub> concentration in the supply air may compensate for a lack of Bca to a certain extent. It was shown that *bca* expression is induced during phases of high bicarbonate demand such as exponential growth and lysine overproduction (Mitsuhashi *et al.*, 2004). Above, the need for Bca activity is stronger at lower external pH values, which is also in agreement with the fact that

bicarbonate as a product of the Bca catalysed reaction is the actual substrate in carboxylation processes.

However, the results regarding growth of *C. glutamicum Δbca* on various carbon sources in liquid culture are highly inconclusive. On alkaline solid medium with additional bicarbonate, *C. glutamicum Δbca* grew only with glucose and 10 % CO<sub>2</sub> and not pyruvate (see Figure 3.12). Even over a wide pH range and without added bicarbonate, growth on glucose was observed on solid minimal medium at 10 % CO<sub>2</sub> (see Figure 3.2). In liquid culture, a completely different picture emerged, since these cells only grew on pyruvate and 10 % CO<sub>2</sub>, while neither glucose nor maltose ensured growth although 10 % CO<sub>2</sub> were supplied as well (see Figures 3.14 and 3.15). This observation was unexpected for two reasons. First of all, growth on glucose should be possible at elevated CO<sub>2</sub> concentrations, since the reason for the growth deficit of *C. glutamicum Δbca* is actually a lack of inorganic carbon. Also, growth in liquid pre-cultures with BHI complex medium was always possible at 10 % CO<sub>2</sub>. Second, pyruvate was expected to be a less optimal substrate which generates a stronger need for inorganic carbon (Netzer *et al.*, 2004). A constrained glucose uptake by *C. glutamicum Δbca* can be ruled out as a reason since the growth deficit occurred on maltose as well (see Figure 3.15). Glucose uptake is mediated by the phosphotransferase system (PTS) subunit E<sub>II</sub> exclusively (Parche *et al.*, 2001). This glucose uptake system is not involved in maltose uptake (Moon *et al.*, 2005), which is realised via the ABC-transporter MuseFGK<sub>2</sub>I (Henrich *et al.*, 2013). Hence, the absence of glycolysis during growth on pyruvate as sole carbon source seems to be the decisive aspect which ensures growth on minimal medium. However, no clear explanation for this phenomenon can be given at this point. Since the observations were made in the *C. glutamicum Δbca* strain provided by Kyowa Hakko, further investigations using a self-constructed *C. glutamicum Δbca* ATCC 13032 strain are indispensable to close this gap.

### **4.1.3 Inorganic carbon supply in *C. glutamicum* wild type**

Since the carbonic anhydrase Bca plays a decisive role for inorganic carbon provision in *C. glutamicum*, it was assumed that overexpression of *bca* in *C. glutamicum* wild type might be beneficial for growth under certain circumstances. Hence, two scenarios were tested that were believed to represent a stronger need for inorganic carbon, since this condition has already been shown to induce *bca* expression (Mitsubishi *et al.*, 2004).

#### 4. Discussion

The first one was growth with a low cell density at the beginning of cultivation since the low metabolic activity leads to the necessity to avoid CO<sub>2</sub> efflux and Bca mediated conversion to bicarbonate is crucial in this context. As shown in Figure 3.8, cells with and without *bca* overexpression showed similar growth behaviour. The observed lag-phase was not shortened by *bca* overexpression. Possibly the assumption that low cell densities represent a low level of CO<sub>2</sub> caused by low metabolic activity is not correct, which means that in fact the substrate CO<sub>2</sub> is not a limiting factor causing the lag-phase. However, it has been shown that the  $\beta$ -type carbonic anhydrase Can in *E. coli* is expressed especially at low growth rates and low cell densities (Merlin *et al.*, 2003). Hence, inorganic carbon provision does seem to be critical under the chosen conditions, so the experimental setup was suitable. Another option is that Bca levels are so high in *C. glutamicum* wild type that elevated amounts of the enzyme do not lead to more bicarbonate in the cell. This second scenario seems more likely, since it also means that the availability of CO<sub>2</sub> as a substrate is limiting and not the amount of enzyme. It has to be noted that an enzymatic characterisation of Bca was not possible, since the only described activity assay (Wilbur & Anderson, 1948) could not be applied due to technical limitations. Expression levels of the *E. coli* carbonic anhydrase Can were not affected by elevated CO<sub>2</sub> levels (Merlin *et al.*, 2003). Thus it might be possible to display benefits of *bca* overexpression at elevated CO<sub>2</sub> concentrations in the supply air during cultivation at low cell densities. Nevertheless, the higher amount of CO<sub>2</sub> might mimic elevated amounts of Bca, so effects of *bca* overexpression in *C. glutamicum* wild type remain difficult to display.

The second approach in this context involved the use of pyruvate as sole carbon source, since it is assumed to be a substrate which generates a higher need for inorganic carbon in anaplerotic reactions (Netzer *et al.*, 2004). Furthermore, a decisive role for a carbonic anhydrase in anaplerosis has been described in *Chlamydomonas reinhardtii* (Giordano *et al.*, 2003). Hence, growth of *C. glutamicum* wild type with and without *bca* overexpression on pyruvate as sole carbon source was monitored. Once more, no differences in growth behaviour were observed (see Figure 3.9). Here again, it appears likely that the amount of Bca in the wild type is not limiting, so no growth benefits emerge from overexpression of the encoding gene. Another possibility lies in the fact that the potential of pyruvate to create a stronger need for inorganic carbon is overestimated. Although the absence of glucose creates an elevated necessity for

#### 4. Discussion

gluconeogenesis, pyruvate as sole carbon source leads to similar amounts of emerging CO<sub>2</sub> compared to the substrate glucose, since CO<sub>2</sub> from the TCA cycle is equally generated. The only additional CO<sub>2</sub> generating step derived from glucose is the pentose-phosphate cycle (Yang *et al.*, 2005). Maybe the use of glutamate or acetate instead of a glycolysis product could lead to more distinct results, since both substrates are known to serve as sole carbon sources and are gluconeogenetic substrates (Gerstmeir *et al.*, 2003; Kramer *et al.*, 1990; Netzer *et al.*, 2004).

Also in terms of pH homeostasis, the influence of Bca remains difficult to display. The results towards pH homeostasis in *C. glutamicum*  $\Delta bca$  upon acidification are inconclusive since both maximum shift pH<sub>i</sub> and steady state pH<sub>i</sub> are lower as in *C. glutamicum* wild type, although a lack of Bca should lead to a decelerated proton formation (see Figure 3.29). Since no measurements were possible with the complementation mutant, it cannot be excluded that the observation is specific for the strain provided by Kyowa Hakko and is possibly based on energetic problems of the mutant. Although *bca* overexpression seems to lead to a higher amount of protons in the cytoplasm of *C. glutamicum* wild type, causing a slightly decreased pH of the crucial extract (see Figure 3.7), no alterations in pH homeostasis were detected in the online pH<sub>i</sub> measurements (see Figure 3.30). The latter method can be regarded as more reliable as it displays the situation *in vivo*. Hence the influence of *bca* overexpression seems negligible in *C. glutamicum* wild type.

Taken together, Bca activity does not seem to influence pH homeostasis in *C. glutamicum* and no optimisation of growth through *bca* overexpression could be displayed in this study. This is most likely due to the generally high amount of Bca in *C. glutamicum* wild type. While the scenario involving low cell densities seems suitable to investigate consequences of varying *bca* expression levels, it is unclear if this is true for the use of pyruvate as a possible anaplerotic substrate.

## 4.2 The impact of bicarbonate import via SbtAB

### 4.2.1 Consequences of additional bicarbonate in *C. glutamicum*

Heterologous expression of the cyanobacterial bicarbonate import system SbtAB restores growth of *C. glutamicum*  $\Delta bca$  at atmospheric CO<sub>2</sub> (see Figure 3.11). Hence, the transporter seems to be functional in *C. glutamicum* and the additionally provided bicarbonate is sufficient to compensate the lack of Bca activity. This is also another hint that bicarbonate is the actual substrate for carboxylation reactions. If grown on solid CgXII minimal medium with additional bicarbonate and an alkaline pH, SbtAB restores growth of *C. glutamicum*  $\Delta bca$  not only on glucose but also on pyruvate (see Figure 3.12). This illustrates the high potential of SbtAB to provide inorganic carbon even on anaplerotic substrates such as pyruvate. However, as discussed in chapter 4.1.3, the elevated need for inorganic carbon during growth on pyruvate is debatable and the results from the solid medium could not be confirmed in liquid culture. Growth of *C. glutamicum*  $\Delta bca$ +SbtAB in liquid CgXII minimal medium with pyruvate as sole organic carbon source was rather poor (see Figure 3.13), even if additional CO<sub>2</sub> was provided in the supply air. While growth rates of *C. glutamicum*  $\Delta bca$ +SbtAB at atmospheric CO<sub>2</sub> and a neutral pH were about 0.25/h on glucose (see Figure 3.11), they only reached about 0.08/h on pyruvate under the same conditions. Interpretation of the results is even more difficult since *C. glutamicum*  $\Delta bca$  grew with pyruvate in liquid culture as discussed in chapter 4.1.2. Nevertheless, the results illustrated in Figure 3.11 strongly argue for the potential of SbtAB to provide decisive amounts of inorganic carbon in *C. glutamicum*. Hence, the impact and possible benefits of this additionally provided bicarbonate were of great interest.

The detection of the SbtB compound in Western Blot analysis (see Figure 3.10) is a proof for the presence of the protein, but not for a functional SbtAB complex. Thus, biochemical characterisation of the transport activity of SbtAB was indispensable. Precise activity measurements were difficult to perform in *C. glutamicum*, which is mainly caused by the fact that there was always background activity in *C. glutamicum* wild type, which made the use of *C. glutamicum*  $\Delta bca$  necessary. Based on the fact that the absence of urea is crucial for precise bicarbonate quantification (see chapter 3.2.3), cultivation in urea-free CgXII is indispensable. Since neither the negative control strain

#### 4. Discussion

*C. glutamicum*  $\Delta bca$  nor the test strain *C. glutamicum*  $\Delta bca$ +SbtAB grew without urea at atmospheric CO<sub>2</sub> (see Figures 3.24.a and b), urea free measurements were impossible. The data gained from uptake measurements with <sup>14</sup>C labelled bicarbonate in urea containing medium showed great aberrations in standard deviations (see Figure 3.22). Nevertheless, they show the activity of SbtAB in *C. glutamicum*  $\Delta bca$ +SbtAB leading to the observed restoration of growth at atmospheric CO<sub>2</sub>.

In *C. glutamicum* wild type, the influence of SbtAB was more difficult to display. A distinct growth benefit emerged during cultivation on solid minimal medium with pyruvate as sole carbon source (see Figure 3.18), but this observation was not confirmed in liquid culture (see Figures 3.19 and 3.20) and the behaviour of *C. glutamicum* on pyruvate as sole carbon source remains difficult to interpret. In contrast, a slight growth benefit in liquid culture with glucose was observed at various pH values (see Figure 3.16). However, it has to be noted that the chosen pH was more decisive for growth than the presence of SbtAB. Also, the pH homeostasis capacity upon acidification is hardly affected by the presence of SbtAB in *C. glutamicum* wild type (see Figure 3.31). Although the buffer capacity of the cytoplasm seems to be elevated due to a SbtAB-derived elevation of the intracellular bicarbonate level, the steady state pH<sub>i</sub> is similar to that of cells without SbtAB. Thus, no long term influence of SbtAB on the intracellular pH is assumed. The fact that SbtAB has also no influence on the lysine yield in *C. glutamicum* DM 1933 (see Figure 3.25) is another hint towards the low impact of SbtAB on the physiology of *C. glutamicum* strains that possess the carbonic anhydrase Bca. Nevertheless, cultivation in a fermenter system might lead to different results here.

To sum up, SbtAB is able to provide bicarbonate in *C. glutamicum* to such an extent that it can replace the essential carbonic anhydrase Bca if urea is provided in the cultivation medium. However if Bca is present, the impact of SbtAB on carbon provision, pH and lysine production appears to be only small. It is possible that inorganic carbon provision is not an aspect of the physiology of *C. glutamicum* that bears great potential for optimisation. Hence, the ability of SbtAB for strain improvement in a biotechnological context did not fulfil initial expectations. Nevertheless, this study presents for the first time the successful expression of a cyanobacterial bicarbonate importer in *C. glutamicum*. Based on these results, other import systems for inorganic carbon from

autotrophic organisms can be tested for their potential to improve inorganic carbon provision in *C. glutamicum*.

### 4.2.2 Possible alternatives to SbtAB

Freshwater  $\beta$ -cyanobacteria like *Synechocystis* sp. are exposed to stronger shifts of inorganic carbon in their environment than marine genera like *Prochlorococcus* sp. Hence, they possess a greater variety of uptake systems for inorganic carbon (Badger *et al.*, 2006). Nevertheless, they harbour bicarbonate uptake systems as well. Generally, five types of inorganic carbon transporters can be distinguished in cyanobacteria, whereas three of them are bicarbonate importers and two are CO<sub>2</sub> uptake systems (Price, 2011).

SbtA, which has been used in this study, is described as an inducible, Na<sup>+</sup>-dependent, high affinity bicarbonate transporter with a possible Na<sup>+</sup>/HCO<sub>3</sub><sup>-</sup>-symport function in *Synechocystis* sp. PCC 6803, which requires 1 mM Na<sup>+</sup> for half maximal activity (Shibata *et al.*, 2002). In *Synechococcus* PCC7942, the *sbtA* gene is collocated with the *sbtB* gene as well and *sbtB* inactivation did not inhibit SbtA activity (B. Forster and GD Price, unpublished). Hence, further investigations towards the function of SbtA alone might lead to promising results in *C. glutamicum*. First experiments showed growth of *C. glutamicum*  $\Delta bca$  equipped with a pEKEx2\_SbtA plasmid on solid BHI complex medium. As possible alternatives, strong SbtA homologues from other  $\beta$ -cyanobacteria (Badger & Price, 2003) could be tested in *C. glutamicum* as well, but this may lead to similar results based on similar structures and transport characteristics.

Another possible Na<sup>+</sup>/HCO<sub>3</sub><sup>-</sup>-symporter that is not related to SbtA and might therefore represent a more interesting candidate is BicA. It belongs to the large ubiquitous family of annotated sulphate transporters and was first described in *Synechococcus* PCC 7002, but homologues can be found in most cyanobacteria (Price *et al.*, 2004). Unlike SbtA, BicA is considered a low-affinity transporter. Another high-affinity bicarbonate transporter that serves as candidate to be tested in *C. glutamicum* is BCT1, an ATP binding cassette (ABC) transporter encoded by the *cmpABCD* operon, which is expressed under inorganic carbon limitation in *Synechococcus* PCC 7942 (Omata *et al.*, 1999). Strong homologues are described in a variety of other species (Price *et al.*, 2008). Based

on their structural and physiological differences from SbtA, BicA and BCT1 might be promising candidates to test their function in *C. glutamicum*. Nevertheless, their properties are difficult to predict in a heterologous system. However, they might have stronger impact on the physiology of *C. glutamicum* and may therefore provide suitable tools for strain improvement.

### 4.2.3 A model of inorganic carbon provision

Based on the results discussed in the previous chapters, new insights into the provision with inorganic carbon in *C. glutamicum* were gained. The initial source of inorganic carbon is CO<sub>2</sub>, which is present in the atmosphere (0.04 %) and is also generated by metabolic activity of the cells. It is able to permeate the membrane passively, so inner and outer concentrations are in equilibrium. At atmospheric CO<sub>2</sub> concentrations, however, the carbonic anhydrase Bca is essential, since the fast enzymatic conversion of CO<sub>2</sub> to HCO<sub>3</sub><sup>-</sup> is indispensable to provide sufficient amounts of inorganic carbon for carboxylation reactions. This essentiality of Bca can be partly compensated by adding 5 % CO<sub>2</sub> to the supply air, but only at neutral or alkaline pH values. Although Bca activity also leads to accelerated proton formation, no influence on the pH homeostasis capacity could be observed. Also a persistently noxious effect of elevated CO<sub>2</sub> concentrations in combination with an acidic external pH can be ruled out, since only short term influences on the internal pH were measured. The cyanobacterial bicarbonate uptake system SbtAB can be functionally expressed in *C. glutamicum* and is able to compensate for the lack of Bca activity in *C. glutamicum*  $\Delta bca$  by import of bicarbonate (HCO<sub>3</sub><sup>-</sup>), which is usually provided via Bca activity. However, this only applies in the presence of urea in minimal medium, so CO<sub>2</sub> derived from urease activity (Nolden *et al.*, 2000; Puskas *et al.*, 2000) is crucial in the absence of Bca as well. In *C. glutamicum* wild type and DM 1933, the impact of SbtAB on growth, pH homeostasis and lysine production is rather low, most probably because those strains still possess Bca activity. Figure 4.1 displays the components involved in inorganic carbon provision in *C. glutamicum*.

#### 4. Discussion

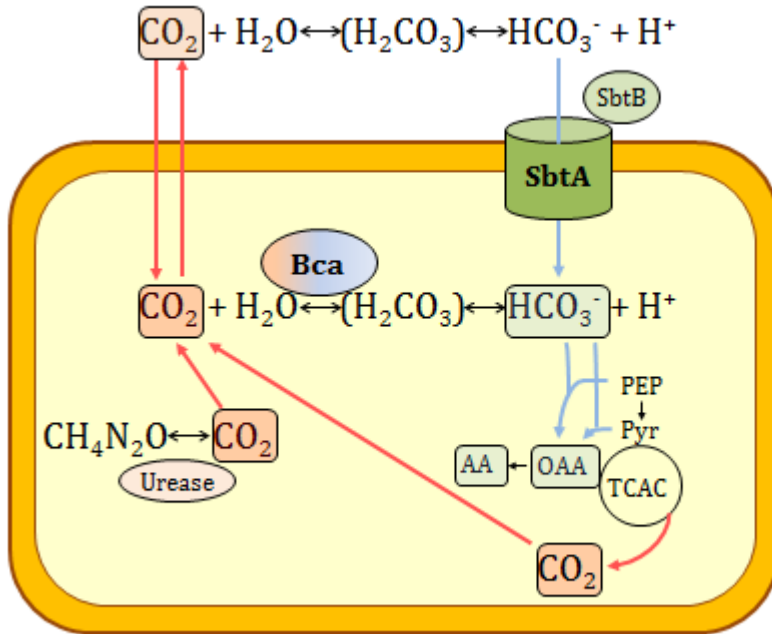


**Figure 4.1: Model of inorganic carbon provision in *C. glutamicum*.** Red arrows mark the fluxes of  $\text{CO}_2$ , blue arrows display bicarbonate ( $\text{HCO}_3^-$ ) fluxes. SbtA: Sodium bicarbonate transporter A from *Synechocystis* sp. PCC 6803; SbtB: periplasmic localised protein SbtB, probably associated to SbtA; Bca:  $\beta$ -type carbonic anhydrase; PEP: Phosphoenolpyruvate; Pyr: Pyruvate; TCAC: Tricarbic acid cycle; OAA: Oxaloacetate; AA: Amino acids.

The model illustrated in Figure 4.1 underlines the central role of the carbonic anhydrase Bca in carbon provision based on the importance to provide bicarbonate as a substrate for PEP and pyruvate carboxylations. It has to be noted that the hydration of  $\text{CO}_2$  takes place also without Bca activity, but proceeds much slower in this case. Nevertheless, a certain amount of spontaneous bicarbonate formation is necessary if SbtAB mediated bicarbonate import is the only source of inorganic carbon as it is the case in *C. glutamicum*  $\Delta\text{bca}+\text{SbtAB}$ , since the mutant shows hardly any growth in the absence of urea as a source of  $\text{CO}_2$ . Hence, at atmospheric  $\text{CO}_2$  concentrations *C. glutamicum* needs either the carbonic anhydrase Bca or SbtAB and urea to ensure sufficient amounts of inorganic carbon in the cell.

### **4.3 The pH homeostasis machinery of *C. glutamicum***

#### **4.3.1 The potential and possible limitations of the established pH<sub>i</sub> detection method**

The Green Fluorescence Protein (GFP) (Tsien, 1998) and many of its mutant forms show certain fluorescence sensitivity to changing pH values and they have been widely used as pH indicators since their discovery (Kneen *et al.*, 1998; Robey *et al.*, 1998; Siegumfeldt *et al.*, 1999). These pH sensitive fluorescence dyes can be separated into two groups. While ecliptic dyes change their intensity depending on the pH values, ratiometric dyes shift their excitation pattern. As described in chapter 3.3.1, ratiometric pHluorin (Miesenböck *et al.*, 1998) was assumed to be a better choice than the ecliptic EYFP for fluorescence based pH measurements because of the unstable EYFP expression levels in *C. glutamicum*. The use of pHluorin to display the intracellular pH and dynamics of pH homeostasis has already been described in eukaryotes like *Saccharomyces cerevisiae* and *Schizosaccharomyces pombe* (Karagiannis & Young, 2001; Pineda Rodo *et al.*, 2012), but also in prokaryotes like *Escherichia coli*, *Bacillus subtilis* and *Lactococcus lactis* (Martinez *et al.*, 2012; Olsen *et al.*, 2002). Above, a more potent variant showing enhanced fluorescence called pHluorin2 has been described recently (Mahon, 2011).

The results in this study present for the first time the successful application of pHluorin in *C. glutamicum*. The protein can be stable and functionally expressed and the physical properties are comparable to those in other organisms, allowing a determination of the intracellular pH between pH 5.8 and 8.5, which is within a physiological range. The results described in chapter 3.3 show the potential of pHluorin for online pH measurements in *C. glutamicum*. Thus, pHluorin bears great potential to determine the intracellular pH of *C. glutamicum* in many other contexts and applications.

Also the setup based on the small bioreactor system combined with the pump unit to apply rapid shifts of the external pH was suitable to investigate the questions in this study. Nevertheless it has to be noted that the culture volume of 50 ml was rather small and so far, no long term applications were tested. It is possible to connect the sample loop also to a larger fermenter unit to monitor the intracellular pH during fermentation

processes. This enables a wide range of applications. However, the use of longer tubes for the sample loop is indispensable in this case, which extends the time cells remain in the sample loop under anaerobic conditions. This is critical in  $\text{pH}_i$  measurements, since there are hints towards a debased pH homeostasis under anaerobic conditions (Andrea Michel, unpublished). Apart from the established setup to measure the pH of *C. glutamicum* cell cultures, single cell measurements using pHluorin should be possible in *C. glutamicum* as well.

### 4.3.2 The role of the respiratory chain

The results regarding pH homeostasis of *C. glutamicum* wild type cells under normal growth conditions (see Figure 3.32) and at elevated  $\text{CO}_2$  concentrations in an acidic surrounding (see Figure 3.28) illustrate the effectiveness of the pH homeostasis machinery. The typical pattern after rapid changes of the external pH including a fast shift of the internal pH followed by a recovery after a few minutes has also been observed in pHluorin based measurements in *E. coli* (Martinez *et al.*, 2012). For *C. glutamicum*, it was assumed that the two branches of terminal oxidases of the respiratory chain are of central importance in this context. Especially the absence of the more efficient *bc<sub>1</sub>-aa<sub>3</sub>*-supercomplex was expected to have negative effects on pH homeostasis. Not only should the lack of this potent proton exporter lead to a reduced acid tolerance, but general effects due to a disturbed energy metabolism were expected. Above, the *C. glutamicum*  $\Delta qcr$  mutant has been shown to exhibit severe defects in growth rate, biomass yield, respiration and proton-motive-force (Koch-Koerfges *et al.*, 2013). Hence, the results for the pH homeostasis pattern of this mutant were surprising, since they were hardly different from *C. glutamicum* wild type (see Figures 3.34.b, 3.35 and Table 3.2). Generally, in *C. glutamicum*  $\Delta qcr$  all parameters were about 0.1 pH units below those of the wild type, but this is probably caused by an altered metabolism of the mutant leading to a slightly more acidic pH of the cytoplasm which was indeed observed regularly at the beginning of the measurements (see Figure 3.33).

The wild type-like results for the *C. glutamicum*  $\Delta cydAB$  mutant fulfilled the expectations, since here only the less efficient cytochrome *bd<sub>1</sub>*-oxidase is absent. The minor impact of the *bd*-branch has been described earlier (Bott & Niebisch, 2003). Also, the determined physiological parameters of this strain hardly differed from

*C. glutamicum* wild type (Koch-Koerfges *et al.*, 2013). The assumption that *C. glutamicum*  $\Delta cydAB$  may show even a better pH homeostasis than *C. glutamicum* wild type was based on the fact that this strain exports protons exclusively via the more efficient supercomplex. However, such an effect was not observed.

The importance of the respiratory chain for pH homeostasis became obvious in measurements conducted with the DOOR strain. If no terminal oxidases are present in *C. glutamicum*, which results in an aerobic fermentative metabolism as described for the *C. glutamicum* DOOR strain (Koch-Koerfges *et al.*, 2013), almost no pH homeostasis was observed (see Figures 3.33.c, 3.34.c and 3.35). Also, the intracellular pH was generally lower, an effect that has been observed in *C. glutamicum*  $\Delta qcr$  as well, but was even stronger in *C. glutamicum* DOOR. It is likely that the formation of organic acids like acetate, succinate and above all lactate (Koch-Koerfges *et al.*, 2013) is the reason for this phenomenon. It has to be noted that *C. glutamicum* DOOR is strongly constrained in its growth and other physiological parameters. Hence, it cannot be ruled out that the severely inhibited pH homeostasis under acidic and alkaline conditions is caused by a generally impaired energy metabolism. A fully functional energy metabolism providing sufficient amounts of ATP has been shown to be crucial for efficient pH homeostasis (Follmann *et al.*, 2009b; Sun *et al.*, 2011). The respiratory chain is of such central importance that a constrained pH homeostasis in the *C. glutamicum* DOOR strain cannot be interpreted as proof of a direct involvement of the terminal oxidases in pH homeostasis. A more promising approach to shed light on this question might be investigation of a possible pH dependent expression of genes encoding the two branches of terminal oxidases. For example, upregulation of proton pumping components of the respiratory chain as part of acidic stress response has been described in *E. coli* before (Slonczewski *et al.*, 2009).

### 4.3.3 A possible involvement of the $F_{(1)}F_{(0)}$ ATPase

Measurements regarding the pH homeostasis capacity of the *C. glutamicum*  $\Delta F_1F_0$  mutant (Koch-Koerfges *et al.*, 2012) conducted in this study revealed that there are no differences to the pH homeostasis pattern of *C. glutamicum* wild type. This is in agreement with the fact that the process of oxidative phosphorylation via  $F_{(1)}F_{(0)}$ ATPase activity is not essential for growth of *C. glutamicum*, although alterations in gene

expression were observed (Koch-Koerfges *et al.*, 2012). However, an involvement of ATPases in pH homeostasis seemed likely based on the fact that there are numerous hints towards pH dependent expression of ATPase encoding genes. The most obvious scenario is upregulation of the ATPase gene expression at alkaline conditions to increase the import rate of protons. Such an effect has actually been described in *E. coli* (Maurer *et al.*, 2005) and *C. glutamicum* (Barriuso-Iglesias *et al.*, 2006). This stands in contradiction to more recent findings arguing for a repressed ATPase gene expression under alkaline conditions in *C. glutamicum* (Follmann *et al.*, 2009b). In the cited study, upregulation at an acidic pH was observed instead. This is a hint towards a possible “reverse” function of the F<sub>(1)</sub>F<sub>(0)</sub>ATPase of *C. glutamicum* under acidic conditions. Such a hydrolytic function of the F<sub>(1)</sub>F<sub>(0)</sub>ATPase together with upregulation of the according genes has been described in *Streptococcus mutans*, *Streptococcus faecalis*, *Lactococcus lactis* and *Lactobacillus acidophilus* (Kobayashi *et al.*, 1986; Koebmann *et al.*, 2000; Kuhnert *et al.*, 2004; Kullen & Klaenhammer, 1999). Nevertheless, it has to be noted that pH homeostasis generally depends on energy consuming transport processes (Krulwich *et al.*, 2011) and the need for ATP in pH homeostasis has been described (Sun *et al.*, 2011). Hence, any upregulation of ATPase encoding genes under acidic conditions might be caused by an elevated need for ATP instead of a direct involvement of the ATPase in proton export. The question whether the F<sub>(1)</sub>F<sub>(0)</sub>ATPase of *C. glutamicum* works in reverse under acidic conditions could not be answered in this study. Instead, the determined homeostasis pattern of the *C. glutamicum* ΔF<sub>1</sub>F<sub>0</sub> deletion mutant revealed a generally low impact of the F<sub>(1)</sub>F<sub>(0)</sub>ATPase on pH homeostasis in *C. glutamicum*.

### **4.3.4 Other putative components of the pH homeostasis machinery of *C. glutamicum***

An important aspect of pH homeostasis that needs to be explored in *C. glutamicum* is the involvement of cation/proton-antiporters. Cations are assumed to play a crucial role in pH stress response since they regulate proton fluxes by changing the electrochemical gradient. The K<sup>+</sup>(Na<sup>+</sup>)/H<sup>+</sup>-antiporter NhaP1 is essential for growth and pH homeostasis at acidic pH values in *Vibrio cholerae* (Quinn *et al.*, 2012). In *C. glutamicum*, the potassium channel CgIK has been shown to be essential at acidic pH values (Follmann *et al.*, 2009a). The involvement of Na<sup>+</sup>/H<sup>+</sup>-antiporters in alkaline stress response is widely spread as reviewed earlier (Padan *et al.*, 2005), but no data are available for

#### 4. Discussion

*C. glutamicum* so far. Mrp-type Na<sup>+</sup>/H<sup>+</sup>-antiporters, which are typically involved in response to alkaline stress, were found in *C. glutamicum* (Follmann, 2008). Nevertheless, their role in pH homeostasis still needs to be explored. The setup for online pH<sub>i</sub> detection developed in this study provides a suitable tool to characterise pH homeostasis patterns of the according deletion and overexpression mutants once these strains are available. A model determined for *Saccharomyces cerevisiae* postulates an involvement of carbonic anhydrases in K<sup>+</sup> homeostasis. The protons derived from its activity may be exported in exchange for potassium ions (Kahm *et al.*, 2012). This scenario implies an indirect contribution of carbonic anhydrases to pH homeostasis, which could be examined by measuring the pH homeostasis capacity of *C. glutamicum*  $\Delta bca$  under potassium starvation. Not only K<sup>+</sup> and Na<sup>+</sup>, but other osmolytes like proline and sucrose are assumed to play a role in the pH homeostasis of *E. coli* cells (Kitko *et al.*, 2010). Thus, this is another interesting aspect of pH homeostasis to be determined in *C. glutamicum* in future experiments.

## 5. Literature

**Abe, S. T., K; Kinoshita,S; (1967).** Taxonomical studies on glutamic acid-producing bacteria. *Journal of General and Applied Microbiology* **Vol.13** 279-301.

**Aguilera, J., Petit, T., de Winde, J. H. & Pronk, J. T. (2005).** Physiological and genome-wide transcriptional responses of *Saccharomyces cerevisiae* to high carbon dioxide concentrations. *FEMS Yeast Res* **5**, 579-593.

**Badger, M. R. & Price, G. D. (2003).** CO<sub>2</sub> concentrating mechanisms in cyanobacteria: molecular components, their diversity and evolution. *J Exp Bot* **54**, 609-622.

**Badger, M. R., Price, G. D., Long, B. M. & Woodger, F. J. (2006).** The environmental plasticity and ecological genomics of the cyanobacterial CO<sub>2</sub> concentrating mechanism. *J Exp Bot* **57**, 249-265.

**Baez, A., Flores, N., Bolivar, F. & Ramirez, O. T. (2009).** Metabolic and transcriptional response of recombinant *Escherichia coli* to elevated dissolved carbon dioxide concentrations. *Biotechnol Bioeng* **104**, 102-110.

**Ballestra P., A. d. S. A., Cuq JL. (1996).** Inactivation of *Escherichia coli* by carbon dioxide under pressure. *J Food Sci* **61**, 829-831.

**Barriuso-Iglesias, M., Barreiro, C., Flechoso, F. & Martin, J. F. (2006).** Transcriptional analysis of the F<sub>0</sub>F<sub>1</sub> ATPase operon of *Corynebacterium glutamicum* ATCC 13032 reveals strong induction by alkaline pH. *Microbiology* **152**, 11-21.

**Barriuso-Iglesias, M., Barreiro, C., Sola-Landa, A. & Martin, J. F. (2013).** Transcriptional control of the F<sub>0</sub>F<sub>1</sub> -ATP synthase operon of *Corynebacterium glutamicum*: SigmaH factor binds to its promoter and regulates its expression at different pH values. *Microb Biotechnol*.

**Bäumchen, C., Knoll, A., Husemann, B., Seletzky, J., Maier, B., Dietrich, C., Amoabediny, G. & Buchs, J. (2007).** Effect of elevated dissolved carbon dioxide concentrations on growth of *Corynebacterium glutamicum* on D-glucose and L-lactate. *J Biotechnol* **128**, 868-874.

**Becker, J., Zelder, O., Hafner, S., Schroder, H. & Wittmann, C. (2011).** From zero to hero--design-based systems metabolic engineering of *Corynebacterium glutamicum* for L-lysine production. *Metab Eng* **13**, 159-168.

## 5. Literature

**Becker, J. & Wittmann, C. (2012).** Systems and synthetic metabolic engineering for amino acid production - the heartbeat of industrial strain development. *Curr Opin Biotechnol* **23**, 718-726.

**Bender, G. R., Sutton, S. V. & Marquis, R. E. (1986).** Acid tolerance, proton permeabilities, and membrane ATPases of oral streptococci. *Infect Immun* **53**, 331-338.

**Blombach, B., Riester, T., Wieschalka, S., Ziert, C., Youn, J. W., Wendisch, V. F. & Eikmanns, B. J. (2011).** *Corynebacterium glutamicum* tailored for efficient isobutanol production. *Appl Environ Microbiol* **77**, 3300-3310.

**Bolten, C. J., Schroder, H., Dickschat, J. & Wittmann, C. (2010).** Towards methionine overproduction in *Corynebacterium glutamicum*--methanethiol and dimethyldisulfide as reduced sulfur sources. *J Microbiol Biotechnol* **20**, 1196-1203.

**Booth, I. R. (1985).** Regulation of cytoplasmic pH in bacteria. *Microbiol Rev* **49**, 359-378.

**Bott, M. & Niebisch, A. (2003).** The respiratory chain of *Corynebacterium glutamicum*. *J Biotechnol* **104**, 129-153.

**Bradford, M. M. (1976).** A rapid and sensitive method for the quantitation of microgram quantities of protein utilizing the principle of protein-dye binding. *Anal Biochem* **72**, 248-254.

**Casey, P. G. & Condon, S. (2002).** Sodium chloride decreases the bacteriocidal effect of acid pH on *Escherichia coli* O157:H45. *Int J Food Microbiol* **76**, 199-206.

**Castanie-Cornet, M. P., Penfound, T. A., Smith, D., Elliott, J. F. & Foster, J. W. (1999).** Control of acid resistance in *Escherichia coli*. *J Bacteriol* **181**, 3525-3535.

**Chapman, B., Jensen, N., Ross, T. & Cole, M. (2006).** Salt, alone or in combination with sucrose, can improve the survival of *Escherichia coli* O157 (SERL 2) in model acidic sauces. *Appl Environ Microbiol* **72**, 5165-5172.

**Clark, D., Rowlett, R. S., Coleman, J. R. & Klessig, D. F. (2004).** Complementation of the yeast deletion mutant DeltaNCE103 by members of the beta class of carbonic anhydrases is dependent on carbonic anhydrase activity rather than on antioxidant activity. *Biochem J* **379**, 609-615.

**Cotter, P. D. & Hill, C. (2003).** Surviving the acid test: responses of gram-positive bacteria to low pH. *Microbiol Mol Biol Rev* **67**, 429-453, table of contents.

## 5. Literature

- Cronk, J. D., Endrizzi, J. A., Cronk, M. R., O'Neill J, W. & Zhang, K. Y. (2001).** Crystal structure of *E. coli* beta-carbonic anhydrase, an enzyme with an unusual pH-dependent activity. *Protein Sci* **10**, 911-922.
- Demain, A. L., Jackson, M., Vitali, R. A., Hendlin, D. & Jacob, T. A. (1966).** Production of guanosine-5'-monophosphate and inosine-5'-monophosphate by fermentation. *Appl Microbiol* **14**, 821-825.
- Dixon, N. M. & Kell, D. B. (1989).** The inhibition by CO<sub>2</sub> of the growth and metabolism of micro-organisms. *J Appl Bacteriol* **67**, 109-136.
- Eikmanns, B. J., Kleinertz, E., Liebl, W. & Sahm, H. (1991).** A family of *Corynebacterium glutamicum*/*Escherichia coli* shuttle vectors for cloning, controlled gene expression, and promoter probing. *Gene* **102**, 93-98.
- Epstein, W. (2003).** The roles and regulation of potassium in bacteria. *Prog Nucleic Acid Res Mol Biol* **75**, 293-320.
- Faust, S. (2011).** Untersuchung der Anwendbarkeit von EYFP als Sensor für den internen pH-Wert von *Corynebacterium glutamicum*. In *Institute for Biochemistry*. Cologne: University of Cologne.
- Follmann, M. (2008).** Untersuchungen zum Einfluß von pH-Variation und erhöhter CO<sub>2</sub> Konzentration auf Stoffwechsel und Aminosäureproduktion mit *Corynebacterium glutamicum*. In *Department of chemistry*. Cologne: University of Cologne.
- Follmann, M., Becker, M., Ochrombel, I., Ott, V., Kramer, R. & Marin, K. (2009a).** Potassium transport in *Corynebacterium glutamicum* is facilitated by the putative channel protein CglK, which is essential for pH homeostasis and growth at acidic pH. *J Bacteriol* **191**, 2944-2952.
- Follmann, M., Ochrombel, I., Kramer, R. & other authors (2009b).** Functional genomics of pH homeostasis in *Corynebacterium glutamicum* revealed novel links between pH response, oxidative stress, iron homeostasis and methionine synthesis. *BMC Genomics* **10**, 621.
- Foster, J. W. (1999).** When protons attack: microbial strategies of acid adaptation. *Curr Opin Microbiol* **2**, 170-174.
- Gale, E. F. & Epps, H. M. (1942).** The effect of the pH of the medium during growth on the enzymic activities of bacteria (*Escherichia coli* and *Micrococcus lysodeikticus*) and the biological significance of the changes produced. *Biochem J* **36**, 600-618.

## 5. Literature

**Gale, E. F. (1946).** The bacterial amino acid decarboxylases. *Adv Enzymol* **6**, 1-32.

**Garcia-Gonzalez, L., Geeraerd, A. H., Spilimbergo, S., Elst, K., Van Ginneken, L., Debevere, J., Van Impe, J. F. & Devlieghere, F. (2007).** High pressure carbon dioxide inactivation of microorganisms in foods: the past, the present and the future. *Int J Food Microbiol* **117**, 1-28.

**Gerstmeir, R., Wendisch, V. F., Schnicke, S., Ruan, H., Farwick, M., Reinscheid, D. & Eikmanns, B. J. (2003).** Acetate metabolism and its regulation in *Corynebacterium glutamicum*. *J Biotechnol* **104**, 99-122.

**Giordano, M., Norici, A., Forssen, M., Eriksson, M. & Raven, J. A. (2003).** An anaplerotic role for mitochondrial carbonic anhydrase in *Chlamydomonas reinhardtii*. *Plant Physiol* **132**, 2126-2134.

**Götz, R., Gnann, A. & Zimmermann, F. K. (1999).** Deletion of the carbonic anhydrase-like gene NCE103 of the yeast *Saccharomyces cerevisiae* causes an oxygen-sensitive growth defect. *Yeast* **15**, 855-864.

**Grant, S. G., Jessee, J., Bloom, F. R. & Hanahan, D. (1990).** Differential plasmid rescue from transgenic mouse DNAs into *Escherichia coli* methylation-restriction mutants. *Proc Natl Acad Sci U S A* **87**, 4645-4649.

**Grigorieva, G. & Sestakov, S. (1982).** Transformation in the cyanobacterium *Synechocystis* sp. 6803. *FEMS Microbiol Lett* **13**, 367-370.

**Henrich, A., Kuhlmann, N., Eck, A. W., Kramer, R. & Seibold, G. M. (2013).** Maltose uptake by the novel ABC transport system MusEFGK2I causes increased expression of ptsG in *Corynebacterium glutamicum*. *J Bacteriol* **195**, 2573-2584.

**Henry, R. P. (1996).** Multiple roles of carbonic anhydrase in cellular transport and metabolism. *Annu Rev Physiol* **58**, 523-538.

**Hermann, T. (2003).** Industrial production of amino acids by coryneform bacteria. *J Biotechnol* **104**, 155-172.

**Hewett-Emmett, D. & Tashian, R. E. (1996).** Functional diversity, conservation, and convergence in the evolution of the alpha-, beta-, and gamma-carbonic anhydrase gene families. *Mol Phylogenet Evol* **5**, 50-77.

## 5. Literature

**Hoang, C. V. & Chapman, K. D. (2002).** Biochemical and molecular inhibition of plastidial carbonic anhydrase reduces the incorporation of acetate into lipids in cotton embryos and tobacco cell suspensions and leaves. *Plant Physiol* **128**, 1417-1427.

**Igamberdiev, A. U. & Roussel, M. R. (2012).** Feedforward non-Michaelis-Menten mechanism for CO<sub>2</sub> uptake by Rubisco: contribution of carbonic anhydrases and photorespiration to optimization of photosynthetic carbon assimilation. *Biosystems* **107**, 158-166.

**Ikeda, M. (2006).** Towards bacterial strains overproducing L-tryptophan and other aromatics by metabolic engineering. *Appl Microbiol Biotechnol* **69**, 615-626.

**Inoue, H., Nojima, H. & Okayama, H. (1990).** High efficiency transformation of *Escherichia coli* with plasmids. *Gene* **96**, 23-28.

**Inui, M., Kawaguchi, H., Murakami, S., Vertes, A. A. & Yukawa, H. (2004).** Metabolic engineering of *Corynebacterium glutamicum* for fuel ethanol production under oxygen-deprivation conditions. *J Mol Microbiol Biotechnol* **8**, 243-254.

**Iyer, R., Williams, C. & Miller, C. (2003).** Arginine-arginine antiporter in extreme acid resistance in *Escherichia coli*. *J Bacteriol* **185**, 6556-6561.

**Kahm, M., Navarrete, C., Llopis-Torregrosa, V., Herrera, R., Barreto, L., Yenush, L., Arino, J., Ramos, J. & Kschischo, M. (2012).** Potassium starvation in yeast: mechanisms of homeostasis revealed by mathematical modeling. *PLoS Comput Biol* **8**, e1002548.

**Kaplan, A. & Reinhold, L. (1999).** CO<sub>2</sub> Concentrating Mechanisms in Photosynthetic Microorganisms. *Annu Rev Plant Physiol Plant Mol Biol* **50**, 539-570.

**Karagiannis, J. & Young, P. G. (2001).** Intracellular pH homeostasis during cell-cycle progression and growth state transition in *Schizosaccharomyces pombe*. *J Cell Sci* **114**, 2929-2941.

**Kashiwagi, K., Suzuki, T., Suzuki, F., Furuchi, T., Kobayashi, H. & Igarashi, K. (1991).** Coexistence of the genes for putrescine transport protein and ornithine decarboxylase at 16 min on *Escherichia coli* chromosome. *J Biol Chem* **266**, 20922-20927.

**Kashket, E. R. (1985).** The proton motive force in bacteria: a critical assessment of methods. *Annu Rev Microbiol* **39**, 219-242.

**Kelle, R., Hermann, T., Bathe, B. (2005).** *L-Lysine production*.

**Kinoshita, S., Udaka, S., Shimono, M. (1957).** Studies on the amino acid fermentation. Production of l-glutamic acid by various microorganisms. *J Gen Appl Microbiol* **3**, 193-205.

**Kitko, R. D., Wilks, J. C., Garduque, G. M. & Slonczewski, J. L. (2010).** Osmolytes contribute to pH homeostasis of *Escherichia coli*. *PLoS One* **5**, e10078.

**Kneen, M., Farinas, J., Li, Y. & Verkman, A. S. (1998).** Green fluorescent protein as a noninvasive intracellular pH indicator. *Biophys J* **74**, 1591-1599.

**Knoll, A., Bartsch, S., Husemann, B., Engel, P., Schroer, K., Ribeiro, B., Stockmann, C., Seletzky, J. & Buchs, J. (2007).** High cell density cultivation of recombinant yeasts and bacteria under non-pressurized and pressurized conditions in stirred tank bioreactors. *J Biotechnol* **132**, 167-179.

**Kobayashi, H., Suzuki, T. & Unemoto, T. (1986).** Streptococcal cytoplasmic pH is regulated by changes in amount and activity of a proton-translocating ATPase. *J Biol Chem* **261**, 627-630.

**Koch-Koerfges, A., Kabus, A., Ochrombel, I., Marin, K. & Bott, M. (2012).** Physiology and global gene expression of a *Corynebacterium glutamicum* DeltaF(1)F(O)-ATP synthase mutant devoid of oxidative phosphorylation. *Biochim Biophys Acta* **1817**, 370-380.

**Koch-Koerfges, A., Pflzer, N., Platzen, L., Oldiges, M. & Bott, M. (2013).** Conversion of *Corynebacterium glutamicum* from an aerobic respiring to an aerobic fermenting bacterium by inactivation of the respiratory chain. *Biochim Biophys Acta* **1827**, 699-708.

**Koebmann, B. J., Nilsson, D., Kuipers, O. P. & Jensen, P. R. (2000).** The membrane-bound H(+)-ATPase complex is essential for growth of *Lactococcus lactis*. *J Bacteriol* **182**, 4738-4743.

**Krämer, R., Lambert, C., Hoischen, C. & Ebbighausen, H. (1990).** Uptake of glutamate in *Corynebacterium glutamicum*. 1. Kinetic properties and regulation by internal pH and potassium. *Eur J Biochem* **194**, 929-935.

**Kronberg, H. L. (1966).** Anaplerotic sequences and their role in metabolism. *Essays in Biochemistry* **2**, 1-31.

**Krulwich, T. A., Hicks, D. B. & Ito, M. (2009).** Cation/proton antiporter complements of bacteria: why so large and diverse? *Mol Microbiol* **74**, 257-260.

## 5. Literature

- Krulwich, T. A., Sachs, G. & Padan, E. (2011).** Molecular aspects of bacterial pH sensing and homeostasis. *Nat Rev Microbiol* **9**, 330-343.
- Kuhnert, W. L., Zheng, G., Faustoferri, R. C. & Quivey, R. G., Jr. (2004).** The F-ATPase operon promoter of *Streptococcus mutans* is transcriptionally regulated in response to external pH. *J Bacteriol* **186**, 8524-8528.
- Kullen, M. J. & Klaenhammer, T. R. (1999).** Identification of the pH-inducible, proton-translocating F1F0-ATPase (atpBEFHAGDC) operon of *Lactobacillus acidophilus* by differential display: gene structure, cloning and characterization. *Mol Microbiol* **33**, 1152-1161.
- Kyhse-Andersen, J. (1984).** Electroblotting of multiple gels: a simple apparatus without buffer tank for rapid transfer of proteins from polyacrylamide to nitrocellulose. *J Biochem Biophys Methods* **10**, 203-209.
- Laemmli, U. K. (1970).** Cleavage of structural proteins during the assembly of the head of bacteriophage T4. *Nature* **227**, 680-685.
- Liebl, W., Bayerl, A., Schein, B., Stillner, U. & Schleifer, K. H. (1989).** High efficiency electroporation of intact *Corynebacterium glutamicum* cells. *FEMS Microbiol Lett* **53**, 299-303.
- Lindskog, S. (1997).** Structure and mechanism of carbonic anhydrase. *Pharmacol Ther* **74**, 1-20.
- Litsanov, B., Kabus, A., Brocker, M. & Bott, M. (2012).** Efficient aerobic succinate production from glucose in minimal medium with *Corynebacterium glutamicum*. *Microb Biotechnol* **5**, 116-128.
- Lopez, M., Kohler, S. & Winum, J. Y. (2011).** Zinc metalloenzymes as new targets against the bacterial pathogen *Brucella*. *J Inorg Biochem*.
- Lu, S., Eiteman, M. A. & Altman, E. (2009).** Effect of CO<sub>2</sub> on succinate production in dual-phase *Escherichia coli* fermentations. *J Biotechnol* **143**, 213-223.
- Lynch, C. J., Fox, H., Hazen, S. A., Stanley, B. A., Dodgson, S. & Lanoue, K. F. (1995).** Role of hepatic carbonic anhydrase in de novo lipogenesis. *Biochem J* **310 ( Pt 1)**, 197-202.

## 5. Literature

- Mahon, M. J. (2011).** pHluorin2: an enhanced, ratiometric, pH-sensitive green fluorescent protein. *Adv Biosci Biotechnol* **2**, 132-137.
- Martin-Galiano, A. J., Ferrandiz, M. J. & de la Campa, A. G. (2001).** The promoter of the operon encoding the F<sub>0</sub>F<sub>1</sub> ATPase of *Streptococcus pneumoniae* is inducible by pH. *Mol Microbiol* **41**, 1327-1338.
- Martinez, K. A., 2nd, Kitko, R. D., Mershon, J. P., Adcox, H. E., Malek, K. A., Berkmen, M. B. & Slonczewski, J. L. (2012).** Cytoplasmic pH response to acid stress in individual cells of *Escherichia coli* and *Bacillus subtilis* observed by fluorescence ratio imaging microscopy. *Appl Environ Microbiol* **78**, 3706-3714.
- Marx, A., de Graaf, A. A., Wiechert, W., Eggeling, L. & Sahm, H. (1996).** Determination of the fluxes in the central metabolism of *Corynebacterium glutamicum* by nuclear magnetic resonance spectroscopy combined with metabolite balancing. *Biotechnol Bioeng* **49**, 111-129.
- Maurer, L. M., Yohannes, E., Bondurant, S. S., Radmacher, M. & Slonczewski, J. L. (2005).** pH regulates genes for flagellar motility, catabolism, and oxidative stress in *Escherichia coli* K-12. *J Bacteriol* **187**, 304-319.
- Mayr, S. (2011).** Etablierung eines Fluoreszenz-basierten Systems zur *in vivo* pH-Messung und Untersuchungen zum Einfluss von CO<sub>2</sub> auf den internen pH-Wert in *Corynebacterium glutamicum*. In *Institut für Biochemie*. Köln: Universität zu Köln.
- McGadey, J. (1970).** A tetrazolium method for non-specific alkaline phosphatase. *Histochemie* **23**, 180-184.
- Meldrum, N. U. & Roughton, F. J. (1933).** Carbonic anhydrase. Its preparation and properties. *J Physiol* **80**, 113-142.
- Merlin, C., Masters, M., McAteer, S. & Coulson, A. (2003).** Why is carbonic anhydrase essential to *Escherichia coli*? *J Bacteriol* **185**, 6415-6424.
- Miesenböck, G., De Angelis, D. A. & Rothman, J. E. (1998).** Visualizing secretion and synaptic transmission with pH-sensitive green fluorescent proteins. *Nature* **394**, 192-195.
- Mimitsuka, T., Sawai, H., Hatsu, M. & Yamada, K. (2007).** Metabolic engineering of *Corynebacterium glutamicum* for cadaverine fermentation. *Biosci Biotechnol Biochem* **71**, 2130-2135.

## 5. Literature

- Minnikin, D. (1982).** *The biology of mycobacteria*: Academic Press.
- Mitchell, P. (1973).** Performance and conservation of osmotic work by proton-coupled solute porter systems. *J Bioenerg* **4**, 63-91.
- Mitsuhashi, S., Ohnishi, J., Hayashi, M. & Ikeda, M. (2004).** A gene homologous to beta-type carbonic anhydrase is essential for the growth of *Corynebacterium glutamicum* under atmospheric conditions. *Appl Microbiol Biotechnol* **63**, 592-601.
- Moon, M. W., Kim, H. J., Oh, T. K., Shin, C. S., Lee, J. S., Kim, S. J. & Lee, J. K. (2005).** Analyses of enzyme II gene mutants for sugar transport and heterologous expression of fructokinase gene in *Corynebacterium glutamicum* ATCC 13032. *FEMS Microbiol Lett* **244**, 259-266.
- Mostafa, S. S. & Gu, X. (2003).** Strategies for improved dCO<sub>2</sub> removal in large-scale fed-batch cultures. *Biotechnol Prog* **19**, 45-51.
- Netzer, R., Krause, M., Rittmann, D., Peters-Wendisch, P. G., Eggeling, L., Wendisch, V. F. & Sahl, H. (2004).** Roles of pyruvate kinase and malic enzyme in *Corynebacterium glutamicum* for growth on carbon sources requiring gluconeogenesis. *Arch Microbiol* **182**, 354-363.
- Nishimori, I., Minakuchi, T., Maresca, A., Carta, F., Scozzafava, A. & Supuran, C. T. (2010).** The beta-carbonic anhydrases from *Mycobacterium tuberculosis* as drug targets. *Curr Pharm Des* **16**, 3300-3309.
- Nolden, L., Beckers, G., Mockel, B., Pfefferle, W., Nampoothiri, K. M., Kramera, R. & Burkovskia, A. (2000).** Urease of *Corynebacterium glutamicum*: organization of corresponding genes and investigation of activity. *FEMS Microbiol Lett* **189**, 305-310.
- Norici, A., Dalsass, A. & Giordano, M. (2002).** Role of phosphoenolpyruvate carboxylase in anaplerosis in the green microalga *Dunaliella salina* cultured under different nitrogen regimes. *Physiol Plant* **116**, 186-191.
- Northrop, D. B. & Simpson, F. B. (1998).** Kinetics of enzymes with isomechanisms: britton induced transport catalyzed by bovine carbonic anhydrase II, measured by rapid-flow mass spectrometry. *Arch Biochem Biophys* **352**, 288-292.
- Okino, S., Noburyu, R., Suda, M., Jojima, T., Inui, M. & Yukawa, H. (2008).** An efficient succinic acid production process in a metabolically engineered *Corynebacterium glutamicum* strain. *Appl Microbiol Biotechnol* **81**, 459-464.

## 5. Literature

- Olsen, K. N., Budde, B. B., Siegumfeldt, H., Rechinger, K. B., Jakobsen, M. & Ingmer, H. (2002).** Noninvasive measurement of bacterial intracellular pH on a single-cell level with green fluorescent protein and fluorescence ratio imaging microscopy. *Appl Environ Microbiol* **68**, 4145-4147.
- Omata, T., Price, G. D., Badger, M. R., Okamura, M., Gohta, S. & Ogawa, T. (1999).** Identification of an ATP-binding cassette transporter involved in bicarbonate uptake in the cyanobacterium *Synechococcus* sp. strain PCC 7942. *Proc Natl Acad Sci U S A* **96**, 13571-13576.
- Onken, U. & Liefke, E. (1989).** Effect of total and partial pressure (oxygen and carbon dioxide) on aerobic microbial processes. *Adv Biochem Eng Biotechnol* **40**, 137-169.
- Padan, E., Bibi, E., Ito, M. & Krulwich, T. A. (2005).** Alkaline pH homeostasis in bacteria: new insights. *Biochim Biophys Acta* **1717**, 67-88.
- Parche, S., Burkovski, A., Sprenger, G. A., Weil, B., Krämer, R. & Titgemeyer, F. (2001).** *Corynebacterium glutamicum*: a dissection of the PTS. *J Mol Microbiol Biotechnol* **3**, 423-428.
- Peters-Wendisch, P. G., Wendisch, V. F., Paul, S., Eikmanns, B. J. & Sahm, H. (1997).** Pyruvate carboxylase as an anaplerotic enzyme in *Corynebacterium glutamicum*. *Microbiology* **143**, 1095-1103.
- Peters-Wendisch, P. G., Schiel, B., Wendisch, V. F., Katsoulidis, E., Mockel, B., Sahm, H. & Eikmanns, B. J. (2001).** Pyruvate carboxylase is a major bottleneck for glutamate and lysine production by *Corynebacterium glutamicum*. *J Mol Microbiol Biotechnol* **3**, 295-300.
- Petersen, S., de Graaf, A. A., Eggeling, L., Mollney, M., Wiechert, W. & Sahm, H. (2000).** In vivo quantification of parallel and bidirectional fluxes in the anaplerosis of *Corynebacterium glutamicum*. *J Biol Chem* **275**, 35932-35941.
- Pineda Rodo, A., Vachova, L. & Palkova, Z. (2012).** In vivo determination of organellar pH using a universal wavelength-based confocal microscopy approach. *PLoS One* **7**, e33229.
- Price, G. D., Coleman, J. R. & Badger, M. R. (1992).** Association of Carbonic Anhydrase Activity with Carboxysomes Isolated from the Cyanobacterium *Synechococcus* PCC7942. *Plant Physiol* **100**, 784-793.

## 5. Literature

- Price, G. D., Woodger, F. J., Badger, M. R., Howitt, S. M. & Tucker, L. (2004).** Identification of a SulP-type bicarbonate transporter in marine cyanobacteria. *Proc Natl Acad Sci U S A* **101**, 18228-18233.
- Price, G. D., Badger, M. R., Woodger, F. J. & Long, B. M. (2008).** Advances in understanding the cyanobacterial CO<sub>2</sub>-concentrating-mechanism (CCM): functional components, Ci transporters, diversity, genetic regulation and prospects for engineering into plants. *J Exp Bot* **59**, 1441-1461.
- Price, G. D. (2011).** Inorganic carbon transporters of the cyanobacterial CO<sub>2</sub> concentrating mechanism. *Photosynth Res* **109**, 47-57.
- Price, G. D., Shelden, M. C. & Howitt, S. M. (2011).** Membrane topology of the cyanobacterial bicarbonate transporter, SbtA, and identification of potential regulatory loops. *Mol Membr Biol* **28**, 265-275.
- Puskas, L. G., Inui, M. & Yukawa, H. (2000).** Structure of the urease operon of *Corynebacterium glutamicum*. *DNA Seq* **11**, 383-394, 467.
- Quinn, M. J., Resch, C. T., Sun, J., Lind, E. J., Dibrov, P. & Hase, C. C. (2012).** NhaP1 is a K<sup>+</sup>(Na<sup>+</sup>)/H<sup>+</sup> antiporter required for growth and internal pH homeostasis of *Vibrio cholerae* at low extracellular pH. *Microbiology* **158**, 1094-1105.
- Robey, R. B., Ruiz, O., Santos, A. V., Ma, J., Kear, F., Wang, L. J., Li, C. J., Bernardo, A. A. & Arruda, J. A. (1998).** pH-dependent fluorescence of a heterologously expressed Aequorea green fluorescent protein mutant: in situ spectral characteristics and applicability to intracellular pH estimation. *Biochemistry* **37**, 9894-9901.
- Rowlett, R. S., Tu, C., McKay, M. M. & other authors (2002).** Kinetic characterization of wild-type and proton transfer-impaired variants of beta-carbonic anhydrase from *Arabidopsis thaliana*. *Arch Biochem Biophys* **404**, 197-209.
- Sambrook, J., Fritsch, E.F., Maniatis, J. (1989).** *Molecular cloning: a laboratory manual*: Cold Spring Harbor Laboratory Press.
- Schaffner, W. & Weissmann, C. (1973).** A rapid, sensitive, and specific method for the determination of protein in dilute solution. *Anal Biochem* **56**, 502-514.
- Schueler, C., Becker, H. M., McKenna, R. & Deitmer, J. W. (2011).** Transport activity of the sodium bicarbonate cotransporter NBCe1 is enhanced by different isoforms of carbonic anhydrase. *PLoS One* **6**, e27167.

## 5. Literature

**Sears, D. F. & Eisenberg, R. M. (1961).** A model representing a physiological role of CO<sub>2</sub> at the cell membrane. *J Gen Physiol* **44**, 869-887.

**Senouci-Rezkallah, K., Schmitt, P. & Jobin, M. P. (2011).** Amino acids improve acid tolerance and internal pH maintenance in *Bacillus cereus* ATCC14579 strain. *Food Microbiol* **28**, 364-372.

**Shibata, M., Katoh, H., Sonoda, M., Ohkawa, H., Shimoyama, M., Fukuzawa, H., Kaplan, A. & Ogawa, T. (2002).** Genes essential to sodium-dependent bicarbonate transport in cyanobacteria: function and phylogenetic analysis. *J Biol Chem* **277**, 18658-18664.

**Siegumfeldt, H., Rechinger, K. B. & Jakobsen, M. (1999).** Use of fluorescence ratio imaging for intracellular pH determination of individual bacterial cells in mixed cultures. *Microbiology* **145 ( Pt 7)**, 1703-1709.

**Slonczewski, J. L., Fujisawa, M., Dopson, M. & Krulwich, T. A. (2009).** Cytoplasmic pH measurement and homeostasis in bacteria and archaea. *Adv Microb Physiol* **55**, 1-79, 317.

**Smith, K. M., Cho, K. M. & Liao, J. C. (2010).** Engineering *Corynebacterium glutamicum* for isobutanol production. *Appl Microbiol Biotechnol* **87**, 1045-1055.

**Smith, K. S. & Ferry, J. G. (2000).** Prokaryotic carbonic anhydrases. *FEMS Microbiol Rev* **24**, 335-366.

**Spilimbergo, S. & Bertucco, A. (2003).** Non-thermal bacterial inactivation with dense CO<sub>2</sub>. *Biotechnol Bioeng* **84**, 627-638.

**Stackenbrandt, E., FRED A. Rainey, F.A. and Ward-Rainey, N.L. (1997).** Proposal for a New Hierarchic Classification System, Actinobacteria classis nov. *Int J Syst Bacteriol* **47**, 479-491.

**Stadie, W. C. a. O. B., H. (1933).** The catalysis of the hydration of carbon dioxide and the dehydration of carbonic acid by an enzyme isolated from red blood cells. *J Biol Chem* **103**, 521-529.

**Sturr, M. G. & Marquis, R. E. (1992).** Comparative acid tolerances and inhibitor sensitivities of isolated F-ATPases of oral lactic acid bacteria. *Appl Environ Microbiol* **58**, 2287-2291.

## 5. Literature

**Summerfield, T. C. & Sherman, L. A. (2008).** Global transcriptional response of the alkali-tolerant cyanobacterium *Synechocystis* sp. strain PCC 6803 to a pH 10 environment. *Appl Environ Microbiol* **74**, 5276-5284.

**Sun, Y., Fukamachi, T., Saito, H. & Kobayashi, H. (2011).** ATP requirement for acidic resistance in *Escherichia coli*. *J Bacteriol* **193**, 3072-3077.

**Supuran, C. T. (2011).** Bacterial carbonic anhydrases as drug targets: toward novel antibiotics? *Front Pharmacol* **2**, 34.

**Towbin, H., Staehelin, T. & Gordon, J. (1979).** Electrophoretic transfer of proteins from polyacrylamide gels to nitrocellulose sheets: procedure and some applications. *Proc Natl Acad Sci U S A* **76**, 4350-4354.

**Tripp, B. C., Smith, K. & Ferry, J. G. (2001).** Carbonic anhydrase: new insights for an ancient enzyme. *J Biol Chem* **276**, 48615-48618.

**Tsien, R. Y. (1998).** The green fluorescent protein. *Annu Rev Biochem* **67**, 509-544.

**Vertes, A. A., Inui, M. & Yukawa, H. (2012).** Postgenomic approaches to using corynebacteria as biocatalysts. *Annu Rev Microbiol* **66**, 521-550.

**Wilbur, K. M. & Anderson, N. G. (1948).** Electrometric and colorimetric determination of carbonic anhydrase. *J Biol Chem* **176**, 147-154.

**Yang, T. H., Heinzle, E. & Wittmann, C. (2005).** Theoretical aspects of <sup>13</sup>C metabolic flux analysis with sole quantification of carbon dioxide labeling. *Comput Biol Chem* **29**, 121-133.

# Danksagung

Herrn Prof. Dr. Reinhard Krämer danke ich dafür, dass er mir ermöglicht hat, diese Arbeit in seiner Gruppe anzufertigen und für die Überlassung des interessanten Themas. Ich danke ihm für sein Vertrauen und seine hervorragende Betreuung, die durch stete Diskussionsbereitschaft geprägt war. Ebenso danke ich Herrn Dr. Kay Marin und Herrn Dr. Gerd Seibold dafür, dass sie diese Arbeit mit betreut und somit durch viele anregende Gespräche und Ideen wesentlich zum Gelingen des Projektes beigetragen haben.

Bei Herrn Prof. Dr. Ulf-Ingo Flügge bedanke ich mich herzlich für die freundliche Übernahme des Koreferats.

Ich bedanke mich bei Abigail Koch-Koerfges für die Bereitstellung der Atmungsketten- und  $\Delta F_{(1)}F_{(0)}$ -Mutanten, sowie für die anregenden Diskussionen und ihre Hilfsbereitschaft. Prof. Dr. Gero Miesenböck danke ich für die Bereitstellung der pHluorin-Plasmide.

Simon Mayr hat durch seine Arbeit zur *online*-pH-Messung entscheidende Beiträge zur Methodenentwicklung geleistet, wofür ihm besonderer Dank gebührt.

Für das stets verlässliche und hilfreiche Korrekturlesen dieser Arbeit bedanke ich mich herzlich bei Dr. Michael Becker, Gwydion Brennan und Dr. Carolin Lange.

Ein besonders lieber Dank geht an meine - zum Teil bereits ehemaligen - Kollegen. Alexander, Andreas, Anna, Benjamin, Carolin, Dimitar, Michael, Markus, Natalie und Stanislav haben meine Zeit in der AG Krämer in vielerlei wissenschaftlicher und nicht wissenschaftlicher Hinsicht enorm bereichert und die gemeinsame Zeit im Labor und darüber hinaus zu einem besonderen Lebensabschnitt voller schöner Erinnerungen werden lassen. Ebenso wäre so manches Experiment mit Sicherheit nicht geglückt ohne die stetige Hilfsbereitschaft und technische Unterstützung von Anja und Gabi. Auch hierfür ein herzliches Dankeschön.

Für ihren vielleicht indirekten, aber zweifellos entscheidenden Beitrag zum Gelingen dieser Arbeit danke ich von ganzem Herzen meiner Familie und meinen Freunden. Ihre schier unerschöpfliche Geduld und Loyalität waren nicht selten der entscheidende Faktor, Mut und Selbstvertrauen nicht zu verlieren. Ein besonders liebevoller Dank gebührt in diesem Zusammenhang Gwydion Brennan, der trotz täglicher Konfrontation mit allen Hochs und Tiefs während dieser Arbeit mir stets den Rücken gestärkt und mich auch in schwierigen Phasen bedingungslos erduldet und immer wieder aufgebaut hat.

# Erklärung

Ich versichere, dass ich die von mir vorgelegte Dissertation selbständig angefertigt, die benutzten Quellen und Hilfsmittel vollständig angegeben und die Stellen der Arbeit - einschließlich Tabellen, Karten und Abbildungen -, die anderen Werken im Wortlaut oder dem Sinn nach entnommen sind, in jedem Einzelfall als Entlehnung kenntlich gemacht habe; dass diese Dissertation noch keiner anderen Fakultät oder Universität zur Prüfung vorgelegen hat; dass sie - abgesehen von den unten angegebenen Teilpublikationen - noch nicht veröffentlicht worden ist sowie, dass ich eine solche Veröffentlichung vor Abschluss des Promotionsverfahrens nicht vornehmen werde.

Die Bestimmungen dieser Promotionsordnung sind mir bekannt. Die von mir vorgelegte Dissertation ist von Prof. Dr. R. Krämer am Institut für Biochemie der Mathematisch-Naturwissenschaftlichen Fakultät der Universität zu Köln betreut worden.

Teilpublikationen: keine

Ich versichere, dass ich alle Angaben wahrheitsgemäß nach bestem Wissen und Gewissen gemacht habe und verpflichte mich, jedmögliche, die obigen Angaben betreffende Veränderung, dem Dekanat unverzüglich mitzuteilen.

Ort, Datum

Unterschrift